МИНИСТЕРСТВО НАУКИ И ВЫСШЕГО ОБРАЗОВАНИЯ РОССИЙСКОЙ ФЕДЕРАЦИИ

ФЕДЕРАЛЬНОЕ ГОСУДАРСТВЕННОЕ АВТОНОМНОЕ
ОБРАЗОВАТЕЛЬНОЕ УЧРЕЖДЕНИЕ ВЫСШЕГО ОБРАЗОВАНИЯ
«САМАРСКИЙ НАЦИОНАЛЬНЫЙ ИССЛЕДОВАТЕЛЬСКИЙ
УНИВЕРСИТЕТ ИМЕНИ АКАДЕМИКА С.П. КОРОЛЕВА»
(САМАРСКИЙ УНИВЕРСИТЕТ)

MECHANICS OF COMPRESSIBLE FLUID

Рекомендовано редакционно-издательским советом федерального государственного автономного образовательного учреждения высшего образования «Самарский национальный исследовательский университет имени академика С.П. Королева» в качестве учебного пособия для студентов, обучающихся по основной образовательной программе высшего образования по направлению подготовки 24.04.05 Двигатели летательных аппаратов

САМАРА
Издательство Самарского университета
2018

УДК 533.6(075)+532.5(075)
ББК 22.253я7
М45

Авторы: ***В.В. Бирюк, Е.В. Благин, Д.А. Угланов, Ю.И. Цыбизов***

Рецензенты: д-р техн. наук, проф. В.Б. Балякин;
д-р техн. наук, проф. А.А. Иголкин

М45 Mechanics of compressible fluid: учеб. пособие / [В.В. Бирюк и др.]. – Самара: Изд-во Самарского университета, 2018. – 156 с.: ил.

ISBN 978-5-7883-1339-9

Приведены основы механики сжимаемых сред. Рассмотрено движение газовой среды в каналах переменного сечения в дозвуковом и сверхзвуковом режиме.

Пособие предназначено для студентов, обучающихся по направлению подготовки 24.04.05 Двигатели летательных аппаратов, а также может быть полезно слушателям курсов, аспирантам и специалистам, изучающим направление «Менеджмент энергосберегающих технологий». Разработано на кафедре теплотехники и тепловых двигателей.

УДК 533.6(075)+532.5(075)
ББК 22.253я7

ISBN 978-5-7883-1339-9

ОГЛАВЛЕНИЕ

INTRODUCTION

Fluid mechanics is a special part of the common mechanics which includes hydraulics (incompressible fluids motion study), aerodynamics and gas dynamics (compressible fluids motion study). In comparison to mechanics of the solid bodies this educational subject is more difficult due to lack of the hard links between particles of the environment. The presence of the high mobile fluid particles provides special difficulties native only to fluid mechanics.

The special feature of the any moving gas or liquid fluid is superposition of the fluid movement with chaotic (undirected) movement of the environment molecules. The calculation of such a difficult fluid movement doesn't seem possible. Schematization and idealization of the flow is necessary i.e. accept of the mathematical model which not only keeps main treats and features of the process under study but also allows to carry out engineering analysis by available means.

At present basis of this common flow model is the well-proved **hypothesis** which determines the compressible fluid (gas) model as media which fills space without creation of any emptiness (**continuity hypothesis**). This hypothesis makes theoretical and experimental researches significantly simpler because it allows considering environment mechanical characteristics as continuous and differentiating parameters as velocity, pressure and density depending upon coordinates and time.

Gas dynamics is an area of science that studies movement of the compressible fluid (gas) in high velocities and temperatures conditions where the laws of the hydraulics are no longer correct. It is a science that requires intimate knowledge of the physics and dynamics and is based on the modern mathematics and computer techniques achievements. Therefore, the equations of the mathematical physics are the basis of the mathematical apparatus of this part of mechanics, and the perfect computer skills are the recipe for success in practical activity.

It is obvious that aviation and rocket industry progress, increasing of the velocity in the flow passages of the rotary machines, development of the different kinds of the jet apparatus requires not only intimate knowledge of the hydrodynamics and gas dynamics but also constant expansion of the knowledge in the area of the sub- and supersonic velocities of the movement.

At present different software is developed and widely used in engineering practice, especially in the hydrodynamics and gas dynamics. This software allows carrying out opportunities of the mathematical modeling of the inner and outer channel 2-D and 3-D flows such as:

- steady and unsteady tasks;
- laminar and turbulent flows (with different turbulence models);
- viscous (Newtonian and non-Newtonian liquids) and non-viscous liquid and gas.

The next features are used:

- effective calculation algorithms;
- adaptive mesh concentration;
- set of the intelligent boundary conditions;
- missed meshes, arbitrary geometric areas, automatized connection of the incompatible meshes;
- moving (deforming, sliding) meshes, dynamic adding and removing of the cells.

It is obvious that verification of the obtained experimental results with calculation results will be criterion of the calculation applicability. All of this requires not only deep studying of the software potential but also knowledge about incompressible fluids flows objective laws and features.

Data about main features of the sub- and supersonic flows, gas dynamic equations, used in engineering activity and engineering methods of the compressible fluid flows calculation in the channels with variable cross section which are suited for the aircraft and ground gas turbine engines, are presented below.

In the chapters 1…3 main definitions and equations of the non-viscous non-heat-conducting compressible liquid (gas) and the accepted simplified models are presented. Also here there are presented data about weak disturbance (acoustic waves) motion. In the chapter 4 strong disturbance, supersonic flows flow phenomena and shock waves are described. In the chapter 5 data about real gas flow features is given and in the chapters 6 and 7 designs of the exhaust devices of the aircraft and ground gas turbine engines are described, flow phenomena and parameter calculation in this channels based on the modern achievements of the gas dynamics. In chapter 8 main definitions and terms of the similarity theory are presented. In chapter 9 the design schemes and operation principals of diffusers are presented. And finally, the basis of the numerical calculation methods and their application in fluid dynamics are presented in chapter 10.

Chapter 1. BASIC TERMS AND DEFINITIONS

It is possible to consider that there is no principle difference between gaseous and liquid conditions because there is continuous transfer from gas to liquid and vice versa. However, it is forbidden to consider liquid as a high pressure gas because their densities are so high quantitative different that liquid properties significantly differ from gas properties. In liquids mean distance between molecules is the same order as its diameters so particles movement in the liquid volume is extremely hindered. Trend of the heat movement of the molecules is next.

There are two groups of the molecules:

- gaseous, chaotic moving (traveling);
- oscillating (settled).

There is dynamic equilibrium between these two groups at the given temperature.

Gas is a system of the discrete molecules that chaotically move and impinge each other. It can be characterized by the mean length of the molecule free path i.e.

length that molecule can move without impact (l). If l is lesser then characteristic dimension of the streamlined body for example, gas can be described as continuous environment.

Example: At air standard conditions 1 cm^3 of air contains $2{,}7 \cdot 10^{19}$ molecules. If cube with 0,001 mm^3 side is considered it will contain $2{,}7 \cdot 10^7$ molecules which is enough for the accept of the mean parameters.

At any moment and position of environment working fluid is situated in the thermodynamic equilibrium which is determined by its pressure, temperature, specific volume and density. Density magnitude depends upon working fluid characteristics and conditions (pressure and temperature). For compressible fluid (gas) density dependence upon pressure and temperature is determined by Clapeyron condition equation:

$$\rho = P/RT.$$

Viscosity. Every really existing gas is viscous. Non-viscous gases are called **ideal**. Viscosity is an ability of the liquids or gases to resist to relative flow of its parts. Newton was first who consider that inner friction force between two layers of the moving fluid is directly proportional to layers velocity difference, surface area of their contact and inversely proportional to distance between layers. **Tangential stress,** which is linked to a viscosity, occurs in a moving media and equal to:

$$\tau = \frac{F}{S} = \mu_в \frac{dw}{dh},$$

where F – viscous force;

S – contact surface area;

dw/dh – velocity gradient;

$\mu_в$ – dynamic viscosity coefficient which depends on working fluid nature and conditions. (Significantly depends on temperature and depends on pressure if it exceeds 100 atm).

Pressure (P) is a force which acts on unit area and directed normal to the volume surface into the interior of the domain.

Mass density is a limit of the working fluid mass to its volume relation with its narrowing to some inner point (such limit exist due to continuity hypothesis).

Compressibility of the media is equal to:

$$B_v = -\frac{(V_1 - V_2)}{V_1 P},$$

where V_1 and V_2 – starting and final volumes during pressure change for Δp magnitude. Increasing of pressure leads to decreasing of volume which explains minus.

Acting forces

In compressible fluids internal and external forces are acting (if related to volume under study).

Inner forces as result of one particles acting on another due to the third Newton law will cause equal response and will not be considered (for exception to special cases).

External forces are divided to mass and surface forces.

External forces include:

- gravity;
- momentum;
- dissipative, magnet and electrical forces.

Surface force is a force which acts on the surface of volume under study. They include:

- superficial tension;
- capillary force;
- friction and normal pressure.

Let’s consider some liquid volume in space.

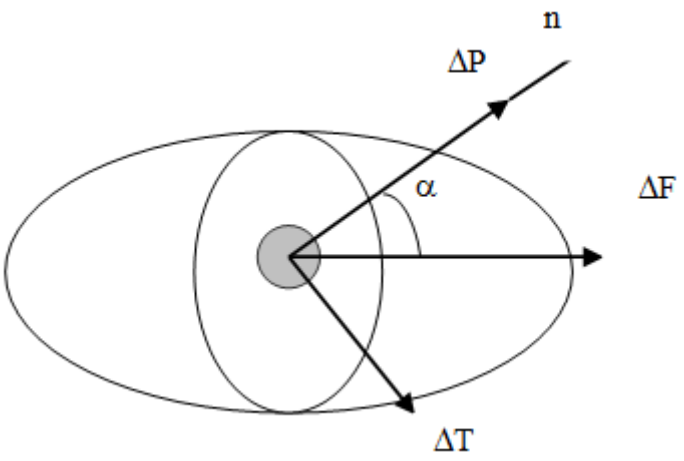

Fig. 2.1. Acting forces.

ΔT is called tangential force of friction force.

ΔP is called stretch or narrowing for or normal pressure force.

Chapter 2. MAIN EQUATIONS FOR THE NON-VISCOUS NON-HEAT-CONDUCTIVE COMPRESSIBLE LIQUID (GAS)

Fluid dynamics is focused on interactions between moving media and channel walls. Compressible liquid movement theory bases on Newton laws for point mass. Equations which describe these interactions are based on continuity, energy and momentum equations for flow tube which parameters can be considered constant in cross-section.

2.1 Continuity equation

In a vector form continuity equation is next:

$$div(\rho w) = -\frac{\partial \rho}{\partial t}.$$

For steady flow:

$$div(\rho w) = 0.$$

In case of 2-D flow with *x* and *y* as variables:

$$\frac{\partial(\rho w_x)}{\partial x} + \frac{\partial(\rho w_y)}{\partial y} = 0.$$

2.2 Eulerian equation of movement

$$\rho \frac{dw}{dt} = \rho g - gradP.$$

For 2-D flow:

$$\rho \frac{dw_x}{dt} = \rho g_x - \frac{\partial P}{dx};$$
$$\rho \frac{dw_y}{dt} = \rho g_y - \frac{\partial P}{dy}.$$

2.3 Condition equations

Common form of this equation is $F(P,\rho) = 0.$ Examples: $P/\rho = const;$ $P/\rho^k = const;$ $P = A - B/\rho$ for elastic media $B > 0,\ dP/d\rho > 0.$

As a rule **perfect gas** is placed under study (not always ideal). Perfect gas has properties:

- internal energy depends only on temperature;
- gas condition can be described as $P = \rho RT.$

Entropy is a state function of the thermodynamic system. Its increment is linked to elemental heat in a reverse process by next relation:

$$dQ = TdS.$$

Perfect gas entropy:

$$S = \frac{gR}{k-1} \ln \frac{P}{\rho k} + const.$$

Any process with S=const is called **isentropic**.

2.4 Energy equation

As an example of mathematical apparatus application, derivation of the energy equation is presented with taking some hydraulics terms into account (flow line, tube of flow).

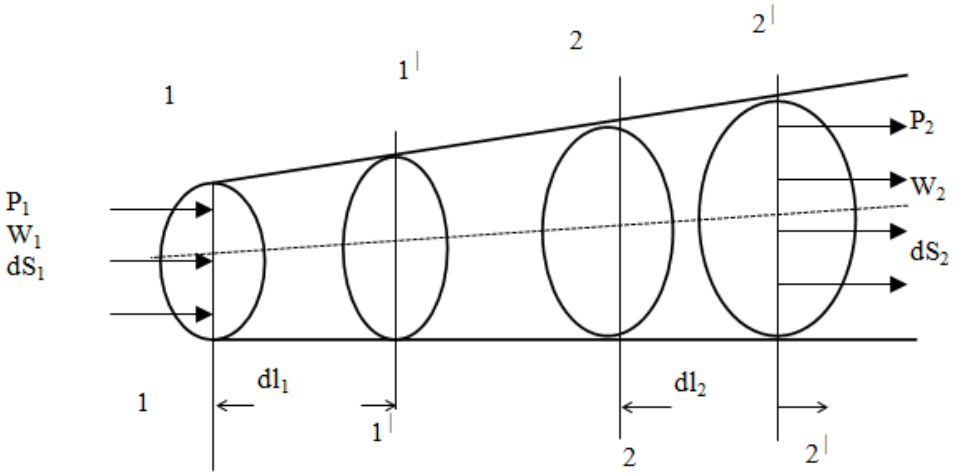

Fig. 2.2 Flow tube

Composition of energy balance.

1. At initial moment t=0 mass of gas $\Delta m = \Delta G / g$ fills volume 1-1…2-2.

2. After Δt sec section 1-1 will move to Δl_1 distance and will be placed into $1'$-$1'$ section.

Kinetic energy in a 1-1 and $1'$-$1'$ sections for Δt:

$$(E_k)_{1-2} = \Delta m_{1-1'} \left(\frac{w^2}{2} \right)_{1-1'} + \Delta m_{1'-2} \left(\frac{w^2}{2} \right)_{1'-2} .$$

$$(E_k)_{1'-2'} = \Delta m_{1'-2} \left(\frac{w^2}{2} \right)_{1'-2} + \Delta m_{2-2'} \left(\frac{w^2}{2} \right)_{2-2'} .$$

Kinetic energy change:

$$\Delta E_k = (E_k)_{1'-2'} - (E_k)_{1-2} = \Delta m_{2-2'} \left(\frac{w^2}{2} \right)_{2-2'} + \Delta m_{1-1'} \left(\frac{w^2}{2} \right)_{1-1'} .$$

If flow tube property $\Delta m_{2-2'} + \Delta m_{1-1'} = \Delta m$ is taken into account, change of the kinetic energy will take next form:

$\left(\frac{w^2}{2}\right)_{2-2'} = \frac{w_2^2}{2}$ and $\left(\frac{w^2}{2}\right)_{1-1'} = \frac{w_1^2}{2}$ because (1-1/…2-2/) volume is infinitely small. So

$$\Delta E_k = \Delta m \frac{w_2^2 - w_1^2}{2}.$$

Potential energy:

$$\Delta E_n = \Delta G\left(z_2 - z_1\right).$$

Pressure work:

$$\Delta E_p = P_2 dS_2 dl_2 - P_1 dS_1 dl_1 = P_2 w_2 dS_2 dt - P_1 w_1 dS_1 dt.$$

Change of the internal energy:

$$\Delta E_T = \left(U_2 - U_1\right)\frac{1}{A}\Delta G = \frac{\Delta G}{A} C_v \left(T_2 - T_1\right)$$

Added and removed heat:

$$\pm \frac{dQ_{1-2}}{A} \pm dL - L_{fr}.$$

In such case

$$\pm dQ_{1-2} \pm dL - L_{fr} = \frac{\Delta G}{q}\left(\frac{w_2^2 - w_1^2}{2}\right) + \left[P_2 w_2 dS_2 dt - P_1 w_1 dS_1 dt\right] + \Delta G C_v \left(T_2 - T_1\right) + \Delta G\left(z_2 - z_1\right).$$

By taking into account that $\frac{dG}{\gamma} = dV = wdSdt$ expression will take the next form:

$$\pm dQ_{1-2} \pm dL - L_{fr} = \frac{\Delta G}{q}\left(\frac{w_2^2 - w_1^2}{2}\right) + dG\left(\frac{P_2}{\gamma_2} - \frac{P_1}{\gamma_1}\right) + \Delta G C_v \left(T_2 - T_1\right) + \Delta G\left(z_2 - z_1\right).$$

If this equation is related to 1 kg of gas ($dq/\Delta G=Q$, $dL/\Delta G=L$, $dL_{fr}/\Delta G=L_{fr}$), energy equation will have its final form:

$$\pm Q_{1-2} \pm L - L_{fr} = \frac{w_2^2 - w_1^2}{2g} + \left(\frac{P_2}{\gamma_2} - \frac{P_1}{\gamma_1} \right) + C_v \left(T_2 - T_1 \right) + \left(z_2 - z_1 \right).$$

If we specify $C_v T + APV$ as I (enthalpy) and $Q_{out} + L_{fr}$ as Q (added and removed heat where friction acts like a source of internal heat), energy equation will take next form:

$$\pm Q \pm L = \frac{w_2^2 - w_1^2}{2g} + i_2 - i_1 + \left(z_2 - z_1 \right).$$

Example. Special cases:

1. Flow in thermal insulated channel (Q=0, L=0). Energy equation will take next form:

$$0 = \frac{w_2^2 - w_1^2}{2g} + i_2 - i_1,$$

which means that, if w_1=0, $w_2 = \sqrt{2g\Delta i}$.

2. Energy adding during compressor work (Q=0, L=L_c):

$$i_1 + \frac{w_1^2}{2g} + L_c = i_2 + \frac{w_2^2}{2g}.$$

3. Energy removing during turbine work (Q=0, -L=L_t)

$$i_1 + \frac{w_1^2}{2g} - L_t = i_2 + \frac{w_2^2}{2g}.$$

2.5 Mechanical form of energy equation (Bernoulli's principle)

Mechanical form of the above derived energy equation for 1 kg of the incompressible fluid is:

$$-L = \frac{w_2^2 - w_1^2}{2g} + \left(z_2 - z_1 \right) + \frac{P_2 - P_1}{\gamma} + L_{fr}.$$

This equation is called common Bernoulli's equation for fluids.

Gas dynamic uses simplified form of this equation without mechanical work and friction (L=L_{fr}=0), and potential energy is not changing (z_2=z_1):

$$\frac{w_2^2 - w_1^2}{2g} + \int_1^2 \frac{P}{\gamma} = 0.$$

In the ideal adiabatic process without adding or removing heat and friction, entropy is constant so this process can be called isentropic. Bernoulli's equation for fluids will take next form.

$$\frac{k}{k-1} \cdot \frac{P_1}{\gamma_1} \left[\left(\frac{P_2}{P_1} \right)^{\frac{k-1}{k}} - 1 \right] + \frac{w_2^2 - w_1^2}{2g} = 0.$$

2.6 Main differential equation of the gas dynamics

Gas dynamic equations, which describe 2-D irrotational flow of the compressible fluid, are next:

$$\left(1 - \frac{u^2}{a^2}\right)\frac{\partial u}{\partial x} - \frac{uv}{a^2}\left(\frac{\partial v}{\partial x} + \frac{\partial u}{\partial y}\right) + \left(1 - \frac{v^2}{a^2}\right)\frac{\partial v}{\partial y} = 0.$$

$$\frac{\partial v}{dx} - \frac{\partial u}{dy} = 0.$$

Let's introduce velocity potential: $\partial\varphi / dx = u,\ \partial\varphi / dy = v.$

Then we get main differential equation of the gas dynamics:

$$\left(a^2 - u^2\right)\frac{\partial^2 \varphi}{\partial x^2} - \left(2uv\right)\frac{\partial^2 \varphi}{\partial x \partial y} + \frac{\partial^2 \varphi}{\partial y^2} = 0.$$

Nonlinear nature of this equation leads to difficulties of its solving. Hence, on practice method of velocity hodograph is widely used. Transfer to variables from velocity components makes this function linear. Chaplygin equation for current function is important for such a conversation:

$$\frac{\partial^2 \psi}{\partial w^2} + \frac{\left(1 - M^2\right)}{w^2}\frac{\partial^2 \phi}{\partial \Theta^2} + \frac{\left(1 + M^2\right)}{w}\frac{\partial \phi}{\partial w} = 0,$$

where current functions are $\frac{\partial \phi}{\partial n} = \rho w$ and $\frac{\partial \phi}{\partial s} = 0$ and n and s are surface normal and current coordinate, which are determined along flow line correspondingly (natural coordinates).

Chapter 3. ACCEPTED SIMPLIFIED FLOW MODELS

Real gas flow in channels of different plants, devices, rotary machines and especially aircraft engines is complicated because of presence of lift-off areas, turbulence, possible compression shock waves etc. Anyway calculation of such complicated flow does not seem possible even by using most perfect computers and this fact slows down further expansion of compressible liquid flow knowledge. This circumstance leads to necessity of more simplified or idealized flow schemes acceptation, its principal diversities and typical features search.

At present, existing practice shows that in some cases simplified models calculation results adequately correspond with real processes and can be used for quantitative assessment. Most common gas flow models for experimental data engineering analysis are next.

1. **Steady** (all parameters don't change depending on time).

2. **Adiabatically** (heat exchange with environment can be neglected).

3. **Isentropic** (entropy of flow is constant).

4. **1-D** (all parameters are similar in one cross-section and depend only on axial coordinate).

5. **2-D** (flow parameters depend on two coordinates).

6. **Laminar** (particle moving is oriented).

7. **Turbulent** (particle moving is chaotic with parameters pulsation either axial or tangential direction).

8. **3-D**.

1-D flow model has significant application on engineering activity for experimental researches analysis and calculation.

3.1 Weak disturbances. Acoustic waves

If body is placed in gas media, disturbances, which cause pressure changing, are arrived. If body movement is slow and smooth and its shape is curved, these disturbances are nearly absent. Fast moving causes positive pressure that pushes environment layers. They are in turn compressed again, and acoustic (weak) wave is generated i.e. streamlined body creates change or disturbance of every gas media parameter in comparison with non-disturbed approached flow. Hence, mechanism of disturbance creation, which is caused by pressure change, is a basis of acoustic or weak disturbance creation and distribution. Main mechanism of flow formation is an ability of gas to transfer parameters disturbance from place of its origin to another places as spherical disturbance waves.

From the point of view of the molecular-kinetic theory to get acoustic wave, it is necessary for molecules to transmit an impulse from area with high pressure and density to molecules with lower pressure. Sound is generated when dimensions of the pressure change area are much more then distance which molecules passes before impact. In an opposite case molecules will pass from peak to a valley and the wave is instantly equalized.

Speed of sound magnitude calculation is performed by expression which set a connection between pressure change and density:

$$a^2 = \frac{\partial P}{\partial \rho}.$$

Here it is important to know how temperature changes.

Newton was the first who try to calculate the speed of sound by consideration that temperature doesn’t change i.e. he calculated isothermal speed of sound. His calculation doesn’t correspond with experiment.

Laplace made a correct consideration that pressure and temperature are changed adiabatically. Heat flux from confluence region to a region of expansion is neglectfully small, if length is high enough in comparison with molecule free passage length. Neglectful heat leakage will lead to neglectful energy absorption

and will not influence a speed of sound. Heat absorption will be amplified if wave-length will reach free passage distance but such waves lengths are smaller than acoustic waves lengths in a factor of 10^6. Speed of sound is equal to $a = \sqrt{kqRT}$. Numerically, it is approximately one half of the mean molecular velocity. Significant part in aero- and gas dynamics is given to a speed of sound term as weak disturbance distribution velocity.

Sound distribution in gas media is linear wave motion, where disturbances are transmitted with certain velocity (speed of sound) which can varies inside a media. (In incompressible fluids small pressure changes are distributed with infinitely high velocity.)

3.2 Mach number

Generally accepted parameter, which characterizes relation between gas velocity *w* and speed of sound *a*, is called Mach number:

$$M = w / a.$$

Depending on M value, there is next flows classification:

- M<1 – subsonic flow;
- 0,9<M<1,2 – transonic flow;
- M>1 – supersonic flow (M>4 – hypersonic flow).

These types of flows, which are determined by Mach number, are fundamentally differed from each other and described by different kinds of mathematical physics equations (subsonic flows are described by elliptic equations, transonic – by parabolic equations, supersonic – by hyperbolic equations).

Physical sense of Mach number is fluid compressibility criterion. Depending on Mach number value, current flow parameters are determined. If M<0,15 compressibility can be neglected.

For inner channel flows analysis and calculation other than Mach number **velocity coefficient** $\lambda = w / a_{cr}$ has significant application, where a_{cr} – critical speed of sound.

3.3.1-D flow

1-D flow is a kind of flow, which have only one direction (usually axial) of parameters change. Gas flow in the channel with slightly cross-section changing and small curvature of axis can be considered as 1-D flows.

Let's study flow in that channel with taking into account that flow has heat exchange and mass exchange with environment (adding or removing of gas), and geometric form of channel is changed, there is a mechanical work over gas and finally gas is perfect and real. If these parameters are inserted into energy equation from Ch.2, we can get differential equation of velocity change along channel axis:

$$(M^2 - 1)\frac{dw}{w} = \frac{dS}{S} - (k-1)\frac{dQ}{a^2} - \frac{dL}{a^2} - k\frac{dL_{fr}}{a^2} - \frac{dG}{G}.$$

This equation is common expression of the **flow reverse-influence law**.

3.4 Typical special cases of 1-D flows

1. Adiabatically isolated isentropic channel (dQ=0, dL=0, dL_{fr}=0, dG=0). So

$$(M^2 - 1)\frac{dw}{w} = \frac{dS}{S}.$$

From this expression it is clearly that in narrowing channel (confusor, $S_2<S_1$) subsonic flow accelerates and supersonic flow decelerates. In diverged channel (diffuser, $S_2>S_1$) subsonic flow decelerates and supersonic flow accelerates.

For continuous flow acceleration channel must be converged at start and then diverged. Therewith, speed of sound will be reached in minimal section if environment pressure is lesser then critical pressure. This converged-diverged channel is called Laval nozzle.

2. Mechanical nozzle.

In this nozzle dS=0, dL_{fr}=0, dQ=0, dG=0. So

$$\left(M^2-1\right)\frac{dw}{w}=\frac{dL}{a^2}.$$

For transfer from subsonic to supersonic flow it is necessary to change direction of influence on flow (fig. 3.1):

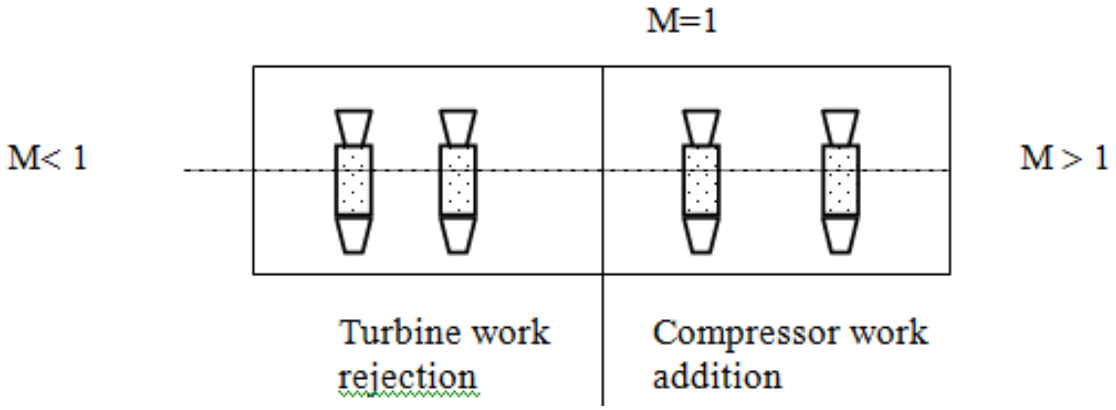

Fig. 3.1 – Mechanical nozzle

if M<1 it is necessary to remove work by turbine;

if M>1 is necessary to add work by compressor.

3. Feed nozzle:

In this nozzle dS=0, dL=0, dQ=0, dG=0. So

$$\left(M^2-1\right)\frac{dw}{w}=-\frac{dL_{fr}}{a^2}.$$

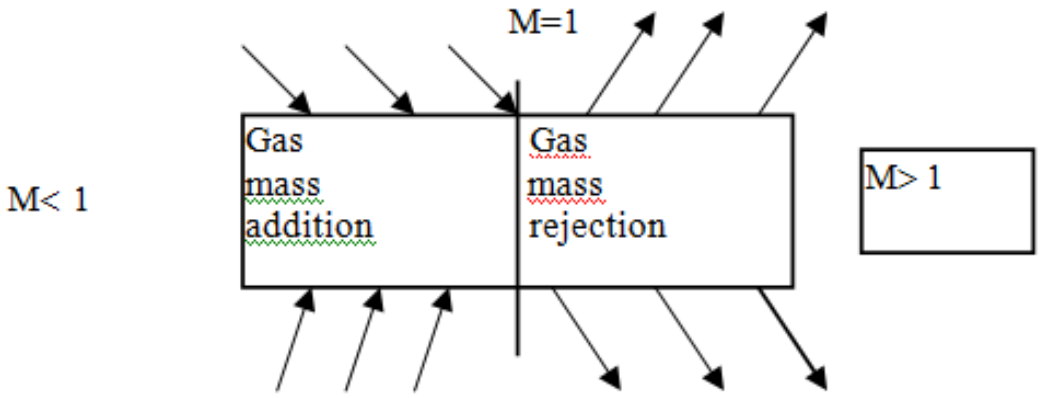

Fig. 3.2 – Flow scheme in the feed nozzle

On practice, except flow acceleration by geometry, combined nozzle is used which has a converged nozzle as subsonic part and feed nozzle as supersonic part. These nozzles found their application in aerodynamic tubes which require uniformity of the supersonic flow at the end.

3.5 Relative parameters of the compressible flows

Energy equation:

$$i^* = i + \frac{w^2}{2}, \qquad (1)$$

where i* – full specific enthalpy of the stagnated flow;

I – specific enthalpy, which characterize potential energy of gas flow.

Equation (1) can be expressed through specific heat:

$$c_p T^* = c_p T + \frac{w^2}{2}. \qquad (2)$$

It is known that

$$\frac{P}{\rho} = RT,\ \frac{P^*}{\rho^*} = RT^*,\ R = C_p - C_v.$$

If (2) is related to $C_p T^*$:

$$1 = \frac{T}{T^*} + \frac{w^2}{2C_p T^*}$$

Then $\frac{T}{T^*} = 1 - \frac{w^2}{2c_p T^*}$.

If $a_{кр}^2 = \frac{2k}{k+1} RT^*$ so

$$\frac{T}{T_*} = 1 - \frac{w^2(k-1)}{2RkT^*}\left[\frac{k+1}{k-1}\right] = 1 - \frac{w^2}{a_{кр}^2}\left(\frac{k-1}{k+1}\right) = 1 - \frac{k-1}{k+1}\lambda^2 = \left[1 + \frac{k-1}{2}M^2\right]^{-1}$$

Correspondingly:

$$\frac{P}{P^*}=\left(\frac{T}{T^*}\right)^{\frac{k}{k-1}}=\left(1-\frac{k-1}{k+1}\lambda^2\right)^{\frac{k}{k-1}}=\left(1+\frac{k-1}{2}M^2\right)^{-\frac{k}{k-1}};$$

$$\frac{\rho}{\rho^*}=\left(\frac{T}{T^*}\right)^{\frac{1}{k-1}}=\left(1-\frac{k-1}{k+1}\lambda^2\right)^{\frac{1}{k-1}}=\left(1+\frac{k-1}{2}M^2\right)^{-\frac{1}{k-1}}.$$

Because of $c_p=R\left(\frac{k}{k-1}\right)$, $i=c_pT$, $a=\sqrt{kRT}$, so

$i=R\left(\frac{k}{k-1}\right)T=a^2\frac{1}{k-1}$ and correspondingly $a^2=(k-1)\,i$.

So $M^2=\frac{w^2}{a^2}=\frac{w^2}{i}\left(\frac{1}{(k-1)}\right)$ i.e. Mach number square is proportional to relation of the flow kinetic energy to its potential energy in this point.

Similar:

Velocity coefficient λ – relation of the flow kinetic energy to its full energy.

Speed of sound a is changing along flow line.

Critical speed of sound a_{cr} is a constant value for adiabatic flow and is a factor of velocity.

3.6 Gas dynamics functions

Gas dynamics calculations and flow research of subsonic and supersonic flow velocities are based on complicated equations of the gas dynamics. So matters of labor intensity decreasing have significant value even nowadays.

Calculation and experimental data analysis of labor intensity decreasing are connected with using of gas dynamics functions which connect main parameters with relative flow velocity (M or λ). Such 1-D non-dimensional functions characterize flow condition in different sections of isentropic flow. Velocity coefficient λ is taken as independent variable. k value is changing from 1,05 to 1,7 and embraces all possible range for the use of industry.

Flow parameters dependence on M and λ:

1. M(λ):

$$M = \sqrt{\frac{2}{k-1}} \frac{\lambda}{\sqrt{1-\frac{k-1}{k+1}\lambda^2}}.$$

2. τ(λ) – relative temperature:

$$\tau(\lambda) = \frac{T}{T^*} = 1 - \frac{k-1}{k+1}\lambda^2.$$

3. ε(λ) – relative density:

$$\varepsilon(\lambda) = \frac{\rho}{\rho^*} = \left(1 - \frac{k-1}{k+1}\lambda^2\right)^{\frac{1}{k-1}}.$$

4. π(λ) – relative pressure:

$$\pi(\lambda) = \frac{P}{P^*} = \left(1 - \frac{k-1}{k+1}\lambda^2\right)^{\frac{k}{k-1}} = \tau(\lambda)\cdot\varepsilon(\lambda).$$

5. q(λ) – relative flow rate:

$$q(\lambda) = \frac{\rho v}{\rho_{кр} v} = \frac{F_{кр}}{F} = \left(\frac{k+1}{2}\right)^{\frac{1}{k-1}} \lambda \left(1 - \frac{k-1}{k+1}\lambda^2\right)^{\frac{1}{k-1}}.$$

6. Function that characterize flow impulse:

$$Z(\lambda) = \frac{J}{J_{кр}} = 2\frac{mv + pF}{ma_{кр} + p_{кр}F_{кр}} = \left(\lambda + \frac{1}{\lambda}\right).$$

Chapter 4. SUPERSONIC FLOW FEATURES. STRONG DISTURBANCES, SHOCKWAVES

Flow of the ideal or real gas is supersonic if Mach number is higher than 1. From the molecular-kinetic theory it is known that kinetic energy of the directed motion is higher than kinetic energy of the molecular motion when the Mach number is higher than $M=(3/k)^{1/2}$ (1,46 for air). However principle differences already start to show itself, when Mach number is equal to 1, when the particle

velocity is equal to weak disturbance distribution velocity (speed of sound) at that point. These principle differences are described by corresponding mathematical physics equations.

In common case, if the flow is supersonic, it has to change its direction in comparison with original one i.e. deflects or rotates to positive or negative angles $\Delta\theta$. If the angle θ is positive there is a flow acceleration ($M_2 > M_1$; $\lambda_2 > \lambda_1$) and in the contrary if the angle θ is negative there is a flow deceleration ($M_2 < M_1$; $\lambda_2 < \lambda_1$).

4.1 Disturbances of the sub- and supersonic flows

Mechanisms of the disturbance distribution in sub- and supersonic flows have its own features. Let's consider examples where point moves uniformly in the space filled by fixed gas (air).

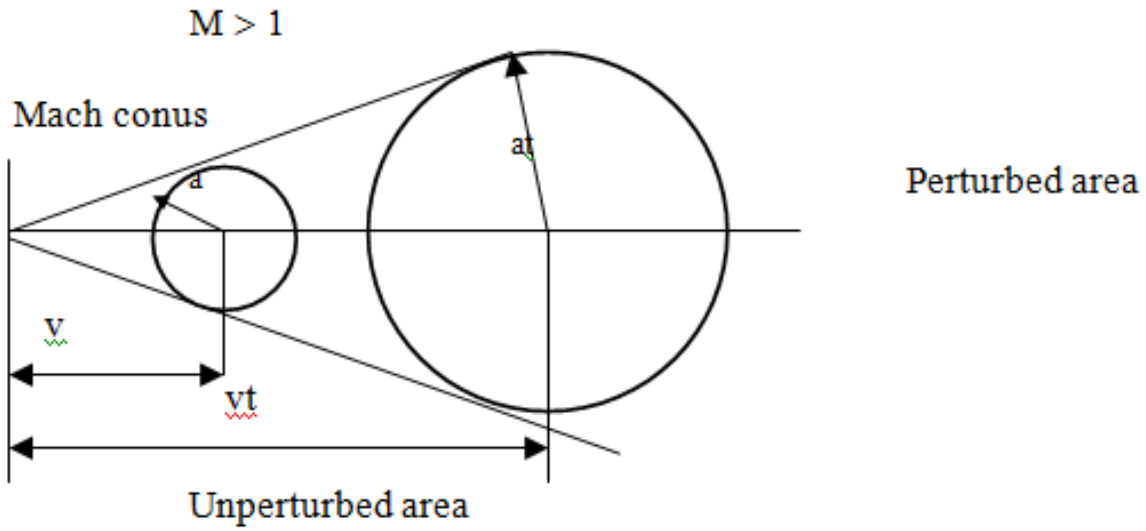

Fig.4.1 Disturbances distribution in the gas media.

Points on the fig 4.1 corresponds to:

1 – fixed media $H=0$, $w=0$;

2 – source of disturbances is moving with velocity $w<a_{cr}$ ($M<1$);

3 – source of disturbances is moving with speed of sound $w=a_{cr}$ ($M=1$);

4 – source of disturbances is moving with speed of sound $w>a_{cr}$ ($M>1$).

If point (source of disturbances) is moving with subsonic velocity, created waves of disturbances are outrunning this point, and it is moving in the flow that was disturbed by the point itself.

If point (source of disturbances) is moving with supersonic velocity, created waves of disturbances and entire disturbance area are placed in Mach cone with opening angle $\alpha = \arcsin(1/M)$.Mach cone is placed beyond disturbance source.

4.2 Simple wave. Prandtl-Meyer flow.

In gas dynamics of the non-vortex isentropic flows, there is class of supersonic flows which called simple wave. (Simple wave of Riemann exists in case of non-steady 1-D sub- and supersonic flows.) In case of the 2-D supersonic flow, simple wave is called Prandtl-Meyer flow.

Let's consider supersonic flow, which bypasses acute angle. In the top of the angle (point A) weak disturbance has arrived which is caused by gas expansion (pressure decreasing) beyond the corner point. In the uniform flow such start disturbance is distributed by Mach straight line (also called characteristics) which makes with a flow velocity direction angle $\alpha_1 = \arcsin(1/M_1)$. Flow turning is over, when the velocity direction corresponds with wall direction after the top of the corner. It should be noted, that flow became uniform by deflection to a $\Delta\theta$ angle and taking the direction of the wall after the top of the corner. In this case, there is finite disturbance with an angle $\alpha_2 = \arcsin(1/M_2)$. Therefore, turning of the uniform supersonic flow i.e. its expansion is carried out as sequence of weak disturbances which have a source in the top of the corner. These disturbances are distributed by the Mach straight lines (characteristics). In such a turning of the supersonic flow near the blunt angle velocity, pressure and density values remain constant along straight characteristics. For analysis it is usable to introduce a concept of the flow expansion angle φ and polar coordinates in the focused simple wave. Expansion angle is equal to:

$$\varphi = \left(\frac{k+1}{k-1}\right)^{1/2} \arcsin\left[\frac{(k-1)\left(\lambda^2-1\right)}{2}\right]^{1/2}.$$

If $\lambda = 1$ so $\varphi = 0.$

In case of discharge to vacuum

$$\varphi = \varphi_{\max} = \left(\frac{k+1}{k-1}\right)^{1/2}\left(\frac{\pi}{2}\right).$$

Dependence of the supersonic flow parameters on angle φ has a next view.

speed of sound $a/a_{cr} - \frac{a}{a_{cr}} = \frac{\cos\varphi}{m}\cdot\left[\frac{k+1}{k-1}\right]^{S}$;

velocity coefficient $\lambda = \frac{w}{a_{cr}} = \left[\frac{k-\cos\left(\frac{2\varphi}{m}\right)}{k-1}\right]^{1/2}$;

pressure $P = P^*\left[\frac{1+\cos\left(\frac{2\varphi}{m}\right)}{k-1}\right]^{\frac{k}{k-1}}$;

density $\rho = \rho^*\left[\frac{1+\cos\left(\frac{2\varphi}{m}\right)}{k-1}\right]^{\frac{1}{k-1}}$,

where P^* and ρ^* are total head parameters of the flow.

Flow line in the Prandtl-Meyer flow is calculated by

$$r = \frac{r_{cr}}{\left(\cos\frac{\varphi}{m}\right)^{m2}},$$

where r_{cr} – is current radius in the critical section of the flow with $\lambda = 1$.

4.3 Shock waves

As it is shown in the chapter 4.1, any increasing of the pressure is distributed in media with finite velocity to all possible directions as pressure waves. Weak pressure waves are moving with speed of sound. However, acoustic pressure and compression are weak in comparison with pressure of the media. Velocity of the media particles itself, which appeared as result of the acoustic wave passing, is also very small in comparison to a speed of sound.

The distinctive feature of the strong pressure wave which appeared as a result of the explosion is that wave front is very narrow (same as molecule's free motion passage) and that's because gas media condition parameters (pressure, density and temperature) are changed discontinuously. Shock waves are the sources of the increased aerodynamic resistance of the moving body because prior to the shock wave the pressure on the body surface is increasing in comparison with the pressure, which appeared without shock wave, and after the shock wave there is a decreased pressure. Resistance, which is caused by shock wave presence, is called wave resistance.

The next flow features are linked to the shock waves. In the ideal compressible fluid resulting force of the pressure is equal to zero (due to D'Alembert's paradox) before shock waves arrival. In the ideal compressible fluid flux energy is wasted in the shock wave to non-adiabatically compression. In real (viscous) liquid energy additionally wasted to a friction work. In total all energy in the shock wave is transferred to heat energy.

Shock wave occurring is linked with supersonic flow deceleration i.e. bypassing of the concave wall or negative angle $\Delta\theta$. Shockwave intensity, i.e. gas parameters changing degree, is increasing with increasing of the $\Delta\theta$ angle.

Riemann justifies the possibility of the discontinuous gas condition parameters changing. Shock wave theory is developed by Rankine and Hugoniot.

4.4 Direct shock wave

Direct shock wave is discontinuity surface which is perpendicular to velocities before and after the shock wave. The gas is perfect (ideal).

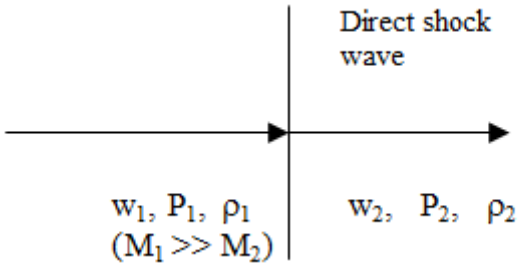

Fig. 4.2 Flow scheme in the straight shock wave.

Three relations (equations of the continuity, momentum and energy) allow deriving equation of the Rankine and Hugoniot adiabatic shock wave for an ideal gas with constant specific heats which connects parameters before and after the shock wave.

$$\frac{P_2-P_1}{\rho_2-\rho_1}=k\frac{P_1+P_2}{\rho_1+\rho_2}=\frac{\Delta P}{\Delta\rho}$$

If ΔP and $\Delta\rho$ are small enough, weak wave is distributed then $\frac{dP}{d\rho}=k\frac{P}{\rho}=a^2$. That means that weak shock wave is distributed with the speed of sound.

Pressure and density changing correspondingly equal to:

$$\frac{P_2}{P_1}=\frac{2kM_1^2}{k+1}-\frac{k-1}{k+1},$$
$$\frac{\rho_1}{\rho_2}=\frac{k-1}{k+1}+\frac{2}{(k+1)M_1^2}.$$

In direct shock wave equalities $w_1w_2=a_{cr}^2$ and $\lambda_1\lambda_2=1$ are correct that means that in the direct shock wave supersonic gas velocity changes to subsonic.

For an ideal gas with binary molecules (k=1,4) it is correct that maximum densities relation is equal to:

$$\frac{\rho_1}{\rho_2} = \frac{k-1}{k+1} = \frac{1}{6}.$$

Corresponding relation for the direct shock wave in case of real (viscous) gas significantly differ from provided relations especially if M>5 and temperature is high, when specific heats are not constant due to molecules oscillatory energy actuation. Thus for perfect gas (k=1,4) densities relation can reach value much more than 6.

4.5 Angle shock wave

More common case of supersonic flow deceleration is angle shock wave. Wave front is oblique to flow direction. In this case only normal component of velocity w_{1n} suffers discontinuity similar to velocity's discontinuity in the straight shock wave. Tangential velocity component w_{1t} remains constant.

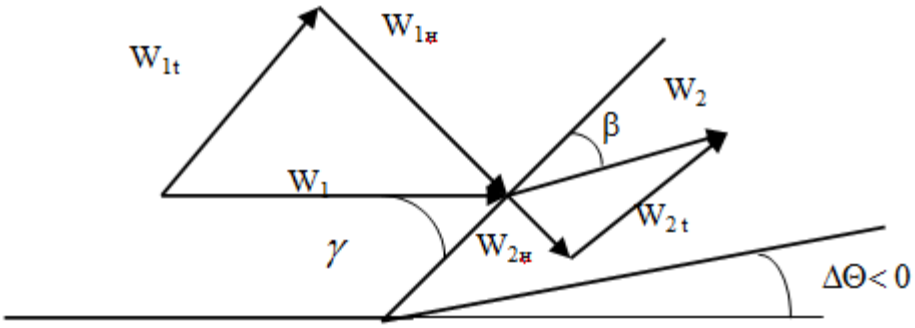

Fig. 4.3 Flow scheme in the angle shock wave.

Pressure, density and temperature changes are determined by relations, which are correct for straight shock wave but only normal components of velocity are used. Prandtl condition is used for calculation:

$$w_{1n}w_{2n} = a_{cr}^2,\ \lambda_{1n}\lambda_{2n} = 1,\ w_{1t} = w_{2t}.$$

Wave velocity after the angle shock is always supersonic i.e. deceleration intensity is less than in the straight shock wave. The kinematic equality $\Delta\Theta = \gamma - \beta$ is correct.

4.6 Detonation wave

Let's consider fundamental principles of the detonation theory. Experiments of flame distribution in tube show that usually slow combustion process in certain circumstances can transform to a fast one (velocity of distribution is more than 2000 m/sec), which is called detonation. Chapman and Jouget, who study detonation, suggest that chemical reaction here happens instantly, i.e. sharp front is created, which travel in unburned gas and transform it to a burned gas. This transfer across the front is similar to transfer from uncompressed gas to a compressed one in the front of the shock wave. The only difference between shock and detonation waves is that chemical properties of the burned gas are differ from the unburned gas and that reaction influences energetic balance, i.e. internal energy of the burned gas is differ from the one of unburned.

So detonation is combustion process, which is caused by shock wave, supported by sharply increasing of the pressure, density, temperature and entropy. Farther pressure and density in combustion process are decreased and temperature and entropy are increased.

Idealized detonation scheme is presented on fig. 4.4. it is supposed that source of the strong disturbance is placed into infinitely long rigid tube without heat transfer across the wall.

One the base of continuity, momentum and energy equations we have:

$$\rho_1 = (W - U)\rho_2;$$
$$W^2\rho_1 + P_1 = (W - U)^2 + P_2;$$
$$E_1 + \frac{W^2}{2} + \frac{P_1}{\rho_1} = E_2 + \frac{(W - U)^2}{2} + \frac{P_2}{\rho_2},$$

where P – pressure,

ρ – density,

E – specific internal energy,

W – velocity of the reaction zone distribution to the explosion zone;

U – velocity changing in the reaction zone.

Thus,

$$W = \frac{1}{\rho_1}\left[\frac{P_2 - P_1}{\frac{1}{\rho_1} - \frac{1}{\rho_2}}\right]^{1/2},$$

$$U = \left[\left(\frac{1}{\rho_1} - \frac{1}{\rho_2}\right)\left(P_2 - P_1\right)\right]^{1/2},$$

$$E_2 - E_1 = \frac{\left[\left(\frac{1}{\rho_1} - \frac{1}{\rho_2}\right)\left(P_2 + P_1\right)\right]}{2}.$$

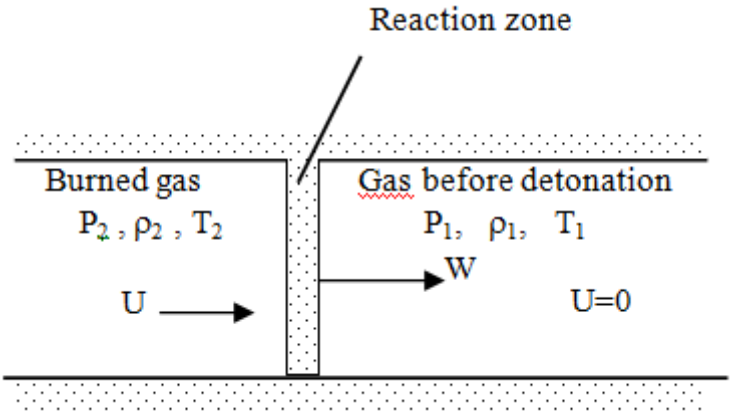

Fig. 4.4 Idealized detonation wave scheme

Internal energy change of the ideal gas can be written as

$$E_2 - E_1 = C_v\left(T_2 - T_1\right) - h,$$

where h – energy which is produced by explosion. Condition energy:

$$P_2 = \rho_2 R_2 T_2.$$

Gas constant R_2 is differ from R_1 because of chemical reaction during explosion.

Calculation task is to determine *W*, *U*, P_2, ρ_2 and T_2 for known value of the heat produced during the explosion and known condition parameters P_1, ρ_1 and T_1. Final term is the Chapman-Jouget condition, which is derived from *P-1/ρ* diagram (fig 4.5).

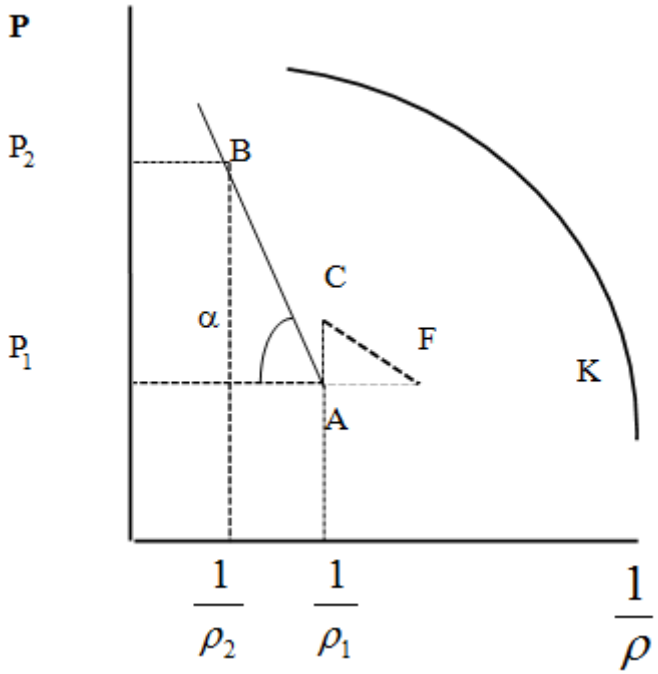

Fig. 4.5 Hugeniot curve for detonation case.

Point *C* is finite state of the combustion with the constant volume ($\rho 1=\rho 2$) and the point *F* is the finite state of the combustion with constant pressure. If finite state lies on the *BC* line we'll have detonation and if the finite state lies on the *FK* line we have normal combustion.

Experimentally validated that detonation velocity is constant for a given gas mixture. It is widely thought that detonation velocity is determined by point *B* which is a point of touch for Hugeniot curve and line which is drawn from the initial state *A*. In this point

$$W_B = U_B + a_2,$$

where a_2 is a speed of sound in the area 2. This condition for *B* is known as Chapman-Jouget condition which is most steady detonation state.

Chapter 5. SOME FEATURES OF THE REAL FLOWS

It is known that viscous and inertial forces make opposite influence on the compressible fluid motion character development. There are laminar and turbulent

flows. Laminar flow is a flow with momentum, energy and mass transfer mechanism is accomplished by microprocesses which have a molecular nature and turbulent flow is related to macroscopic molar transfer processes which are caused by finite mass mixture.

Turbulence is chaotic velocity pulsations which are laid on mean motion and differ from the volumetric non-uniformity of the main flow. Turbulence is isotropic if root mean square value of the pulsation component of the velocity doesn't depend on direction. Turbulence intensity is characterized by the relation of the pulsation velocity component to velocity mean value.

Due to the Landau's hypothesis turbulence is kind of motion which has a viscosity decreasing due to less complicated flow steadiness losses corresponding with the stage-to-stage increasing of the flow complexity. Transfers from one discrete condition to another are discrete. Mathematical description of the transfer from laminar to turbulent flows which is based on the steadiness theory was not succeeded and theories which describes such nonlinear phenomena is not finished. Transfer from the laminar flow to the turbulent and vice versa and the flow breakdown presence are the real flow features.

5.1 Boundary layers

Real flows are linked to conception about boundary layer which is flow area where viscosity influence leads to significant total pressure losses for example as a result of the friction to the channel walls surface. Boundary layer thickness δ is a distance between from the wall to the place where velocity rises up to 99% of the velocity in the middle of the flow. So δ value separates the boundary layer of the flow from the flow core.

Another characteristics of the flow which is decelerated near the wall surface are the displacement thickness δ* and impulse loss thickness δ**.

Wall thickness:

$$\delta^* = \int_{R-\delta}^{R} \left(1 - \frac{\rho w}{\rho_1 w_1}\right) dy,$$

where w – current velocity in the boundary layer,

w_1 – velocity on the boundary layer border,

R – channel section radius,

y – distance from the wall.

Introduction of the wall thickness value allow to substitute real channel by the equivalent with ideal gas flowing inside.

Similar the impulse loss thickness value:

$$\delta^{**} = \int_{R-\delta}^{R} \left(1 - \frac{w}{w_1}\right) \frac{\rho w}{\rho_1 w_1} dy.$$

Chapter 6. MAIN PARAMETERS AND CHARACTERISTICS ASSESSMENT

6.1 Main requirements to the exhaust nozzles (jet nozzles)

Exhaust nozzle of the modern gas turbine engine is complicated and major part of the engine which has a significant Impact to its efficiency. Commonly exhaust nozzle includes intermediate (extensible) tubes for gas input to a jet nozzle, part of direction reverse, noise suppression and design elements

6.3 Jet nozzles main characteristics

Main parameter which is characterized an amount of potential energy transformed to jet kinetic energy in the exit of this nozzle is a available exhaust pressure ratio

$$\pi_c = \frac{P_1^*}{P_н},$$

which is equal to the total pressure at the nozzle P_1* beginning to the environment pressure P_H.

During engine ground operation π_c slightly exceed critical pressure fall $\left[\frac{2}{k+1}\right]^{-\frac{k}{k-1}} = 1{,}86$ with k=1,33 for exhaust gas.

If π_c<5 (Mach number =1,2…1,4) subsonic (convergent) nozzles are usually used. If Mach number is 2,3…3 value of the $\pi_c \approx 20$ that causes to use supersonic nozzle which has exit section area more than critical section area in a factor of 2,5…3.

6.4 Discharge ratio.

During the designing and work analysis of the different plants and apparatus assessment of the nozzle capacity has a significant influence. Real air or gas flow is differ from the real and this difference is very suitable to take into account by using discharge ratio

$$\mu = \frac{G}{G_T}.$$

Theoretical mass flow rate G_T is determined during isentropic 1-D discharge process across the nozzle of the same geometric dimensions with the same available pressure loss by

$$G_T = \left(\frac{2}{k+1}\right)^{\frac{k+1}{2(k+1)}} \sqrt{\frac{kq}{R}} \frac{P_{01} F_{cr} g(\lambda_{cr})}{\sqrt{T_{01}}} = \frac{m P_{01} F_{cr} g(\lambda_{cr})}{\sqrt{T_{01}}}$$

where $m = \left(\frac{2}{k+1}\right)^{\frac{k+1}{2(k+1)}} \sqrt{\frac{kq}{R}}$.

P_{01} and T_{01} are total pressure and temperature;

F_{cr} critical section area;

$g(\lambda_{cr})$ – specific flow density;

k – isentropic exponent;

R – gas constant.

μ value depends on amount of the channel narrowing, nozzle working condition which is determined by $\pi_c = P_{01}/P_H$ (where P_H is a pressure of the

environment), critical section generatrix angle or spherical radius. Real gas flow rate is differ from the theoretical due to velocity fall in the boundary layer and flow non-uniformity in the critical section. There are two regimes of discharge: subcritical which corresponds to a area where μ depends on π_c and supercritical where acoustic line is stabilized μ reaches its maximum value of μ_{**} and doesn't change if π_c is changed.

Chapter 6.4.1. Narrowed nozzle

Narrowed nozzle feature is that it section became critical if $\pi_c > \left[\frac{2}{k+1}\right]^{-\frac{k}{k-1}}$.

(further it is suitable to insert a pressure relation term $\beta = 1/\pi_c$).

For graded nozzles and relatively small flow contraction $n = F_2 / F_1$ (where F_1 is a entrance area and F_2 is an exit area) μ_{**} value is close to 1 and equal to 0,99-0,995. Current value of the μ is determined by boundary layer dimensions at nozzle section and linked to displacement thickness δ* by relation

$$\mu = 1 - \frac{4\delta^*}{D_2}.$$

Second critical pressure relation β** for gas turbine engine combustion gases is 0,47…0,5.

In the conical narrowed nozzles which have most widely use in the different plants and gas turbine engines boundary layer influence on the μ significantly less in comparison to non-uniformity influence which is caused by acoustic line deformation due to its conical shape.

On the basis of the experimental data consolidation μ value can be determined by

$$\mu = \mu^{**}\left(\frac{k+1}{2}\right)^{\frac{1}{k-1}} \zeta \cdot \sqrt[\frac{1}{\lambda}]{\frac{k+1}{k-1}\left(1-\zeta^{\frac{k-1}{k}}\right)} \cdot \frac{1}{g(\lambda)},$$

where $\zeta = \frac{\left[(\beta - \beta^{**}) + (1-\beta)\beta^{*}\right]}{1-\beta^{*}}$, $\beta = \frac{1}{\pi_c}$ and β** is second critical pressure relation $\beta^{**} > \beta^{*} = \left(\frac{2}{k+1}\right)\frac{k}{k-1}$; g($\lambda_{cr}$) is relative flow density in critical section which is determined by $g(\lambda_{cr}) = \left(\frac{k+1}{2}\right)^{\frac{1}{k-1}} \lambda \left(1 - \frac{k-1}{k+1}\lambda^2\right)^{\frac{1}{k-1}}$ or by reference data. If $\beta < \beta^{*}$ g(λ_{cr}) is equal to 1.Second critical pressure relation β** depends on geometric dimensions of the nozzle and gas physical properties and by consolidation of the experimental data can be determined by

$$\alpha = \frac{2}{c} \cdot \left(\frac{k+1}{k-1}\right)^{\frac{1}{2}} \cdot \frac{arctg\left[\frac{2}{k-1} - (\beta^{**})^{\frac{k-1}{k}}\right]}{(\beta^{**})^{\frac{k-1}{k}}} - \frac{arctg\left[\frac{k+1}{(k-1)}\left(1 - (\beta^{**})^{\frac{k-1}{k}}\right)\right]}{(\beta^{**})^{\frac{k-1}{k}}},$$

where c is experimental constant, α is nozzle cone generatrix angle. If that angle is changed from 20º to 60º and contraction n from 1,45 to 4 c value is changed by c = 0,433 + 0,66 n.

Gas physical properties have significant influence on μ and this influence can be taken into account through μ**, β** and k. There is universal dependence between them:

$$\mu^{**} = \mu_{90}^{**} + \left(\mu_0^{**} - \mu_{90}^{**}\right)\left[\frac{\left(\beta^{*} - \beta_{90}^{**}\right)}{0,5 - \beta_{90}^{**}}\right]^{1/k},$$

where μ_{90}^{**} and μ_0^{**} are maximum values of the discharge ratios for conical subsonic nozzle with generatrix angle α = 90 ^{0} and 0 ^{0} (for graded nozzle) correspondingly, β_{90}^{**} is the second critical pressure relation for a nozzle with angle α = 90^0 (for air β_{90}^{**} = 0,04).

μ** dependence on α и β^{**} which is necessary for discharge ratio μ calculation are presented below.

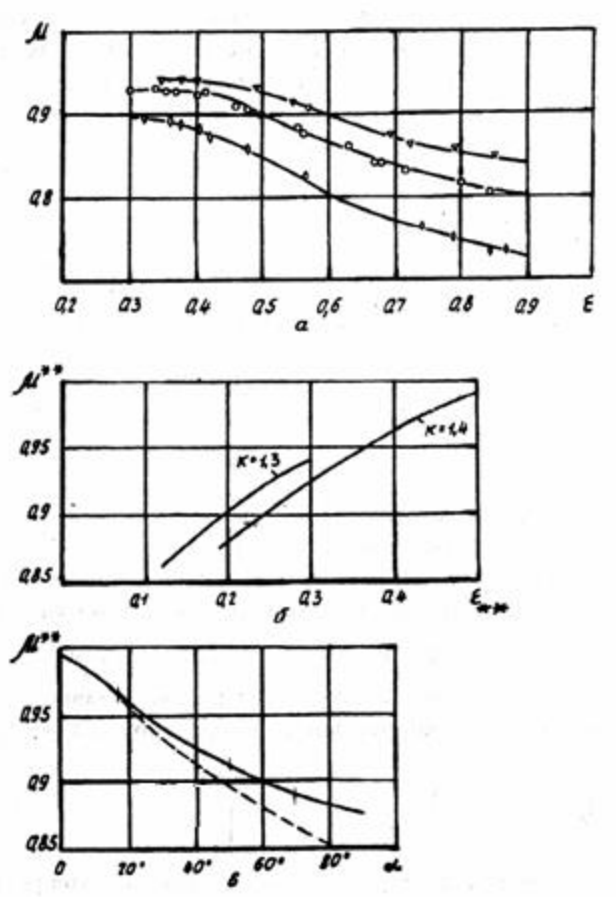

Fig.4.1. Discharge ratio of the contracted conical nozzle:

a) calculation results comparison with experimental results;

b) dependence of the maximum discharge ratio μ** on second critical pressure relation β**;

c) dependence of the maximum discharge ratio μ** on generatrix angle α.

Chapter 6.4.2. Laval nozzle

Laval nozzle is characterized by the fact that exit area of the nozzle is bigger than critical section area ($F_2>F_{cr}$). Experimental data and results of the flow analytical research show that gas flow rate through the Laval nozzle with spherical radius of the minimal section is determined by the shape of the subsonic part and depends weakly on the generatrix angle α. Relation of the spherical radius of the nozzle throat to critical section radius makes significant impact to μ_λ. As well as in the narrowed nozzle there is subcritical $\beta>\beta_{**}$ and supercritical $\varepsilon<\varepsilon_{**}$ discharge

regimes. In case of the supercritical regime maximum value of the Laval nozzle discharge ratio μ_λ** is congruent to the μ** value of the narrowed nozzle which has geometric dimensions similar to the subsonic part of the Laval nozzle.

μ_λ of the conical Laval nozzle is determined by expression from the chapter 6.4.1 where ζ variable is determined from the relation

$$\zeta = (\beta - \beta_{**}) + \beta_*,$$

where β_{**} is the second critical pressure relation after that in the critical section of the Laval nozzle flow stabilization comes. During the calculation of the μ_λ value as well as in the case of the narrowed nozzle gas dynamic function g (λ) is equal to 1 if $\beta<\beta_*$ but as opposed to Laval nozzle value $\beta_{**} > \beta_* = \left[\frac{2}{k+1}\right]^{\frac{k}{k-1}}$.

6.5 Thrust coefficient

Expansion process perfection is determined by the nozzle thrust coefficient $R = R/R_{id}$, where

$$R_{id} = k\left(\frac{2}{k+1}\right)^{\frac{k}{k-1}} F_{cr}\ \mu\ P_1^*\ q(\lambda_{cr})\sqrt{\frac{k+1}{k-1}\left(1-\left(\frac{1}{\pi_c}\right)^{\frac{k-1}{k}}\right)}.$$

Thrust coefficient is a relation of the real thrust to an ideal nozzle thrust during the real gas mass expansion in it without losses to the pressure of the environment P_H. Specific nozzle thrust losses are equal to $\Delta R = 1 - \bar{R}$. Real thrust is differ from the ideal by presence of the viscous friction, probability of the shock waves inside the nozzle, non-uniformity and angular displacement of the velocity in the exit area section and also losses due to operation on off-design regime (flow overexpansion or underexpansion).

Typical characteristics of the different nozzle schemes ($R = f(\pi_c)$ dependencies) are presented on fig. 6.2. For narrowing nozzle (curve 1) thrust

coefficient slightly depends on generatrix angle to an axis α within the range from 0^o to 40^o and amount of the channel narrowing n. Maximum value of the R is reached when π_c is low. During the π_c increasing (starting from the $\pi_c \geq 2{,}5$) R value drops due to the flow underexpansion losses.

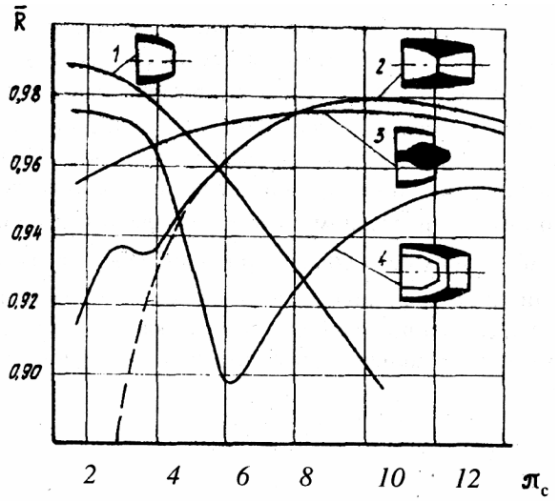

Fig.6.2. Thrust coefficient R of the different types
of the gas turbine engine nozzles

For Laval nozzle (curve 2) R value has its maximum on design regime. When π_c is low Laval nozzle thrust coefficient is significantly lower than thrust coefficient of the narrowing nozzle due to flow overexpansion in it. $R = f(\pi_c)$ dependency is non-monotonic due to the changing of force which acts on supersonic part during the flow separation from the wall ($R = f(\pi_c)$ changing for non-separated flow is shown on fig. 6.2 by dashed line). R increasing during the flow separation results from atmospheric pressure penetration to the separation zone from the nozzle section side and losses from the overexpansion are smaller I comparison to a case with non-separated flow. After the flat maximum on regimes which are close to a design regime R is decreased again due to underexpansion.

Nozzle with central body (curve 3) unites the well characteristic of the narrowing nozzle if π_c is low (due to impossibility of the high flow overexpansion) and Laval nozzle when π_c reaches design regime.

Also characteristics of ejector nozzle which has a circuit breakdown near the critical section are presented here (curve 4). If the dimensions of the ejector are optimal and π_c is low during discharge regime with flow separation when the jet doesn't touches walls of the supersonic part pressure of the jet is close to PH and its characteristics reach characteristic of the narrowing nozzle. However on starting regimes when the jet starts to adhere to walls of the supersonic part with heavy flow overexpansion nozzle characteristics significantly decrease. If π_c is close to a design regime R value has flat maximum. However, if the section areas are equal R value of the Laval nozzle is higher because of the free flow jet presence near the critical section and afterward joining of the free jet with a resulting shock wave.

6.6 Effective thrust coefficient

Thrust of the aircraft engine nozzle, where not only inner characteristics but also bypassing of the outer surfaces, outside flow interaction with the jet of exhausted gas, base drag etc. are taken into account, is estimated by nozzle effective thrust coefficient and correspondingly thrust effectiveness losses

$$\bar{R}_{ef} = \frac{R_{ef}}{R_{id}} = \frac{R - X}{R_{id}}, \quad \Delta\bar{R}_{ef} = 1 - \bar{R}_{ef}.$$

where R_{ef} – effective nozzle thrust (with taking outside resistance X into account); R_{id} – ideal thrust.

Resistance of the tail part X consists of friction resistance and pressure resistance. Outside resistance depends on bypasses shapes and the relation of the outside nozzle cross-section area F_n to master cross-section area F_{mid}. The more smooth bypasses of the nozzle outside surface, the less pressure resistance. Outer resistance values is calculated by known coefficient of the outside resistance c_x ($X = c_x \frac{\rho \varpi_n^2}{2} F_{mid} = c_x \frac{k}{2} M_n^2 P_н F_{mid}$) or by real pressure distribution. If the flight speed is subsonic or transonic analytical determination of the pressure on the outside nozzle surface is quite complicated and not reliable so experimental data

consolidation on the c_x values is used. Thrust losses dependency on the Mп number for Laval nozzle and ejector nozzle is presented on fig. 6.3. The largest effective thrust losses of any type of the nozzles take place in the transonic flight velocities, because in this case appearing of the supersonic areas is possible, which is followed by resistance increasing.

Also the static pressure changing along the outer surface of the Laval nozzle with optimal geometry and ejector nozzle is presented during their flowing with the velocity value $M_f \approx 0.8$. It is seen that in the case of the Laval nozzle the level of rarefaction is lesser and pressure recovery to a section is bigger. It is a result of the underexpansion flow interaction with an external flow. In the ejector nozzle which is operating on the separated state (fig. 6.3), this effect is less pronounced which results in increasing of the effective losses.

It should be noted, that gas flow, which is ejected from the nozzle, influences on the pressure distribution along the tail part. Because of that imitation of the inner gas jet has a great importance during the c_x determination.

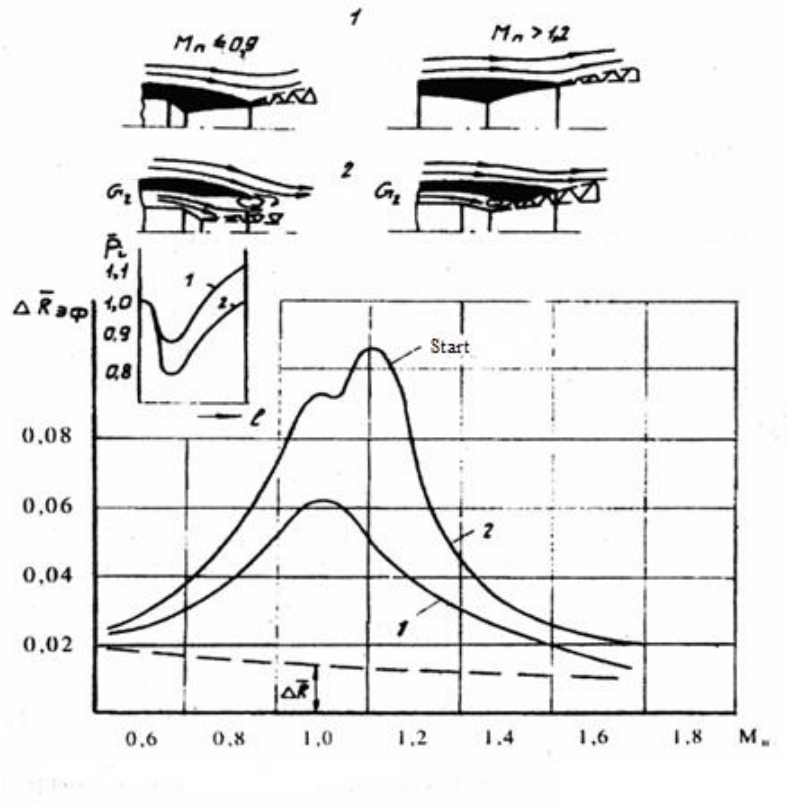

Fig. 6.3. Effective thrust losses comparison of the different types of the GTE nozzles

6.7 Another types if the nozzle perfection estimation

In the engineering calculations estimation of the losses is performed by relative decrement of the nozzle discharge by introducing the velocity coefficient

$$\varphi_c = \frac{w_2}{w_{2id}},$$

which is equal to real axial velocity relation to the velocity of the perfect expansion to geometric area on the nozzle outlet area. On the design condition $\overline{R} = \varphi_c$, and on the other regimes it is fair that $\varphi_c > \overline{R}$.

For estimation of the inner thrust losses and for flow character determination (separated or self-pressuring) as it will be showed below it is possible to use impulse coefficient (relative impulse) which is calculated by

$$\overline{I} = \frac{I}{I_p},$$

where $I = R + p_H F_2$ is real nozzle impulse; I_p is calculated ideal impulse which is determined by real flow rate and expansion without loss to a geometric exit area.

Engine thrust P_{eng}, which is determined as difference of the outlet and inlet thrusts, is always less or equal to nozzle thrust in bench ground condition and on start. Relation $K_c = R / P$ is called losses amplification factor which value depends on airplane velocity and engine operating condition. K_c value characterizes degree of the nozzle perfection influence on the engine thrust and effectiveness and for modern engine it is varies from 1 to 3,5.

6.8 Working regimes

For nozzle designing and parameters and characteristics calculation it is necessary to obtain the data about flight conditions and engine operation regimes in these conditions. In this case flight path (flight profile) can be separated into several individual parts (profile of the flight to maximum distance is considered).

The main parts are flying-off and raising the height, acceleration to a cruiser speed and the part of the flight with that speed (it is usually the longest part of the flight), gliding flight and landing. Correspondingly with these considerations main engine regimes are appointed and required engine thrust, engine effectiveness and regimes duration are determined. The mentioned regimes are described below.

1. Flying-off corresponds to a maximum thrust i.e. maximum frequency of the engine rotor rotation and for engine with afterburning it will be corresponded to maximum afterburning. For modern engines the value of the maximum available pressure ratio π_c on this regime is equal to 1,9 to 2,5.

In the ground bench conditions parameters and effectiveness of the engines with afterburner are controlled on the maximum regime without afterburning for predictions of the characteristics in high heights conditions.

2. Regimes of the acceleration to a cruiser speed correspond to condition of the gaining maximum thrust on the height. For the supersonic airplanes parameters of the transfer through the speed of sonic are additionally controlled. Operation regime is maximal with afterburning, π_c varies from 3,5 to 5. In case of the engine without afterburning for a planes with Мп=0,75…0,85 parameters of the maximal thrust regime are controlled (π_c=2,6…3,2).

Cruiser flight conditions. For subsonic airplane engines in these conditions operation regime thrust is less than maximal and usually corresponds to minimal fuel consumption rate. For engine of the airplane with Мп from 1,7 to 3 π_c varies from 7 to 20 and for maximal nozzle effectiveness maximal outlet section area is necessary and it is restricted by engine micelle dimensions.

7. Gliding and landing correspond to a decreased frequency of the engine rotor rotation, small thrust and low π_c. But in these conditions too gaining of satisfied nozzle thrust losses is required.

From the analysis of the mentioned before condition it can be seen that engine nozzle must provide high efficiency and working capacity in the wide range of π_c, gas temperature and, consequently, dimensions of the critical and outlet

sections. Typical flight profile, changing of the π_c and calculated outlet section area from the Mach number are presented on fig. 6.4.

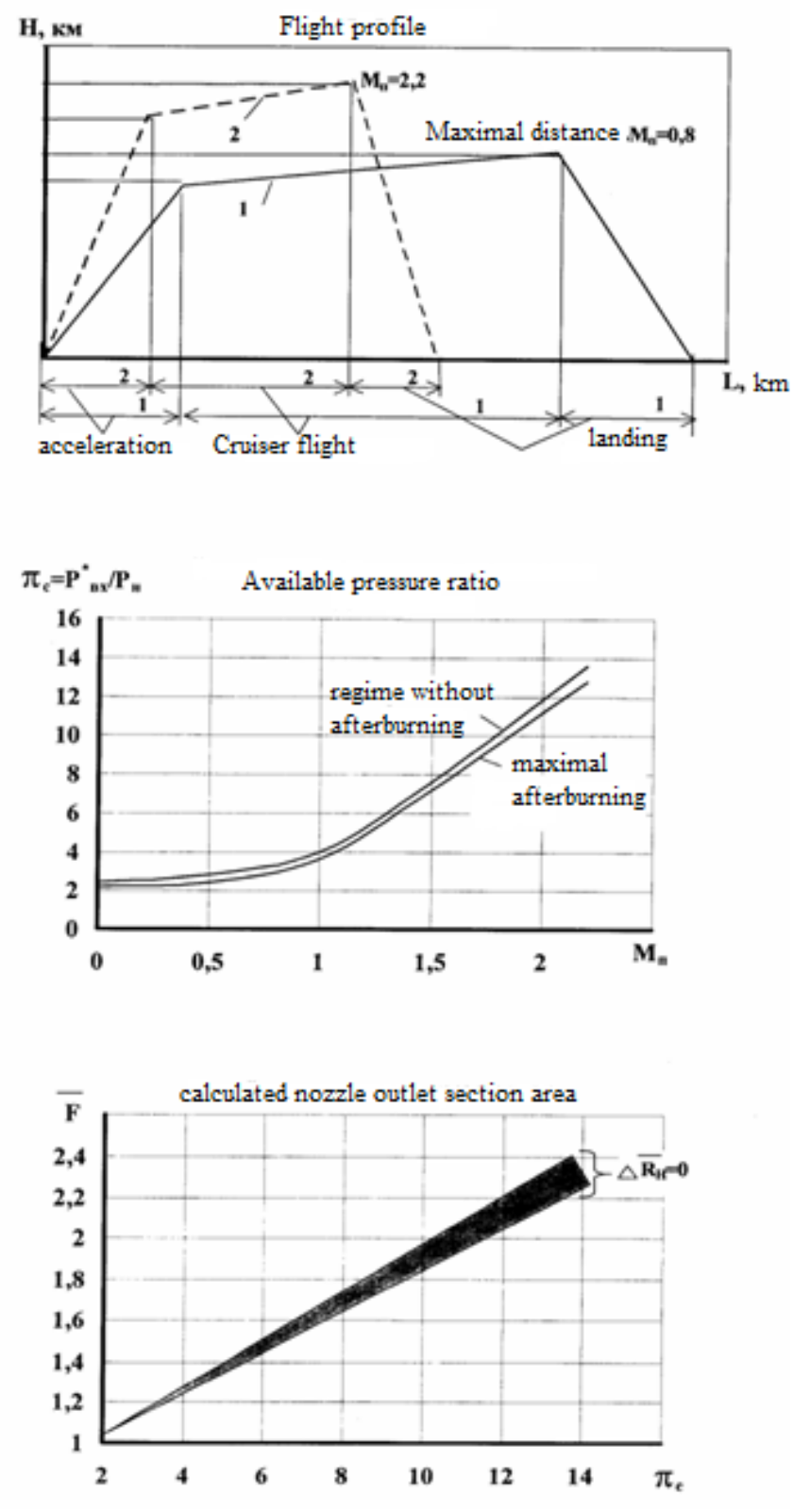

Fig. 6.4. Flight profile and nozzle parameters changing (π_c, F)

6.9 Shape features of the Laval nozzle

Analysis of the perspective engine developments for the airplanes with relatively high supersonic flight cruiser speeds (Mп>2) shows that farther nozzle development is followed by sophistication of their design scheme and converging of the nozzle air circuit to a theoretical. Innovation is transfer to a nozzle with continuous circuit in supersonic part with self-pressuring flow regime which is corresponding with a current trend of using afterburning turbofan engine instead of afterburning turbojet engine.

Unlike to traditional Laval nozzle of liquid propellant engine fully-variable nozzle of gas turbine engine which is presented in fig 6.5 and fig 6.6 is characterized by the following features of geometric shape:

- spherical radius of the inlet part in the junction of the afterburning chamber shell to a flap-type subsonic part is absent;
- geometry of the subsonic part is changing (changing of the α angle varies from 3^o on the regimes of maximal afterburning to a 40^o on regimes without afterburning);
- as a rule spherical radius of the minimal section can be neglected;
- geometry of the supersonic part is changing (changing of the Θ angle varies from 30^o to 2^o for subsonic and transonic speeds and from 9^o to a 12^o for supersonic flight speeds).

The results of the investigation of the Laval nozzles with that shape allow establishing some feature of the flow behavior.

One of the possible design schemes of the regulated Laval nozzle for three regimes of engine operation is presented on fig. 6.5.

These regimes are:

- Regime without afterburning (closed position);
- cruiser regime with afterburning (middle position);
- maximal open position (maximal afterburning).

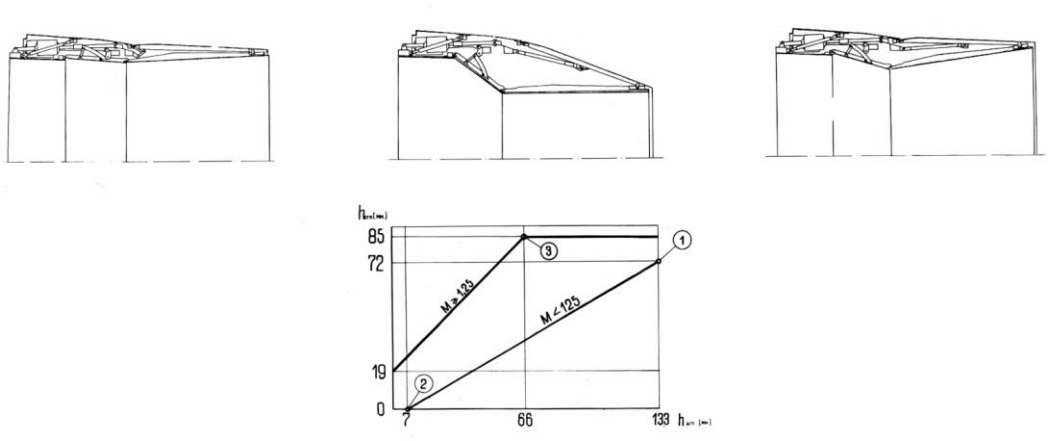

Fig. 6.5. Design of the regulated Laval nozzle of the aircraft gas turbine engine: 1 – maximal afterburning; 2 – regime without afterburning; 3 – cruiser afterburning; 4 – nozzle regulation program

6.10 Stream pattern in the Laval nozzle

Corresponding scheme and typical curve of relative pressure ($\overline{P}_i = P_i / P_i^*$) which is measured along the walls of the Laval nozzle in projection to the axis are presented on fig. 6.6. Dimensions of the presented nozzle (large angles α and Θ and small $\overline{F}_2$) are typical for operation with small π_c, in starting condition, flying-off and cruiser subsonic flight during engine operation without afterburning. However, with the increasing of the $\overline{F}_2$ and decreasing of the α and Θ many other flow features which was described before take place.

Relative pressure distribution which was calculated by 1-d flow theory is presented on the fig. 6.6 by dashed curve for comparison. Pressure distributions are presented for special nozzle regimes which are marked by corresponding values of the π_c with asterix.

Acoustic zone π_{c*} occurs if the low subsonic pressure falls take place. If $\pi_c > \pi_{c*}$ the flow is subsonic in every point similar to the flow in Venturi tube. When π_c exceed π_{c*} sudden pressure fall appears. Pressure fall value continuously decreasing with increasing of the π_c. If angles α high enough and π_c low enough flow separation near the critical section became possible. After that jet flow appears (flow scheme presented on fig. 6.6). And finally if $\pi_c = \pi_{c*}$ relation

pressure reaches its minimal value of 0.2. In this case formation of the acoustic line if fully finished, air flow rate reaches its maximal value and discharge ratio does not depend on π_c.

Thus, if $\pi_c > \pi_{c*}$ in the area of the minimal nozzle section near the walls flow is supersonic, i. e. acoustic line moves towards flow. It seems to be connected with appearing of the high negative pressure gradient in the angle point neighborhood. Appearing area of decreased pressure is distributed trough the boundary layer up to the flow which causes local flow acceleration to supersonic speed in the area near the wall in subsonic part.

Shadow photo and flow visualization show that after the angle point "hanged' angle shock wave caused by circuit break appears. Shock wave intensity is increasing with increasing of the total break angle of the circuit $\alpha+\Theta$. Positive pressure gradient created by the shock wave determine flow separation threat. if the total break angle is small ($<5^o$) remarkable separation area is not observed. However if $\alpha+\Theta>26^o$ separation area is clearly seen.

It is specified that during circuit break increasing two mechanisms of the flow separation take place. If the circuit break is small separation starts not from the angle point but from the point somewhere downstream in supersonic and this separation is caused by interaction of the hanged shock wave with boundary layer. If the circuit break angle is high flow separation starts immediately after the angle point after which it accelerates in expansion fan and then joins the walls of the supersonic part. Angle shock waves system takes place in the point of the reattachment after the separation area. Interaction of this shock wave with direct shock wave in the nozzle section area on the overexpansion regimes leads to its curvature i.e. causes additional flow non-uniformity.

It is also specified pressure distribution along generatrix fall and the depth of the fall are connected with flow separation. If $\pi_c = \pi_{c**}$ self – pressuring flow regime occurs. In this case shock wave structure stabilizes after minimal section, separation and farther flow joining to the walls area fully forms. Starting from π_{c***} relative pressure which is measured on the walls after the joining point become

independent from π_c. Relative pressure distribution along the walls is greatly correlates with 1-d flow theory calculation.

Special investigation of the working fluid influence on the stream pattern makes clear that changing of the isentropic coefficient k does not cause any significant differences in the separated flow structure. However, if k decreases separation area dimensions and intensity of the joining shock wave increase.

The results of the stream pattern in the conical Laval nozzle investigations consolidation and static pressure falls areas after the angle point during flow separation and the lengths of the separation area are presented on fig. 6.6 and 6.7.

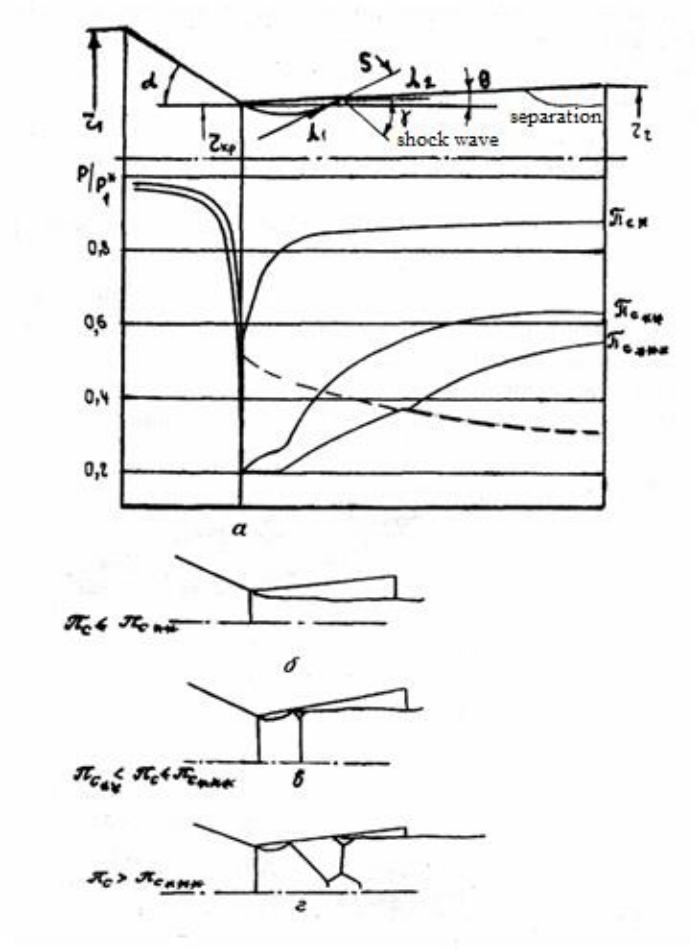

Fig. 6.6. Stream pattern in the conical Laval nozzle:

a – dimensions, flow scheme and change of the relative pressure $\overline{P}_i = P_i / P_i^*$ during different flow regimes vs π_c; b – flow separation from the angle point; c – flow structure stabilization in the critical section; d – angle shock wave interaction with direct shock wave interaction in the nozzle section area during flow overexpansion.

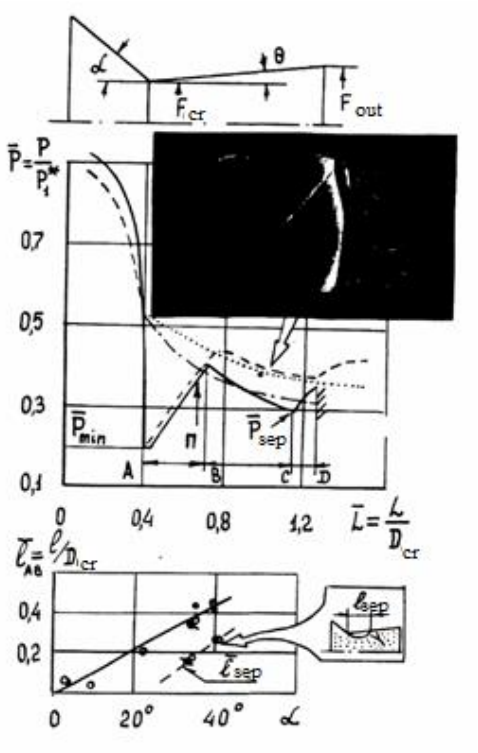

Fig. 6.7. Separation area after the angle point:

• – flat; o, ↵ – axis-symmetric Laval nozzles

6.11 Determination of the separation after the angle point conditions

Stream pattern with flow separation in the critical section obtained by V. F. Novikov in Central Institute of Aerohydrodynamics by flow in the conical axis-symmetric Laval nozzle visualization is presented on fig. 6.8.

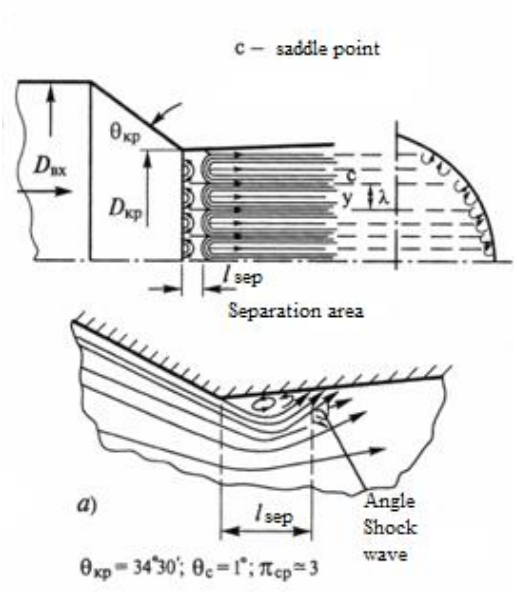

Fig. 6.8. Flow visualization with flow separation

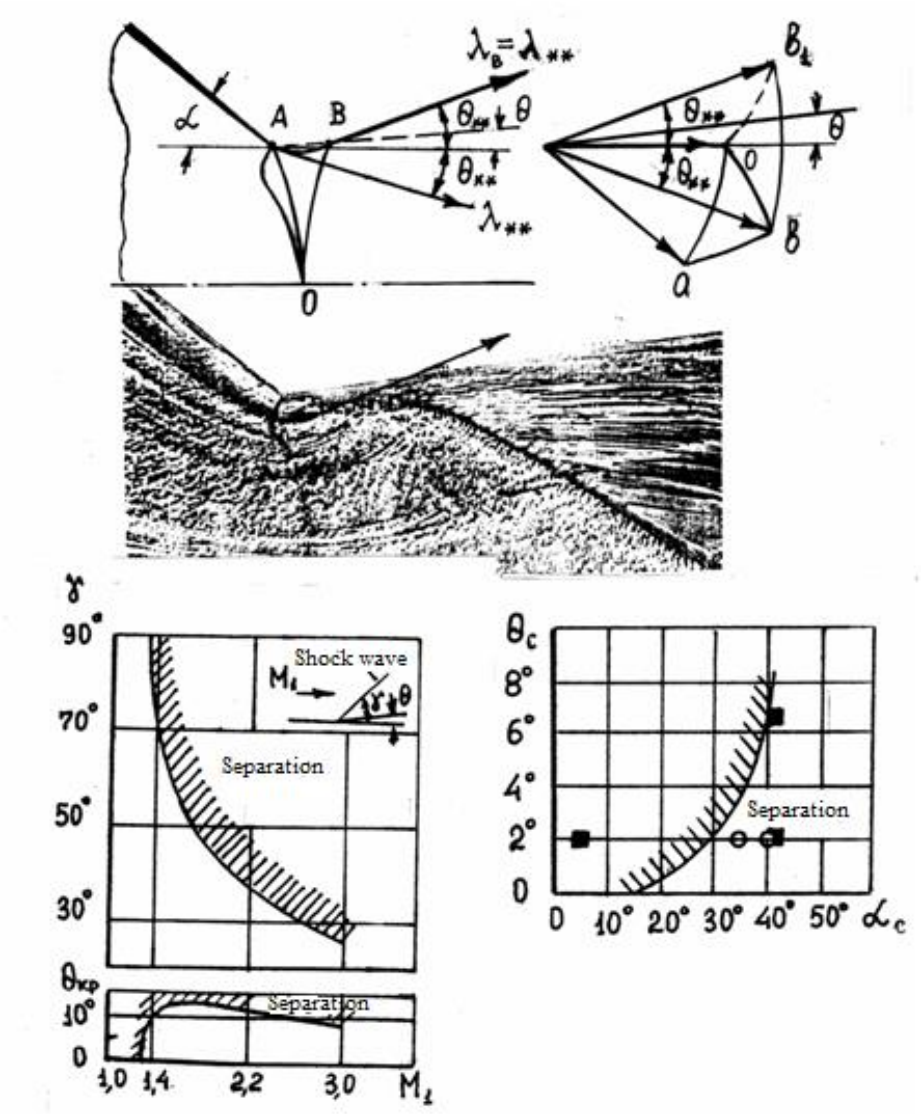

Fig. 6.9. Non-design discharge regimes from the Laval nozzle

Let’s consider stream pattern of the ideal gas in flow plane and velocity hodograph (presented of fig. 6.8) for determination of the flow separation after the angle point in the conical Laval nozzle.

On the acoustic line π_{c**} stabilization regime gas flow rate become maximal and expansion and pressurizing of the flow area which is placed between acoustic line and limiting characteristic AO does not reach free flow boundary. Than the velocity on the boundary of the discharging flow in the A point is determined by radius-vector value in the junction of the epicycloids which start in the point O and A of the hodograph and its angle equal to $\theta_{**} = \alpha/2$ to the nozzle axis.

In the area between the limiting characteristics AO and OA1 U turn of the stream lines with constant velocity along them takes place. On the boundary of the flow velocity coefficient $\lambda_в$ is equal to λ^{**} which is calculated by angle value of $\Theta^{**} = \alpha / 2$ in Prantl-Meyer expansion flow. The direction of the stream line in B1 point after the U turn is determined by radius-vector which circumscribes epicycloid OB arc which is mirror image of the OB arc. In this case velocity inclination angle is equal to Θ^{**} and directed up from the nozzle axis.

If we consider that described narrowing nozzle (fig.) has supersonic part nozzle with an angle $\Theta < \Theta_{**}$, so we will have an example of the flow deceleration after the angle point. Information of the critical wall inclination angle which causes turbulent flow separation is presented on fig. vs M_1 number of incoming flow. It is obvious that separation after the angle point condition is an inequation $\Theta_{**} - \Theta = \alpha/2 - \Theta > \Theta_{кр}$.

On this inequation basis on fig. separation condition after the angle point in the Laval nozzle with circuit break is presented as a curve which is reflective of minimal limit angle of the supersonic part Θ dependency on subsonic part inclination angle α.

6.12 Overexpansion and flow separation

When the pressure in the wall is less than some critical value during Laval nozzle operation on overexpansion non-design regimes separation of the flow from the walls takes place (fig. 6.7, 6.8 and 6.9). In the flow without separation boundary layer still hold pressure increasing in the angle shock wave after the nozzle outlet section. Theoretically, such a discharge regime can be considered in non-viscous flow up to angle shock wave transfer to a direct shock wave.

In the flow (Fig. 6.9) flow separation inside the nozzle is followed by creation of system of angle shock waves which are became direct shock waves on the axis with creation of the subsonic flow areas.

Flow regime of the boundary layer significantly impact on the area of shock wave interaction with boundary layer. Turbulent boundary layer maintain significant resistance to a separation and more intensive pressure increasing takes place after the separation point.

Universal pressure dependency $P_{sep} = P_{sep} / P_н$ in the separation point on $\bar{\pi}_c = \pi_c / \pi_{c\,p}$ and boundary layer condition, where $\pi_{c\,p}$ is calculated expansion ratio which is calculated from

$$\left(\frac{1}{\pi_{c\,p}}\right)^{\frac{1}{k}}\left[1-\left(\frac{1}{\pi_{c\,p}}\right)^{\frac{k-1}{k}}\right]^{\frac{1}{2}}=\left(\frac{k-1}{2}\right)^{\frac{1}{2}}\left(\frac{2}{k+1}\right)^{\frac{k+1}{2(k-1)}}\frac{\mu F_{cr}}{F_{cr}}.$$

On the fig. 6.10 $P_{sep} = f(\bar{\pi}_c)$ has three pronounced areas fro the next flow regimes in the boundary layers:

$\bar{P}_{sep\ lam}$ – for laminar (Re $<10^6$); $\bar{P}_{sep\ т}$ – for fully turbulent (Re $\geq 5 *10^6$); $\bar{P}_{sep\ i}$ – for intermediate ($10^6 <$ Re $< 5 *10^6$). For similar $\bar{\pi}_c$ inequation $\bar{P}_{sep\ т} < \bar{P}_{sep\ i} < \bar{P}_{sep\ l}$, i.e. conclusion that separation in turbulent case take place later because of higher particle kinetic energy near the walls is made. Starting from Re $> 5 *10^6$ Re number almost doesn't impact on the $P_{sep\ t}$ and is approximated by the expression $P_{sep\ т} = 0{,}96\ \bar{\pi}_c + 0{,}042$.

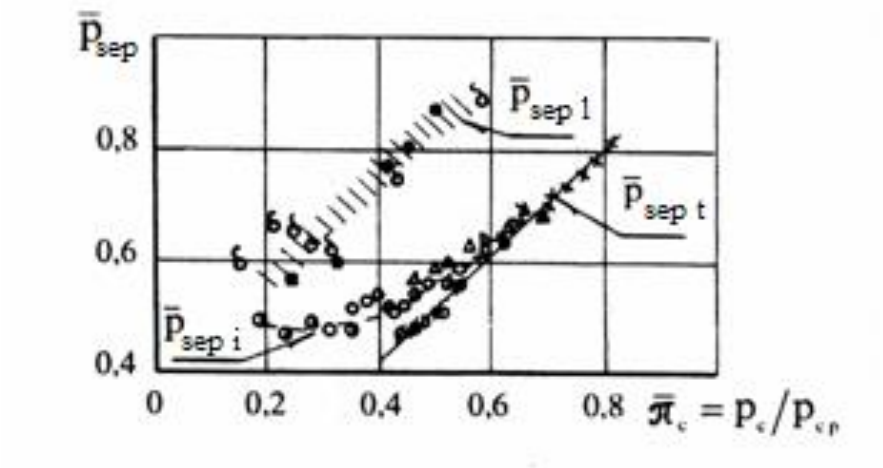

Fig. 6.10. Pressure in the separation point dependency on the $\bar{\pi}_c$ during flow overexpansion in the Laval

	□	•	δ	o	+	Δ	∅	×	*
α, deg	3	40	10	40	0	3	35	34	3
Θ, deg	2	2	10	2	2	2	2	0,5	2
Re 10^6	0,1	0,1	0,8	2,3	2,3	3	7	7	13

It is necessary to take flow in the nozzle features described before into account during the gas turbine engine nozzle designing and operation analysis.

6.13 Land gas turbine engines nozzles

6.13.1 Common requirements

The main feature of the ground gas turbine engine nozzles operation is low value of the available pressure ratio (π_c<2).

Nozzle must provide disposal of the exhausted gas with minimal resistance due to the significant influence of the pressure losses to the effective efficiency.

During the engine nozzle designing which serve, for example, as gas compressor unit drive the next requirements are taken into account:

1. Providing of the acceptable dimensions;

2. Ability to provide acceptable length of the shaft which connects engine to a compressor unit;

3. Providing of the exhaust gas turning to 90 degrees and its disposal to a waste treating unit with minimal hydraulic losses;

4. Providing of the stable flow and uniform pressure field after the turbine on all operation regimes.

Meeting of the first requirement is connected with concerns about railroad transportation and its service.

Meeting of the second requirement is connected with critical rpm detuning of the shaft which connects engine with compressor unit.

Meeting of the third and fourth requirements allows high fuel efficiency of the gas turbine engine and simultaneously solving of the durability increasing task of not only turbine elements but entire exhaust system.

It is obvious that creation of the effective gas turbine engine exhaust system which will meet all requirements that mentioned before is complex problem. Compromise decision is usually accepted.

6.13.2 Main design elements

On the fig. 6.11 one of the typical nozzle schemes of the converted gas turbine engines which serves as gas compressor unit drive is presented.

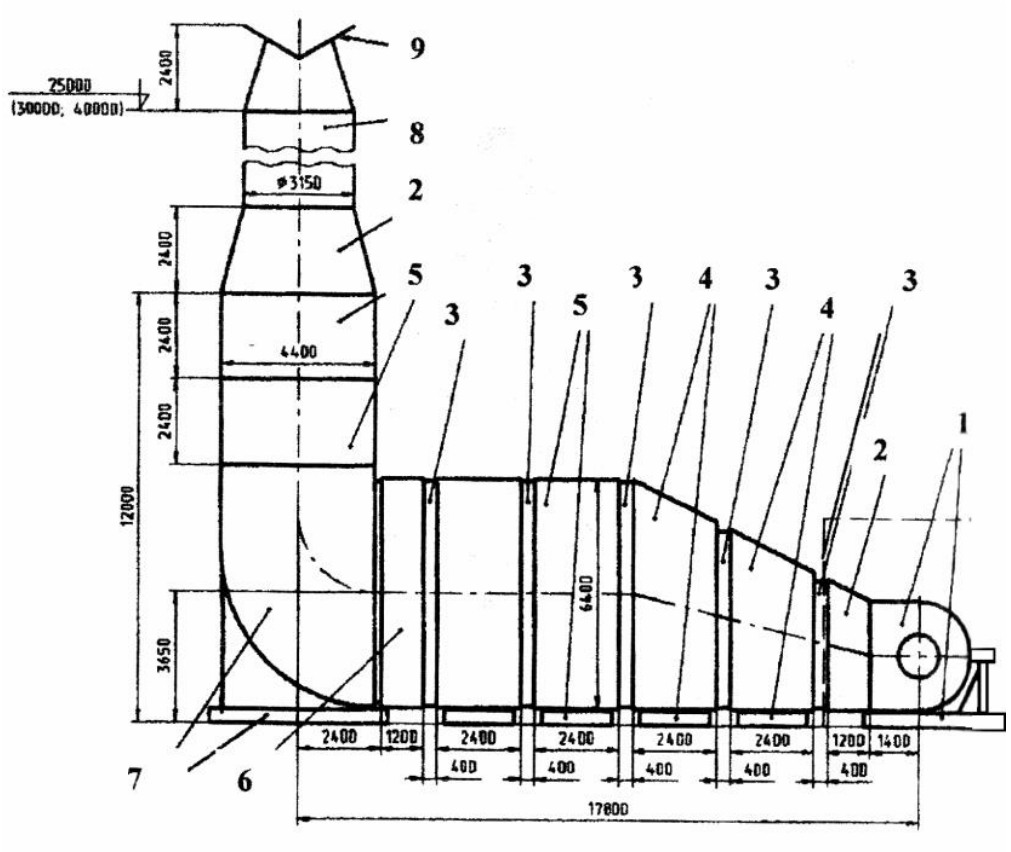

Fig. 6.11 Nozzle scheme

1 – gasholder; 2 – adapters; 3 – compensators; 4 – gas ducts; 5 – silencers; 6 – chamber for heat recovery unit installation; 7 – turning device; 8 – tube; 9 – all-weather hood

Exhaust volute which consists of axial-radial diffuser and gasholder is suited for smooth deceleration and flow turning to 90 degrees in diffuser and followed turning the flow up to 24 degrees from the horizontal axis in gasholder. Outer surface of the gasholder and inner shell of the axis-radial diffuser have liner from the heat- and sound- insulation material with 120 mm thickness.

Adapter with a rectangle section serves for connection of the exhaust volute with gasholder with and 10 degrees angle between its axis and horizontal axis of the exhaust channel.

Gas ducts of the rectangle section provide smooth transfer of the swirling gas flow to an axial one. In this case it is necessary to reach a flow velocity decreasing by channel expansion. Inner surfaces of the gas ducts are made from stainless steel plate as moving screen backed on “cushion” from the heat insulated materials with 60 mm thickness. The thickness of the heat insulation of the gas duct wall outer surface is equal to 240 mm.

Silencer is suited for providing required noise levels and represents channel with rectangle section with 18 shields which are placed across the width of a channel.

Heat exchanger for heat recovery is suited for using of the exhaust gases heat to heat supplying combustion chamber and outside customers. Heat exchanger for heat recovery with heat capacity of 5-6 MW must have regulation range between 50 and 100% of nominal capacity. Screens before the heat exchanger are suited for this purpose.

Turning device makes flow turning from the horizontal direction up to 90 degrees and is suited for providing uniform velocity and temperature fields on the entrance to the silencer.

Compensators are installed between nozzle elements and serve for providing opportunity to their possible expansion. The design of every compensator is two holders and represent telescopic group with rectangle section which is field with heat- and sound- insulated material.

6.14. Estimation of the hydraulic resistance

During the nozzle designing the task of the creation of the device with minimal possible resistance is set due to significant influence of the pressure losses to an effective gas turbine engine efficiency.

Losses in axial-radial diffuser

Estimation of the hydraulic losses is carried out by known and quite time-tested calculation relations. Nozzle hydraulic resistance is determined by the value of the total pressure losses due to:

- sudden expansion of the gas flow discharged from turbine diffuser during the flow entering in the rectangle area of the axial-radial diffuser;
- wall friction losses;
- flow expansion in the diffuser channel losses;
- flow turning;
- losses in gasholder.

Total pressure losses are determined by the expression:

$$1-\sigma_{\Sigma}=\Delta p^{*}\Big/ p_{in}^{*}=\sum_{i=1}^{m}\delta_{i}$$

where Δp^* – total pressure losses in the duct; p^*_{in} is a total pressure on the entrance to the axial-radial diffuser; m – number of duct elements; I – number of calculated area.

the losses on every area are calculated by the expression:

$$\delta_{i}=\frac{k}{k+1}\cdot\xi_{i}\cdot\lambda_{i}^{2}$$

where k – specific heat ratio; ξ_I – hydraulic resistance coefficient of the ith area; λ_i – superficial velocity on the entrance to the concerned area.

Sudden expansion losses

With regard to annular diffusers sudden expansion of the channel losses are calculated by the specified (to the velocity field non-uniformity) expression of Bord-Carnot:

$$\zeta_{\mathrm{i}} = \frac{\Delta \mathrm{H}}{\rho \mathrm{w}_0^2/2} = \frac{1}{\mathrm{n}^2} + N - \frac{2M}{n}$$

where $n = F_{ex}/F_{in}$ is flow section expansion ratio (F_{in} – area of the inlet section; F_{ex} – area of the exit section).

$N = \frac{(2m+1)^3(m+1)^3}{4m^4(2m+3)(m+3)}$ is coefficient of the flow kinetic energy on the exit from the narrow channel to wide one;

$M = \frac{(2m+1)^2(m+1)}{4m^2(m+2)}$ is momentum coefficient in the same section;

ρ and w_0 are flow density and velocity in the entrance;

m – coefficient which depends on flow velocity profile (by the results of the consolidation measurements m=1,8).

Friction and expansion losses

Friction losses coefficient in axial-symmetric annular diffuser is determined by the expression:

$$\zeta_{Fr} = \xi \frac{L_i}{2(R_{2i} - R_{1i})} y,$$

where ξ – friction coefficient which depends on Reynolds number and wall roughness;

L_i , R_{1i} , R_{2i} are calculated area length, outer and inner radiuses on the area entrance correspondingly (Fig.)

y – coefficient which takes into account geometric relation between inlet and outlet sections.

Losses coefficient due to the expansion in diffuser is calculated by the expression:

$$\xi_p = (\varphi 1 - 1/n)^2,$$

where n – diffusion degree; $\varphi = 3{,}5(\mathrm{tg}\theta/2)^{1,22}$ is coefficient which corrects degree of flow expansion suddenness for the expansion angles $8^\circ < 0 < 40^\circ$.

Flow turning losses

In the radial diffuser flow turning takes place. Flow turning losses are determined as a function of expansion degree and relative diffuser diameter $\bar{D}$:

$$\xi_{\text{пов.}} = \mathrm{f}(n,\ \bar{D}).$$

Expansion of the radial-annular diffuser is equal to

$$n = 2\left(\frac{L_1}{l_2}\left(\frac{\bar{D}}{1+\bar{d}}\right)\right),$$

where $\bar{D} = \frac{D_3}{D_2}$ and $\bar{d} = \frac{D_1}{D_2}$ are relative diameters of the diffuser and hub;

n – diffusion degree.

Common diffuser resistance degree due to the flow turning is determined by nomogram $\xi_n = \mathrm{f}(D, f)$.

Gas ducts losses

Adapter (fig. 6.11) represents differ with rectangle are with nearly the same areas of inlet and outlet sections. Total pressure losses along the channel length are caused by friction and local losses.

Duct №1,2 represents pyramidal diffuser with different angles (α and β) of the expansion in planes (α = $27^0 42'$ by upper wall and β = $8^0 36'$ by side wall).

Duct №3 represents plane diffuser with wall expansion in only one plane with an angle $27^0 42'$.

Common diffuser resistance coefficient ζ_{con} consist of coefficient of local resistance due to the flow overexpansion ζ_{exp} and friction resistance coefficient ζ_{fr}.

$$\frac{\Delta H}{\frac{\gamma \cdot w^2}{2 \cdot g}} = \zeta_{com} = k_1 \zeta_{exp} + \zeta_{fr},$$

where k_1 is coefficient which takes non-uniform velocity field in the inlet section into account.

Expansion coefficient ζ_{exp} is determined through impact fullness coefficient φ_{exp} and diffuser expansion degree by approximated expression

$$\zeta_{exp} = \varphi_{exp}\left(1 - \frac{F_1}{F_0}\right)^2$$

where F_1 is an area of the gas duct outlet section;

F_0 is an area of the gas duct inlet section.

Friction resistance coefficient ζ_{fr} of the flat diffuser with inlet section sides a_0 and b_0 depends on expansion angle (α) sides relation a_0/b_0 and diffuser expansion degree

$$\zeta_{fr} = f\left(\alpha, a_0 / b_0, F_0 / F_1\right)^2.$$

There are blockages in the ducts in the form of cover plates (lock of duct plates to a frame), screws and prickers with height up to 30 mm. Pointed blockages cause additional local losses of total pressure.

Relative value of the blockage area is equal to $F = F_{bl} / F_{in} = 0{,}018$ (F_{bl} is total blockage area, F_{in} – area of the gas duct inlet section).

Decreasing of the inlet area due to the blockage presence causes increasing of the inlet specified flow velocity λ and velocity head H and, consequently, total pressure losses. For gas duct №1 estimation of the hydraulic losses of the total flow pressure shows that without blockage gas with the flow velocity equal to 50 m/s duct losses are equal to 21 mm w.g. and with with blockage this value reaches 21,2 mm w.g.

Thus, for gas ducts №2-3 with less flow velocity level blockage influence can be neglected. it is confirmed by the boundary layer thickness calculation along the nozzle duct.

The estimation of the boundary layer thickness is accomplished by the expression for flat plate [6]:

$$\delta = 0,37\left(\frac{\nu}{\frac{w_g}{2}}\right)^{0,2} \cdot L^{0.8},$$

where ν is coefficient of the kinematic viscosity;

w_g is exhaust gases velocity in the inlet section of the diffuser;

L is gas duct length.

Provided boundary layer thickness estimation (δ ≈ 40 mm) in the gas ducts shows that the height of blockages (h≈ 30 mm) does not exceed thickness of boundary layer (δ ≥ h). Because of that blockage presence in the gas ducts was not taken into account during hydraulic losses determination.

The losses in silencer №1

Silencer represents channel with constant section area with 18 shields which are placed across the width of a channel. The relative flow section area is equal to 0,365.

The hydraulic resistance of the silencer is determined as the resistance of the bar screen. Common losses in the screens are consolidated from entrance area

losses, friction losses and sudden expansion losses during the exiting from the narrowed section between the shields to the channel.

Turning device losses

Turning device makes flow turning up to 90 degrees. It is known that turning channels require special approach to designing. It is caused by not only possible increased resistance during the flow turning but also flow instability with higher turbulence which is distributed to the long distances. Coefficient of the resistance of the turning channel mainly depends on relative spherical radius R/D (R is turn radius and D is channel diameter) in the case of circular turning channel and in the case of rectangle channel additionally from the H/h value (H is width, h is height of the channel).

In the case of calculated estimation for accepted turning device design with velocity equal to 10 m/s hydraulic losses does not exceed 5 mm w.g.

Silencer №2 losses

Total pressure losses are determined the same way as silencer №1 losses because their designs are similar.

6.15 Ground gas turbine engine nozzles with silencing

6.15.1 Nozzle design

As an example of design and parameter calculation, nozzle of gas turbine locomotive engine considered which is converted aircraft gas turbine engine working on liquefied natural gas and mounted on locomotive as power drive.

Nozzle serve for disposal of the exhausted gases from the engine in vertical direction with minimal resistance due to the significant pressure losses impact on the effective efficiency.

The next requirements was taken into account during the nozzle designing:

- providing of the acceptable dimensions;

- providing of the gas after turbine turning up to 90 degrees and its disposal vertically to atmosphere with minimal hydraulic losses;
- providing of the required silencing according to GOST R 50951-96;
- providing of the necessary requirements for cryogenic fuel gasification.

The main nozzle design elements are presented on fig. 6.12. The nozzle consists of axial-radial diffuser, gas-holding volute and silencer.

Exhaust volute which consists of axial-radial diffuser 2 and gas-holding volute 3 is suited for smooth deceleration and flow turning up to 90 degrees from the horizontal axis. Silencer 1 is suited for providing necessary noise requirements and represents channel with constant rectangle section area with 18 shields which are placed across the width of a channel. Silencing elements in the walls and shields are _____. On the exit from silencer protecting cast grid is mounted with vertical flow direction.

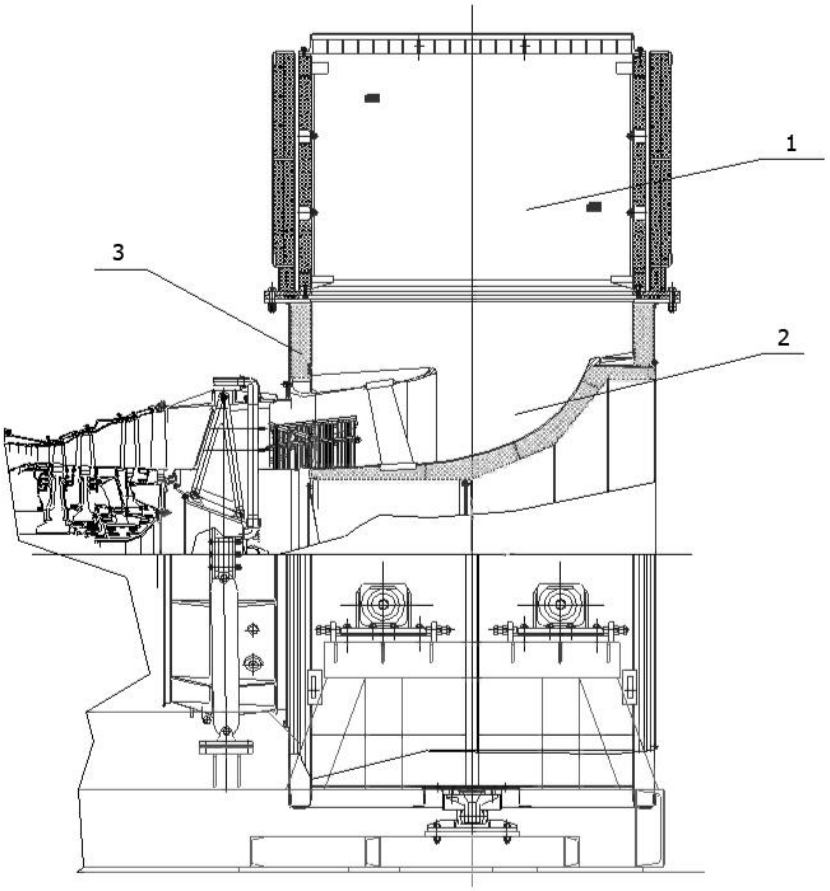

Fig. 6.12. Gas turbine locomotive engine nozzle

1 – silencer, 2 – axial-radial diffuser; 3 – gas-holding volute.

6.15.2 Gas dynamic calculation of the nozzle

The arrangement of the nozzle with placing silencing and heat exchanger elements in it which will serve for gasification of the liquefied natural gas or hydrogen.

The main thermodynamic parameters of the exhaust gases on maximal regime during operation on liquid natural gas which are necessary for hydraulic resistance estimation are presented in table 8.

Table 8 – **Thermodynamic parameters**

Parameters	Dim	Value
Environment temperature	K (^{0}C)	288(15)
Capacity	kW	8300
Exhaust gases mass flow rate	kg/s	53,71
Exhaust gases temperature	K (^{0}C)	667 (394)
Total pressure of exhaust gases in the entrance of the a diffuser	kPa (kg/sm^2	105 (1,076)
Total hydraulic pressure loss in the nozzle	Pa (mm w.g	3382 (345)*
∗ Heat exchanger resistance is a part of this value		

Estimation of the hydraulic losses value was carried out by numerical method of gas dynamics. Applied numerical method shows good correlation with experimental results of hydraulic losses in diffuser and gasholder determination on the example of NK-16ST. Hydraulic resistance of exhaust volute is determined by the value of total pressure losses due to:

- wall friction losses;
- flow expansion in diffuser channel losses;
- flow turning;

- gasholder and silencer losses.

The results of calculated estimation of the nozzle hydraulic losses with three possible types of the heat exchanger are presented in table 9.

Table 9 – **Calculation results**

	Parameter	Dimension	Basic variant	Basic variant + 200 mm	Basic variant + 200 mm with shelf
			Variant №1	Variant №2	Variant №3
Geometry	α	degree	8,1	4,7	8,1
	β	degree	2,25	2,25	2,25
	b	mm	546	426	450
	L	mm	1592	1792	1792
Losses	Axial-radial diffuser with heat exchanger with	mm w. g. (%)	370 (63)	359 (77)	245 (71)
	Silencer	mm w. g. (%)	220 (37)	105 (23)	100 (29)
	Total losses	mm w. g.	590	465	345

Basic variant calculation shows unsatisfied total pressure losses values because of heat exchanger presence in the diffuser duct lead to flow field distortion in the smooth part and flow separation and creation of vortex in the turning part of the nozzle.

Prolongation for 200 mm of the nozzle duct by means of reserves allows increasing of the flow section area of the channels which are created by silencing screens. It leads to a total pressure losses decreasing. At the same time losses value with outlet velocity remains on the same level.

Flow organization with shelf in diffuser i.e. with two areas of sudden expansion allows decreasing of the losses by 345 mm w.g. Exceedance by 45 mm w.g. the technical requirements is compensated by heat recovery from the exhaust gases to a engine working cycle.

Variant №1 (basic) is axial-radial diffuser design similar to real design used on the NK engine series. The outer section width from the axial-radial diffuser is equal to b=546 mm;

Variant №2 is prolongated by 200 mm basic variant with decreased width of the outer section equal to b=426 mm;

Variant №3 is prolongated by 200 mm basic variant with decreased width of the outer section equal to b=450 mm and with shelf on the inner surface of diffuser.

Hydraulic losses are presented as total pressure losses correspondingly on the area of the axial-radial diffuser with heat exchanger and silencer. Analysis of the results mentioned above show that minimal total pressure losses in the nozzle with heat exchanger are realized in variant №3 and are equal to 345 mm w.g. Variant №3 was accepted for design development.

Chapter 7. PLANE NOZZLES

For some promising airplanes and especially for hypersonic aircrafts matters of the plane nozzles application are considered and simulation tests of the power plant tail parts are carried out.

Plane nozzles have the next advantages:

1) maneuverability and plane stability increasing;

2) resistance decreasing during cruiser flight condition and maneuvers with high ascentional power by more propitious engine and airframe arrangement;

3) decreasing of the infrared and radar-location detection;

4) cost decreasing and nozzle design simplification by moving parts number decreasing;

5) High fitness for thrust vector control and thrust reverser.

However, plane nozzles have some disadvantages which include:

1) inner pressure losses increasing caused by transition channel from the axial-symmetric section to plane presence;

2) weight increasing which is connected with nozzle design features;

3) refrigeration problem appearance caused by increased nozzle and adapter wall surface.

Plane nozzles also find extensive use in pneumonics, rocket technique and serve for gas flow acceleration in the powerful lasers aerodynamic sluices.

7.1 Supersonic part profiling

Let's take into consideration that for gaining of the acoustic line form similar to straight line it is necessary to narrowing part circuit to be accomplished as interlinked circles arcs. One of these arcs which is placed in the entrance of the subsonic part has radius which is equal or exceed critical section radius and another one has radius equal to the diameter of critical section.

Laval plane nozzle supersonic part profiling and calculation are carried out by well planned characteristic method and presented as circuit tables for the M numbers in the outlet section range and limited range of the specific heat ratio values. Application of the presented velocity hodograph, consolidated polar coordinates for r and φ variables, where φ is supersonic flow expansion angle in the Prandtl-Meyer flow, allows task simplification and gaining of the analytical decision for any spontaneous M number and k value.

Let's consider, that surface of the speed of sound transition is plane. As it can be seen of fig. 7.1a, 1-d ideal flow of the perfect gas expansion occurs near the angle points O and O_1. Profiling task is separated in two: the first one is acceleration area calculation ABB_1C and the second one is smoothing area calculation MM_1DD_1.

1. Acceleration area. Flow acceleration from the plane surface of OO_1 transition for given value of $M_2 = M_c$ takes place in the ABB_1C of the simple

centered rarefaction wave from the perturbed points O and O_1. Physical flow area ABB_1C (where AB_1BC, AB_1 and B_1C are characteristics) corresponds to the area abb_1c (fig. 7.1b) of the velocity hodograph. In the case of uniform flow on the exit of the nozzle (i.e. during straight line CB characteristic) angles of the flow deflection**,** caused by the perturbed points O and O_1, are equal and, consequently, the next expression is correct:

$$\theta_b = \theta_{b1} = \frac{1}{2}\theta_c = \frac{1}{2}\left[m\ arctg\frac{\sqrt{M_c^2 - 1}}{m} - arctg\sqrt{M_c^2 - 1} \right] \qquad (7.1)$$

where θ_c is a flow deflection angle (angle between velocity vector and flow axis);

M_c – design Mach number,

$$m = \sqrt{\frac{k+1}{k-1}}.$$

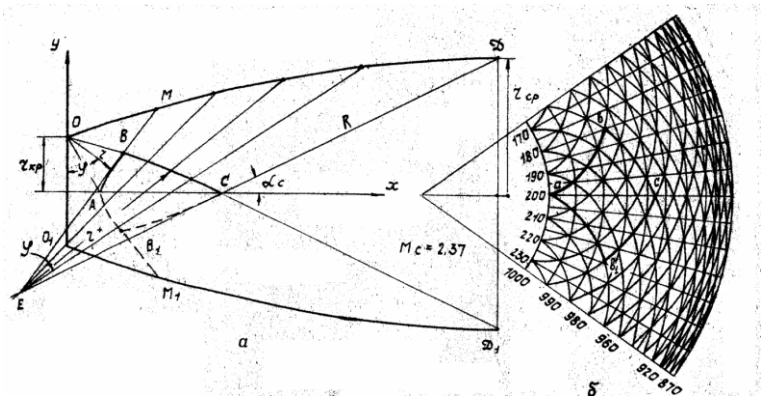

Fig. 7.1 Laval nozzle supersonic part profile:
a – physical plane; b – hodograph plane.

Condition 7.1 fully determines λ (where $\lambda = W/a_{cr}$ is velocity coefficient) and Θ parameters of the characteristic circuit abb_1c of the hodograph circuit (curves ab and bc are epicycloids).

For flow calculation in the physical plane it is comfortable to introduce the polar coordinate system with r and φ variables where φ is supersonic flow expansion angle. Dependencies of the flow parameters vs angle φ are the next:

For flow density: $\rho = \rho^* \cdot \left(\frac{1+\cos 2\varphi / m}{k-1} \right)^{\frac{k}{k-1}}$;

For pressure: $P = P^* \cdot \left(\frac{1+\cos 2\varphi / m}{k-1} \right)^{\frac{k}{k-1}}$;

For velocity coefficient $\lambda = \sqrt{\frac{k-\cos 2\varphi / m}{k-1}}$;

Speed of sound $a = a_{cr} \cos \varphi/m$,

where ρ* and P* are stagnation density and pressure.

Differential equation of the characteristics in simple wave has the next view:

$$\frac{1}{r}\frac{dr}{d\varphi} = ctg\,2\alpha,$$

where $\alpha = \arcsin\frac{1}{M}$ is a Mach number.

Integrating of this equation gives

$$r = \frac{const}{\sqrt{\sin(\phi / m)\left(\cos(\phi / m)\right)^{m^2}}} = \frac{const}{\left(\lambda^2 - 1\right)^{\frac{1}{2}}\left(1 - \lambda^2 / m^2\right)^{\frac{m^2}{2}}} = \frac{const}{j(\phi)}$$

Considering polar coordinate system origin in the point O and the fact that staring point A of the expansion fan interaction from O and O_1 belongs to the stream line in the Prandtl-Meyer flow

$$r = r_{cr} \cdot \left(\frac{\cos\varphi}{m} \right)^{m^2},$$

curve AB equation will have the next form:

$$r = r_{cr}\left[\frac{\sin\varphi_A / m}{\left(\cos\varphi_A / m\right)^2} \right]^{\frac{1}{2}} \left[\frac{\sin\varphi / m}{\left(\cos\varphi / m\right)^2} \right]^{-\frac{1}{2}} = r_{cr}\frac{\gamma(\varphi_A)}{j(\varphi)},$$

where $2 \cdot r_{cr}$ is a critical section area OO_1 and current value of the angle φ varies in the limits of $\varphi_A < \varphi < \varphi_B$. Angle of the starting characteristic can be considered equal to 1^o with enough accuracy. Value of the φ_B angle is determined from the (7.1) condition by the expression

$$\varphi_B + arcctg(m\, tg\varphi_B / m) = \frac{\pi}{2} - \frac{1}{2}\left[m\, arctg \frac{\sqrt{M_c^2 - 1}}{m} - arcrg\sqrt{M_c^2 - 1} \right].$$

BC characteristic of the ABB_1C area has new coordinate system with origin in the point E. Angle between radius-vector $\bar{r}_b$ of the new system and r_b of the old coordinate system in common point B is equal to $2a_b = 2arctg\left(\frac{m \cdot tg\varphi_b}{m}\right)$. BC curve equation is next:

$$\bar{r} = \bar{r}_E \frac{1}{j(\phi)}, (\varphi_B \le \varphi \le \varphi_C).$$

Validation of the profiling is carried out by:

1. Flow rate through enclosing characteristic CD calculation:

$$G_{CD} = \frac{1}{2}\rho_c a_c \left(R_{CD} - \bar{r}_c\right) = \frac{1}{2} G_{cr}$$

2. Angle between enclosing characteristics and nozzle axis calculation:

$$\alpha_c = 2\alpha_B - \left(\varphi_c - 2\varphi_B\right) - \frac{\pi}{2}$$

7.2 Outlet momentum determination in the shortened nozzle

On practice it is often necessary to know the dependency of outlet momentum on the shortened nozzle length. Such dependency as a function of φ_I angle is described in r and φ variables and has a next form.

$$\bar{I}_i = \left(\sqrt{\frac{k - \cos\left(\frac{2\varphi_i}{m}\right)}{k-1}} \cdot \cos\left(2\theta_B - (\varphi_i) + arcctg\left(m\, tg\left(\frac{\varphi_i}{m}\right)\right) - \frac{\pi}{2}\right) + \right.$$

$$\left. + \frac{\cos\left(\frac{\varphi_i}{m}\right)}{k} \right) \cdot$$

$$\cdot \left[\frac{\gamma(\varphi_A) \pm R_E}{j(\varphi_B)} \right] \left(\cos\left(\frac{\varphi_B}{m}\right)\right)^{m^2} - \left(\sqrt{\frac{k - \cos\left(\frac{2\varphi_c}{m}\right)}{k-1}} + \frac{\cos\left(\frac{\varphi_c}{m}\right)}{k} \right) \frac{R_E}{\gamma(\varphi_c)}.$$

$\bar{I}$ is related to a next product: $2\rho \cdot r_{cr} \cdot a_{cr}^2 \left(\frac{2}{k+1}\right)^{\frac{1}{k-1}}$.

On the fig. 7.2 circuits of the supersonic nozzle part for Mc=4 and k=1,25 1,3 and 1,4 and outlet momentum dependency vs nozzle length are presented. It is seen, that shortening of the nozzle level by 10-15% does not have an impact on its characteristics.

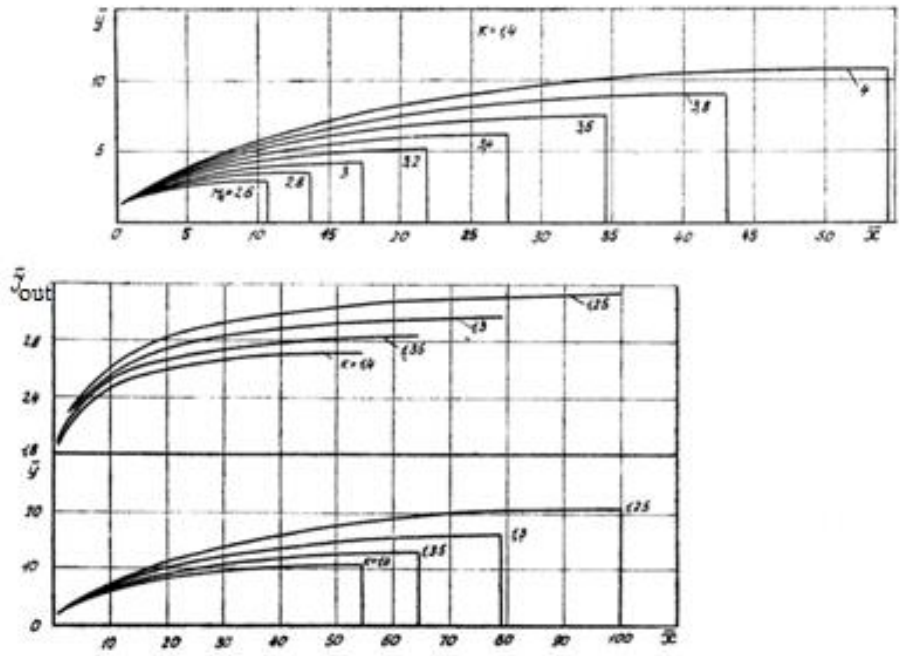

Fig. 7.2 Circuit of the Laval nozzle supersonic part with Mc=4 in the outlet section for various k values; relative outlet momentum dependency on nozzle length.

7.3 Supersonic flow in the channel with sudden expansion calculation

The tasks of the separation area boundary and supersonic flow parameters determination are decided with a help of hodograph and r and φ variables introduction.

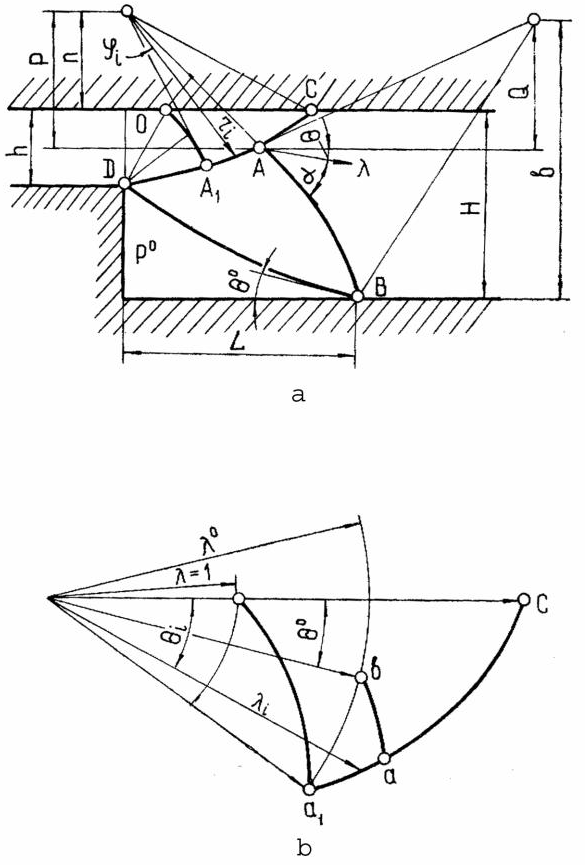

Fig. 7.3. Supersonic flow in the channel with sudden expansion

Full analytical description of the flow structure in given area which includes se

On the basis of the experimental and theoretical data it is known that in the isobaric separation area total pressure on the flow layer line is equal to the end of the joining flow compression area and as main parameter, which characterizes viscous layer, allowable flow angle in the joining point Θ^0 should be used.

On the fig. 7.3 supersonic flow with M=1 in the plane channel during the sudden expansion of the narrow section from the dimension h in the entrance (let consider h=1) to the dimension H on the exit is presented. Assumptions:

1) flow parameters change including compression in the joining area (from the shock wave from the B point) takes place isentropically;

2) starting thickness of the boundary layer before the separation point can be neglected;

3) viscous layer in the joining area is characterized by the determined value of the allowable angle.

Velocity hodograph of this flow is presented on fig. 7.3, b. Point D (fig. 7.3, a) is a source of the centered rarefaction waves where the flow accelerates from the speed of sound $\lambda=1$ to a velocity λ_{A1}.

Upper wall of the OC channel, which is limited by characteristics OA_1AC, is a stream line along which the velocity increases from 1 to λ_c (note that flow character in the area OA_1C and the area oa_1c of the hodograph correspond to an area of acceleration in the Laval plane nozzle).

Boundary stream line DB in the starting point D of the separation area has direction which converge with velocity λ_{A1} vector and in the joining point b it has an Θ^0 angle. In the hodograph plane boundary stream line is enclosed between epicycloids a_1a arc which corresponds to a compression characteristics AB.

Then on the basis of the mentioned above task decision separation area boundary is described by next dependencies:

- relative shelf height

$$\overline{H}=\frac{H}{h}=\gamma(\varphi_C)\,A\left[\frac{\cos\left[\pi-\left(2\varphi_{A_1}-\varphi_A-2\alpha_{A_1}\right)\right]}{j(\varphi_A)}-\frac{\cos\left[\pi-\left(2\varphi_A-\varphi_B+2\alpha_{A_1}\right)\right]}{j(B)}\right]+$$

-

$$+B\left[\frac{\gamma(\varphi_A)}{\frac{\gamma(\varphi_A)}{j(\varphi_{A_1})}-1}\right]\cdot\left\{\frac{\sin\left[\frac{\pi}{2}-\left(2\varphi_A-\varphi_B\right)+2\left(\alpha_B-\alpha_{A_1}\right)\right]}{j(\varphi_B)}-\right.$$

$$\left.-\sin\left[\frac{\pi}{2}-\left(2\varphi_{A_1}-\varphi_A\right)+2\left(\alpha_A-\alpha_{A_1}\right)\frac{1}{j(\varphi_A)}\right]\right\}$$

- relative distance to a joining point

$$\bar{L} = \frac{L}{h} = \frac{\gamma(\varphi_A)}{j(\varphi_{A_1})}\sin(\varphi_{A_1}) + \gamma(\varphi_C)\, A \times$$

$$\left\{\sin\left[\pi - (2\varphi_{A_1} - \varphi_A - 2\alpha_{A_1})\right] * \frac{1}{j(\varphi_A)} - \sin\left[\pi - (2\varphi_A - \varphi_B + 2\alpha_{A_1})\right]\frac{1}{j(\varphi_B)}\right\} +$$

$$+ B\left\{\left[\frac{\gamma(\varphi_A)}{\frac{\gamma(\varphi_A)}{\gamma(\varphi_{A_1})} - 1}\right]\right\}\left\{\begin{array}{l}\cos\left[\left(2\varphi_{A_1} - \varphi_A\right) + 2(\alpha_A - \alpha_{A_1}) - \frac{\pi}{2}\right]\frac{1}{j(\varphi_A)} - \\ \cos\left[\frac{\pi}{2} - (3\varphi_{A_1} - 2\varphi_A) - 2(\alpha_{A_1} - \alpha_A)\right]\frac{1}{j(\varphi_{A_1})}\end{array}\right\}$$

where $A = \dfrac{\gamma(\varphi_{A_1}) - \gamma(\varphi_0)}{\gamma(\varphi_C) - \gamma(\varphi_{A_1})}, \quad B = 1 - A\left[\dfrac{\gamma(\varphi_C) - \gamma(\varphi_A)}{\gamma(\varphi_A)}\right]$

Comparison of the calculated value of the relative base pressure P^0/P_1, where P^0 is pressure after shelf and P_1 is static pressure in a narrow channel, with experimental value show good correlation (fig. 7.4).

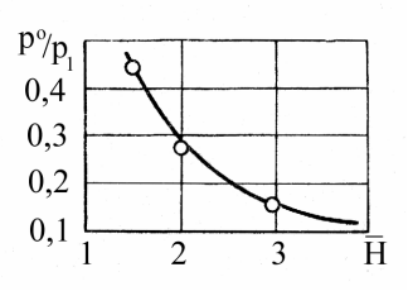

Fig. 7.4 Comparison of the calculation and experimental results.

Chapter 8. SIMILARITY THEORY AND DIMENSIONAL ANALYSIS

8.1 Similarity of the physical processes

Complex fluid flow studying is usually connected with physical experiment. Such experiments usually require large material costs. Sometimes significant or even irresistible difficulties take place during testing. Scientific statement of the experiment bases on physical processes similarity theory. This theory is a basis of modeling i.e. substitution of the full-scale testing by model testing. Local modeling of the most complex structure part often takes place. Similarity theory provides a

scientific statement of the experiment on the nature and the model and the minimum cost for its holding. In addition, it allows us to extend the results to all such phenomena under study. The main objectives of this theory is to identify the necessary and sufficient conditions for the similarity of model and full-scale processes, scientific methods of experimentation and obtain generalized dependencies. Physical processes are similar if systems, in which they occur and at similar times at similar points in space all the same parameter proportional, are geometrically similar.

From this definition it should be concluded that:

1. Similar may be homogeneous physical phenomena described by the same form and content of differential equations. If an analytical description of the two processes similar in shape, but different processes in the physical sense, they are called similar, such as the diffusion $G = -D\frac{dc}{dn}$ of and thermal conductivity $q = -\lambda\frac{\partial T}{\partial n}$.

Geometric similarity is necessary for the similarity of any physical processes. Complete similarity is similarity of fields similar quantities, i.e., at similar times at similar points in space any parameter φ_2 can be obtained from the same parameter $\varphi_1$of this process by multiplication by a constant similarity $\varphi_2 = \mathrm{C}_{\varphi(1-2)}\varphi_1$.

In relation to hydrogasdynamic processes we receive that the terms of their similarity are:

geometric similarity

Kinematic similarity or velocity fields similarity

$$\frac{u_2}{u_1} = \frac{v_2}{v_1} = \frac{w_2}{w_1} = C_{u(1-2)}.$$

Dynamic similarity or likeness of fields of forces acting in the fluid

$$\frac{t_2}{t_1} = C_{t(1-2)};\ \frac{p_2}{p_1} = C_{p(1-2)};\ \frac{\rho_2}{\rho_1} = C_{\rho(1-2)};\ \frac{v_2}{v_1} = C_{v(1-2)}.$$

Thermal similarity or similarity of temperature fields and heat fluxes

$$\frac{T_2}{T_1} = C_{T(1-2)};\ \frac{q_2}{q_1} = C_{q(1-2)};\ \frac{\lambda_2}{\lambda_1} = C_{\lambda(1-2)};\ \frac{\chi_2}{\chi_1} = C_{\chi(1-2)}.$$

Constant similarity of different parameters may vary in magnitude but can not be chosen at random and are linked by the equation, which is called the condition of similarity.

It is obtained by the transformation of equations connecting parameters that determine the course of similar processes. Consider as an example the condition of simple geometric similarity for the compressor blades. We have the formula for calculating the area of $S_1 = b_1 h_1$, $S_2 = b_2 h_2$.. And such a transformation formula $S_2 = S_1 C_{s(1-2)}$ and $S_1 C_{s(1-2)} = b_1 h_1 C^2_{l(1-2)}$.

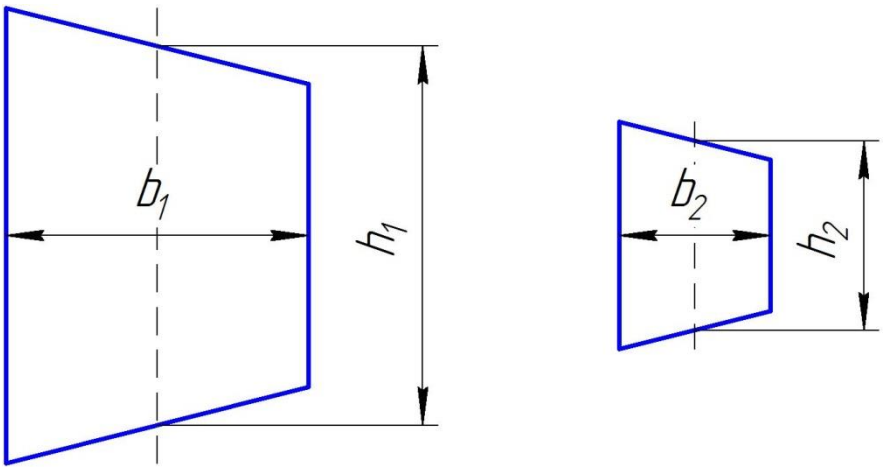

Fig. 8.1 Geometric similarity

Comparing this expression with equation $S_1 = b_1 h_1$ gives

$$C_{s(1-2)} = C^2_{l(1-2)} \text{ или } C_s / C_l^2 = 1. \qquad (4.1.1)$$

Similar calculations for any other pair of similar figures can be concluded that the equation (4.1.1) between the constants is valid for all the similar figures and the condition for their similarity. Therefore, in (4.1.1) indices (1-2) are omitted. The left side of (4.1.1) is an indicator of similarity. For such flows

similarity indicators must be equal to unity. Substituting in (4.1.1) values of the similarity constants, we find that the dimensionless expression:

$$\frac{S_1}{b_1^2} = \frac{S_2}{b_2^2} = \frac{S_3}{b_3^2} = \frac{S}{b^2} = inv. \quad (4.1.2)$$

remains unchanged (invariant) value for all similar figures and is called invariant or similarity criterion. Hydrodynamic similarity criteria are more complex dimensionless complexes.

Three theorems of similarity theory Theorem I. For similar processes criteria of the similarity with the same names are equal. This means that the indicators of similarity are equal to 1. Theorem allows us to determine the similarity criteria on the basis of this similarity transformation equations describing these processes.

Theorem II. If a physical phenomenon is described by a system of differential equations, it their solution can always be represented as a consolidated criterion equation establishes a relationship between the similarity criteria obtained on the basis of Theorem I, or other way:

$$K_1 = f(K_2, K_3, \dots, K_n) \quad (4.2.1)$$

Form of the f function and the values of certain constants in it are determined on the basis of the original differential equation and, if necessary, by experiment.

Theorem III. For physical processes similarity it is necessary and sufficient to conditions of uniqueness be similar and independently determined similarity criteria with the same name to be equal. Thus, equality of the determined similarity criteria is provided automatically. Non-dimensional complexes which are composed from the parameters in the uniqueness condition are called determinantive similarity criteria $K_2, K_3, \dots, K_n$. Non-dimensional complex which includes the parameter determined in the task is called determined similarity criterion K_1. Similarity criteria are divided into: a) hydrodynamic similarity criteria derived by analyzing the differential Navier-Stokes equations; b) thermal similarity criteria derived on the basis of an analysis of the energy equation.

8.2. Criteria of hydrodynamic similarity

On the basis of the first theorem we establish criteria for the hydrodynamic similaritydetermining. For this we write the differential Navier-Stokes equations of one-dimensional flow for the full-scale (index 1) and similar model (index 2) flows. Assuming that the mass forces – is the force of gravity, i.e. $X_1 = X_2 = g$, we obtain:

$$\frac{\partial u_1}{\partial t_1} + u_1 \frac{\partial u_1}{\partial x_1} = g - \frac{1}{\rho_1}\frac{\partial p_1}{\partial x_1} + \nu_1 \frac{\partial^2 u_1}{\partial x_1^2} + \frac{1}{3}\nu_1 \frac{\partial^2 u_1}{\partial x_1^2}. \qquad (4.3.1)$$

$$\frac{\partial u_2}{\partial t_2} + u_2 \frac{\partial u_2}{\partial x_2} = g - \frac{1}{\rho_2}\frac{\partial p_2}{\partial x_2} + \nu_2 \frac{\partial^2 u_2}{\partial x_2^2} + \frac{1}{3}\nu_2 \frac{\partial^2 u_2}{\partial x_2^2}. \qquad (4.3.2)$$

Both flows are similar. Performing transformations corresponding to the geometric, kinematic and dynamic similarity and substituting the values of the parameters with index 2 in the equation (4.3.2) we obtain the equation of the model flow in full-scale parameters:

$$\frac{C_u}{C_t}\frac{\partial u_1}{\partial t_1} + \frac{C_u}{C_l} u_1 \frac{\partial u_1}{\partial x_1} = C_g g - \frac{C_p}{C_\rho C_l}\frac{1}{\rho_1}\frac{\partial p_1}{\partial x_1} + \frac{C_\nu C_u}{C_l^2}\frac{4}{3}\nu_1 \frac{\partial^2 u_1}{\partial x_1^2}. \qquad (4.3.3)$$

Equations (4.3.1) and (4.3.3) are identical and, therefore, all members of the dimensionless factors of equation (4.3.3) equal to each other. Thus, the condition of hydrodynamic similarity of flows is equal:

$$\frac{C_u}{C_t} = \frac{C_u^2}{C_l} = C_g = \frac{C_p}{C_\rho C_l} = \frac{C_\nu C_u}{C_l^2}. \qquad (4.3\ 4)$$

This is connection between the constants of similarity. They point to the similarity of all the forces acting in such flows. Indeed, the equation (4.3.2) and (4.3.3) are identical, i.e. term by term equal to, for example, $\frac{C_u}{C_t}\frac{\partial u_1}{\partial t_1} = \frac{\partial u_2}{\partial t_2}$, consequently, $\frac{C_u}{C_t} = (\frac{\partial u_2}{\partial t_2})/(\frac{\partial u_1}{\partial t_1})$ is the ratio of inertial local forces of the model and full-scale flows. $\frac{C_u^2}{C_l}$ is convective inertial forces relation, C_g is a mass forces

relation; $\frac{C_p}{C_\rho C_l}$ is pressure forces relation; $\frac{C_\nu C_u}{C_l^2}$ is viscosity and compressibility forces acting on the model and full-scale flows relation.

So, in such flows relationship of similar strength are the same. For indicators and criteria gaining all members of similarity (4. 3. 4) are compared with the second term $\frac{C_u^2}{C_l}$.

$$\frac{C_u}{C_t} = \frac{C_u^2}{C_l} \text{ similarity indicator } \frac{C_b}{C_t C_u} = 1;$$

$$C_g = \frac{C_u^2}{C_l} \text{ similarity indicator } \frac{C_u^2}{C_l C_g} = 1;$$

$$\frac{C_p}{C_\rho C_l} = \frac{C_u^2}{C_l} \text{ similarity indicator } \frac{C_p}{C_\rho C_u^2} = 1;$$

$$\frac{C_\nu C_u}{C_l^2} = \frac{C_u^2}{C_l} \text{ similarity indicator } \frac{C_l C_u}{C_\nu} = 1.$$

Substituting the indicators of similarity values of constants and taking the choice of processes 1 and 2 randomness, we obtain the following criteria which determine the hydrodynamic similarity.

Strauhal or time non-uniformity number

$$Sh = \frac{l}{Wt} = \frac{lh}{W}. \qquad (4.3.5)$$

where l – is the characteristic dimension of the body, located in the flow channel or path traversed by a particle in a time unit; w – the characteristic velocity of the fluid flow; t- characteristic time of the process or the time period of the phenomena occurring at a frequency of h = 1 / t. Sh criterion is the ratio of the local component of the inertial forces to the convective component of the inertial forces. Sh criterion excluded from determining: criteria for the study of steady flow.

Froude number

$$Fr = \frac{w^2}{gl}. \qquad (4.3.6)$$

Characterizes the ratio of convective inertia forces to the forces of gravity in the flow is determinative one if the gravity significantly affect the motion of the fluid (the tube or powerful vane pump). If the motion is due to the free fluid convection in the media of variable density, to a Navier-Stokes equation it is necessary to add the Archimedes force. In this case, instead of the Froude number a criterion Grashoff is introduced in the number of defining criteria.

Grashoff criterion:

$$Gr = \frac{gl^3\beta\Delta T}{\nu^2},$$

where $\beta = \frac{\rho_0 - \rho}{\rho_0 \Delta T}$ is a coefficient of thermal expansion of the liquid; ρ_0 and ρ are the densities of cold and hot particles in the media; ΔT is a temperature difference which causes by free convection, for example, $\Delta T = T_w - T_\infty$. Grashof criterion expresses the ratio of Archimedes forces causing convection to the viscous forces that prevent it.

Eulerian criterion:

$$Eu = \frac{P}{\rho W^2}.$$

characterizes the ratio of hydrodynamic pressure forces and inertial forces in the flow. In gas dynamics Euler criterion is represented using the expression for the speed of sound $a^2 = \frac{kp}{\rho}$ and the Mach number $M = w/a$ in the form $Eu = \frac{1}{kM^2}$.

Therefore, specific heat ratio $k = \frac{C_p}{C_v}$ and Mach number, which characterize has compressibility and must be equal in similar flows, can be used in gas dynamics instead of Eu

Reynolds number

$$Re = \frac{\rho W l}{\mu} = \frac{Wl}{\nu}. \qquad (4.3.8)$$

Characterizes the ratio of inertial forces to viscous forces in the stream.

Aerodynamic coefficients are the dimensionless complexes containing unknown quantities and is therefore determined by the similarity criteria.

1. Coefficient of drag is equal to $C_x = R_x / \left(\frac{\rho_\infty W_\infty^2}{2} S\right)$, where $R_x$is the drag force of the body; $\frac{\rho_\infty W_\infty^2}{2}$ is the undisturbed flow velocity head, Pa; S – typical area of the body; for a wing is is an area in its plan.

2. The coefficient of lift.

$$C_y = R_y / \left(\frac{\rho_\infty W_\infty^2}{2} S\right),$$

where R_y is a lift force.

3. The coefficient of the total aerodynamic force

$$C_R = R / \left(\frac{\rho_\infty W_\infty^2}{2} S\right),$$

where $R = \sqrt{R_y^2 + R_x^2}$ is total aerodynamic force.

4. Pressure coefficient

$$\overline{p} = (p_1 - p_2) / \left(\frac{\rho_\infty W_\infty^2}{2}\right).$$

5. The drag coefficient of friction

$$C_f = r / \left(\frac{\rho_\infty W_\infty^2}{2}\right).$$

For every aerodynamic coefficient it is remarkable that forces in them are related to a velocity head.

8.3. Criteria of thermal similarity

Thermal similarity in the streams is performed under the condition:

1) hydrodynamic similarity

2) the similarity of the temperature fields,

3) The equality of the same name similarity criteria.

At low flow velocities temperature fields similarity means equality of corresponding relations T_∞/T_W or excessive temperatures relations:

$$\frac{\Delta T}{\Delta T_0} = \frac{T - T_W}{T_\infty - T_W}. \quad (4.4.1)$$

In this case, constant of temperature can be represented as:

$$\mathrm{C}_T = \frac{\Delta T_2}{\Delta T_1} = \frac{\Delta T_{02}}{\Delta T_{01}}. \quad (4.4.2)$$

At high speeds of the gas flow temperature criteria will be:

$$\theta = \frac{W_\infty^2}{\mathrm{C}_p \Delta T_0} = 2\frac{T_\infty^* - T_W}{T_\infty - T_W} = 2\frac{\Delta T_\infty^*}{\Delta T_0}. \quad (4.4.3)$$

where $T, T_\infty, T_w, T_\infty^*$ are the temperatures in the same undisturbed flows, body surfaces and total temperature of the undisturbed flow itself. temperature fields similarity determines the similarity of the heat fluxes, for example, if $(T_\infty/T_W) > 1$ heat flux is directed from the fluid to the body and vice versa.

For thermal similarity criteria, based on the similarity transformation of the Navier-Stokes equations, simplistically we transform the energy equation using the constants of similarity. We have the original equation

$$\frac{dT}{dt} = \frac{1}{\rho C_p}\frac{dp}{dt} + a\nabla \mathrm{T} + \frac{1}{C_p}\frac{dq_{\text{тр}}}{dt},$$

where $a = \frac{\lambda}{\rho C_p}$ is thermal diffusivity.

We get (in the projection on the x axis):

$$\frac{C_T}{C_t}\frac{\partial T}{\partial t} + \frac{C_u C_T}{C_t} u \frac{\partial T}{\partial x} = \frac{C_p}{C_\rho C_{Cp} C_t}\frac{1}{\rho C_p}\frac{\partial p}{\partial t} + \frac{C_u C_\rho}{C_\rho C_{Cp} C_l}\frac{1}{\rho C_p} u \frac{\partial p}{\partial x} + \frac{C_a C_T}{\mathrm{C}_l^2} a \frac{\partial^2 T}{\partial x^2} + \frac{C_\nu \mathrm{C}_u^2 \nu}{C_{C\rho} \mathrm{C}_l^2 C_p}\left(\frac{\partial u}{\partial x}\right)^2.$$

Condition of thermal similarity we obtain by equating complexes composed of the constants of similarity:

$$\frac{C_T}{C_t} = \frac{C_u C_T}{C_l} = \frac{C_p}{C_\rho C_{Cp} C_t} = \frac{C_u C_p}{C_\rho C_{Cp} C_l} = \frac{C_a C_T}{\mathrm{C}_l^2} = \frac{C_\nu \mathrm{C}_u^2}{C_{Cp} \mathrm{C}_l^2}. \quad (4.4.4)$$

Equality of the second and sixth members (4. 4. 4) provides an indicator of similarity $\frac{C_u^2}{C_{Cp}C_T} = \frac{C_\nu}{C_l C_u} = 1$ and criterion $\frac{W_\infty^2}{Cp\Delta T_0}\frac{\nu}{lW_\infty} = \frac{\theta}{Re}$. Equality of the second and fourth members (4. 4. 4) provides an indicator of similarity $\frac{C_p}{C_\rho C_u^2}\frac{C_u^2}{C_{Cp}C_T} = 1$ and criterion $\frac{p}{\rho W_\infty^2}\frac{W_\infty^2}{C_p\Delta T_0} = E_u\theta$. Equality of the first and second members and also third and fourth members gives an indicator $\frac{C_l}{C_t C_u} = 1$ and Strauhal criterion $Sh = \frac{1}{Wt}$, i.e. in all cases we will not get the new independent similarity criteria.

Fourier criterion or criteria heat homochronicity:

$$F_0 = \frac{at}{l^2} \qquad (4.4.)$$

Obtained by comparing the first and fifth members (4. 4. 4) and characterizes the ratio of heat transferred thermal conductivity to a change in enthalpy due to non-stationary process. Fourier is the determining criterion in the study of transient heat transfer.

Peclet number $Pe = \frac{Wl}{a}$ is obtained from the comparison of the second and fifth members (4. 4. 4) and is the ratio of convective heat transfer to the enthalpy, transmitted by molecular conductivity. Here χ – coefficient of thermal diffusity.

Prandtl number $Pr = \frac{Pe}{Re} = \frac{\nu}{a}$ is convenient because it is composed only of physical constants and ν a, characterizing the intensity of the molecular transfer of momentum and heat. Defining parameters for the criteria calculation can be selected in some extent arbitrary, but must be the same for all compare similar processes.

8.4. Compilation of criteria equations

On the basis of the second similarity theorem let compose consolidated criteria equation, for example, for the group of similar processes which have drag coefficient as a defining similarity criterion.

Form of the function is determined on the basis of a system of differential equations of motion with the help of an experiment performed under the same the

defining criteria of similarity as in the full-scale experiment This similarity is complete. Studies show that complete similarity, i.e. complete simulation of complex phenomena is not feasible – it leads to the identity of the currents. For practice it is enough the accomplishment of the partial similarity. During the partial modeling only those defining criteria are accepted that significantly impact on defining criterion value. Non-defining criteria are determined from the task uniqueness condition and estimation of the equation members relative value which describe the process. Range of values of the criterion, in which its change does not affect the value of the determining criterion, called automodel – similarity is performed automatically for all values of the criterion. For example, instability of the process can often be neglected and the Strauhal Sh criterion is eliminated, in studies of incompressible fluid flows – Poisson number k and the Mach M.

Conditions $F_{r_M} = F_{r_H}$ and $Re_M = Re_H$ for decreased in C_l times model cannot be satisfied: the first require the decreasing of the model flow velocity $W_M = W_H\sqrt{C_l}$ and the second one require increasing of the $W_M = W_H/C_l$.

To resolve this contradiction, we must either pursue modeling experience using liquid whose properties are determined by the equations of similarity criteria and C_l values, or introduce additional restrictions in terms of uniqueness, narrowing the group of similar processes.

The number of the similarity criteria is always less then number of dimensional parameters which define the process. It is also the advantage of the criteria equation in comparison to the equation which consist of physical parameters. The substitution of the dimensional variables to non-dimension is the essence of the similarity theory as it is mentioned in similarity π – theorem.

Physical equation, which contains $n \geq 2$ dimensional parameters, $m \geq 1$ of them has independent uniformity, will contain $n - m = \pi$ non-dimensional value after its transformation to non-dimensional form.

Chapter 9. DIFFUSERS

9.1 Subsonic gas turbine engine diffusers. Diffusers for moderate supersonic velocities

Diffusers are used to convert kinetic energy into potential pressure energy (briefly in head) of liquid. For an incompressible fluid diffusers are expanding channels $\left(W_2 = W_1 S_1 / S_2\right)$. Lets consider a gas turbine engines diffusers which are divided into the next categories depending on the flight velocity:

for subsonic velocities $M_H < 1$;

for small supersonic velocities $M_H < 1{,}5$;

for supersonic flight velocities $M_H > 1{,}5$.

All diffusers must have minimum dimensions, weight and losses.

Subsonic diffusers are expanding channels with smoothly rounded leading edge to prevent flow separation at the inlet (fig. 10.1). The larger $dS/dx > 0$, the more dp/dx and the less the weight and length of the diffuser. In practice, is necessary to limit dp/dx in order to avoid boundary layer separation which is the source of the most significant loss of total pressure. The second source is the friction loss in the boundary layer.

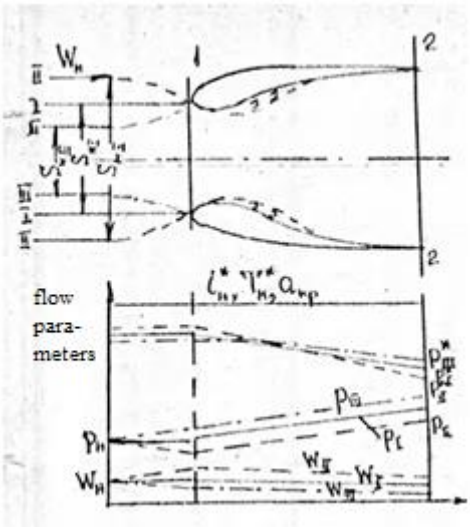

Fig. 9.1. Subsonic diffuser operation regimes

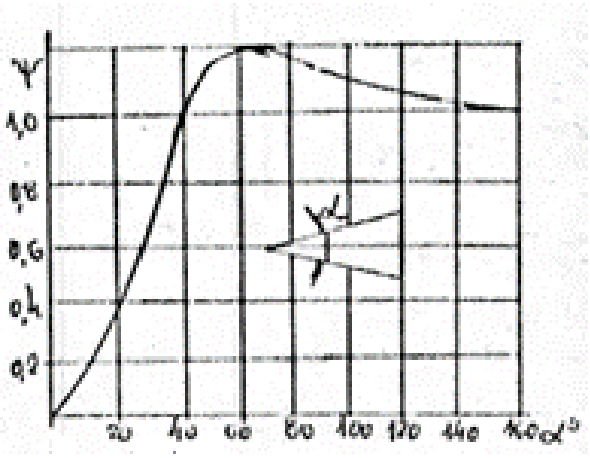

Fig. 9.2. Impact damping coefficient dependency vs circle diffuser angle of expansion

The total temperature of the energy isolated flow in the diffuser remains constant $T_2^* = T_1^* = T_H^*$. The total pressure due to pressure loss is reduced, resulting in a loss of engine efficiency and thrust. Static pressure and the density increase due to the decrease of the velocity.

Calculation in the diffuser boundary layer flows is difficult, so the loss in the diffuser is usually calculated using experimental coefficients.

Lets calculate the total pressure loss associated with the separation of the boundary layer, the formation and maintenance of vortex regions, such as the loss of Borda-Carnot impact at sudden expansion of the channel from S_1 to S_2 which is softened by the smooth extension of the diffuser. Typically, the calculations can be given a specific velocity λ_2 at the outlet of the diffuser.

Therefore, we express total pressure coefficient in fractions of velocity head not in the inlet section but in the diffuser outlet. Assuming that gas is approximately incompressible, i.e. $\rho_2 = \rho_2^* = \rho_H^*$, and taking $p_H^* / \rho_H^* = RT^* = \frac{k+1}{2k} Q_{кр}^2$ into account we get:

$$\sigma = \frac{p_2^*}{p_H^*} = 1 - \frac{p_H^* - p_2^*}{p_H^*} = 1 - \psi\left(\frac{S_2}{S_1} - 1\right)^2 \frac{\rho_H W_2^2}{2 p_H^*} = 1 - \psi\left(\frac{S_2}{S_1} - 1\right)^2 \frac{k}{k+1}\lambda^2$$

where $\left(\frac{S_2}{S_1} - 1\right)^2 = \zeta_{y\partial}$ – losses coefficient on the Borda-Carnot impact during the sudden channel expansion from S_1 to S_2, ψ is experimental coefficient of the impact damping which depends only on diffuser angle of expansion α (fig. 10.2). Maximal value ψ=1,2 is gained if α=60°, i.e. the losses value with that angle is bigger then at the sudden channel expansion ($\alpha=180^0$). The reason is that during $\alpha=180^0$ the the flow is stable, while during α=60° flow is unstable and periodically sweeped by stream. The additional energy of the flow is spent on the continuous recovery of the vortex zone. Minimal losses correspond to $\alpha \simeq 6^0$. On practice in the sake of diffuser length shortening this angle is usually $\alpha \simeq 8^0 ... 12^0$. At such angles, the visible boundary layer separation from the walls of the diffuser is usually not yet been observed. If $\alpha > 15^0$ it is advisable to perform curved wall of the diffuser with a gradually increasing angle α, so that the pressure gradient along the axis of the force was constant $dp/dx = const$. Reduction of losses may be 40%. Step diffuser with a organized flow separation also gives good result. Reduction of losses in the diffuser at large α can be achieved by suction or blowing boundary layer.

Let the plane flies at a constant speed W_H at a constant altitude H. Then changing the compressor speed, ie, the three different modes of operation of the diffuser can be obtained by changing p_2 (fig. 10.1):

I. Mode without converting speed and air pressure before the diffuser $W_1 = W_H$ and $p_1 = p_H$. Air stream enters the diffuser from the environment without changing of density (section $S_H = S_1$). Feed coefficient $\psi = 1$.

II. Regime with external flow expansion $W_1 > W_H$, $p_1 < p_H$, $\rho_1 < \rho_H$, $\psi = \frac{S_H}{S_1} > 1$. This regime occurs during the p_2 pressure decreasing by means of compressor rotation velocity increasing. Regime II is undesired because it is followed by increased total pressure losses $\sigma_{II} < \sigma_I$ by increasing of λ_1 и λ_2 and appearing of the boundary layer separation on the diffuser entrance due to inflow angle increasing to the leading edge of the diffuser.

III. Regime with external flow compression $S_1 > S_H; \psi = \frac{S_H}{S_1} < 1; W_1 < W_H;$ $p_1 > p_H$; $p_1^* = p_H^*$. This regime occurs during the compressor rotation velocity decreasing and p_2 pressure increasing. Experiments show the optimal mode of operation is a subsonic air intake mode where $W_1 = 0,5W_H$. In this case isentropic gas deceleration appears before the diffuser where nearly 75% of total compression ratio p_2 / p_H of diffuser is realized. Further increase in the compression of air before the diffuser causes an excessive air inflow angles to the leading edge of the diffuser and may cause separation of the boundary layer from the outer surface of the diffuser, which would increase drag. If the diffuser is throttle down completle on the outlet section, air outsid the diffuser will decelerate isentropically and $p_2 = p_H^*$; $\sigma = 1; \psi = 0$. When the throttle is open, air feed ($\psi > 0$) and diffuser losses ($\sigma < 1$) occur.

Diffuser compression ratio $\pi_Д = p_2 / p_H$ depends on diffuser operation regime, M number, section relations S_2 / S_1 and hydraulic losses. Calculations and experiments show that during diffuser normal operation increasing of the expansion ratio S_2 / S_1 more than on 4 is inefficient. So, if $M_1 = 0,75$ and $S_2 / S_1 = 4$: $\pi_Д = 1,32$,if $S_2 / S_1 = 5$: $\pi_Д = 1,33$.

9.2 Diffusers for moderate supersonic velocities

If $M \le 1,5$ common expansion diffusers with sharp edges are used. The next operation regimes of such diffusers are observed (fig. 10.3).

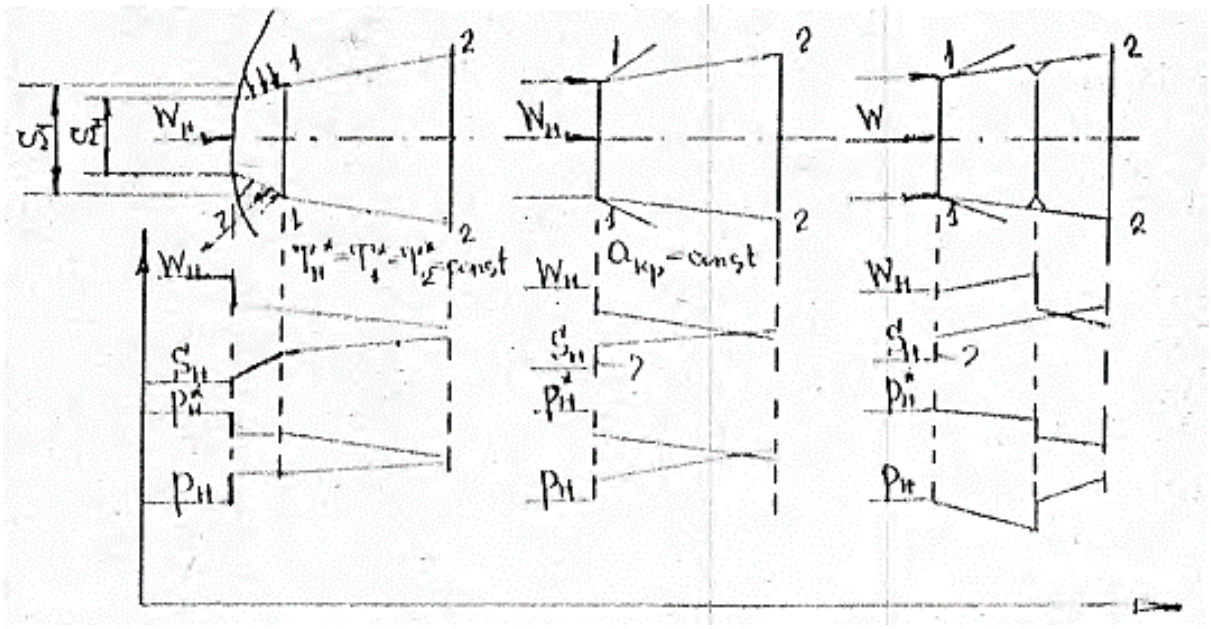

Fig. 9.3 One-step diffuser operation regimes

I. If $\psi < 1$ detached shock wave take place. The jet with $S_H < S_1$ section which enters the diffuser cross the area of the shock wave which is similar to direct one. Subsonic flow $\lambda_1' = 1/\lambda_H$ is isentropically decelerate on the area between shock wave and inlet diffuser section to $\lambda_1 < \lambda_1'$ in subsonic diffuser and then to $\lambda_2 < \lambda_1$. Simultaneously on the jet surface between the shock wave and 1-1 section increased pressure, caused by centrifugal forces of the air particles which are moving on the boundary surface. Projection of this pressure total force on x axis is called additional diffuser resistance.

II. If the air feed coefficient increase to $\psi = 1$ shock wave takes place immediately in the inlet section 1-1 of the diffuser and external flow decelerate in the angle shock waves which corresponds to a minimal external diffuser resistance.

On this regime losses in subsonic diffuser are bigger then on the first regime due to λ_1 and λ_2 caused by feed coefficient decreasing.

III. If air flow rate through section 2 increase due to compression rotation velocity increasing and corresponding decreasing of p_2, supersonic jet with a section $S_H = S_1$ enters the diffuser, accelerate in the expansion channel and decelerate in the more intense shock wave inside the diffuser. Therefore, total pressure $\sigma_{II} < \sigma_I$ loss still increase. On this regime $\psi = 1$ and $W_1 = W_H$. $\psi > 1$ in the supersonic flight is not realized.

Coefficient of the total pressure conservation of the considered gas turbine diffuser is determined by the expression:

$$\sigma = p_2^* \Big/ p_H^* = \frac{p_1^*}{p_H^*} \frac{p_2^*}{p_1^*} = \sigma_{П.С.} \sigma_Д$$

where $\sigma_{П.С.} \sigma_Д$ – total pressure conservation coefficients in the direct shock wave and subsonic diffuser. Total pressure losses in the direct shock wave are small $\sigma > 0,93$ if $M_H \le 1,5$. It allows application of the simplest diffuser with one shock wave.

9.3 Supersonic diffusers

Total pressure losses in the direct shock wave, which are small during M_H slightly bigger then 1, sharply increase with increase of M_H. If $M_H = 2$ we have $\sigma = 0,72$. Due to this total pressure losses gas turbine engine thrust must decrease on 40% in comparison with a gas turbine engine thrust with isentropic compression which make effective flight impossible. Researches show that shock wave losses in supersonic diffuser are decreased during substitution of the strong direct shock wave by the system of weak angle shock waves with further weak direct shock wave. The velocity after these angle shock waves remains supersonic. Consequent

angle shock wave row appears on the supersonic diffuser deceleration surfaces which are place at the angle ω with supersonic flow.

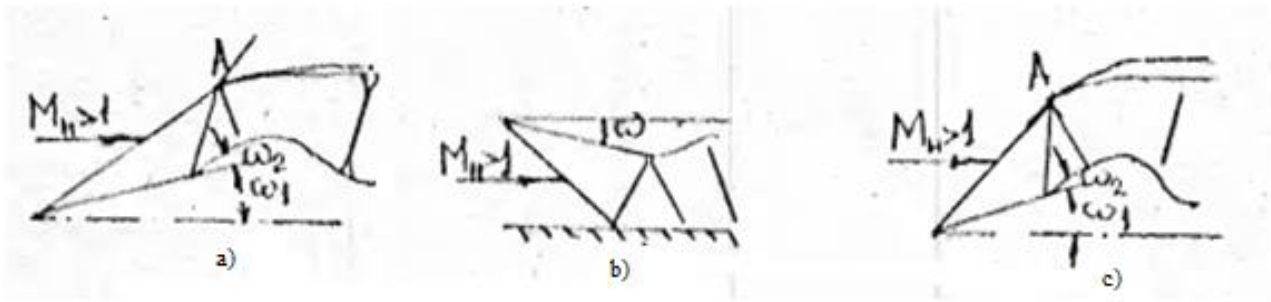

Fig. 9.4 Diffusers:
a) with external compression; b) with internal compression;
c) with mixed compression

Depending on shock wave position relatively on inlet plane, diffusers are divided on three categories:

a) with external compression: angle shock waves are placed before inlet plane;

b) with internal compression: part of the shock waves is placed inside the channel;

c) with mixed compression: part of the shock wave is placed inside the channel and other part is placed outside.

Each type of air inlets has its advantages and disadvantages, which are not considered here. We note only that the figure 10.4 shows that for the same area of the entrance, the air intake of external compression has a maximum external resistance and air intake of internal compression has minimal resistance. Input devices generally are flat or rotationally symmetric. Number of the system shock waves is selected from the high total pressure conservation coefficient σ value condition at calculated M_H flight number in the inlet device of acceptable dimensions, mass. The other condition is regulation with minimal possible amount of the regulated elements.

In an optimal system of external compression all shock waves should converge on the front edge of the shell (Fig. 10.4). In this case maximal values σ_m of the air flow rate ($\psi = 1$) and minimal external resistance are provided.

Researches show that maximal value $(\sigma_m)_{\max}$ for system which consists of m flat shock waves, i.e. from (m-1) angle shock waves and on closing direct shock wave:

$$(\sigma_m)_{\max} = \sigma_1 \sigma_2 ... \sigma_{m-1} \sigma_m .$$

takes place with the same intensity of all angle shock waves

$$\sigma_1 = \sigma_2 ... \sigma_{(m-1)} \sigma_k .$$

It means that for every angle shock waves of the optimal system normal components of the numbers $M_{in}, \lambda_{in} = W_{in} / Q_{i_{kpn}}$, pressure, temperature, density and entropy increasing are the same, i.e.

$$M_{Hn} = M_{1n} = ... = M_{(m-2)n}; \quad p_1 / p_H = p_2 / p_1 = ... = p_{m-1} / p_{m-2};$$
$$T_1 / T_H = T_2 / T_1 = ... = T_{m-1} / T_{m-2}; \rho_1 / \rho_H = \rho_2 / \rho_1 = ... = \rho_{m-1} / \rho_{m-2};$$
$$S_1 - S_2 = S_3 - S_2 = ... = S_{m-1} - S_{m-2}.$$

Closing direct shock wave of the optimal system is much weaker then angle shock waves if $1{,}5 < M_H < 5$:

$$M_{m-1} = 0{,}94 M_{Hn} = 0{,}94 M_H \sin \alpha_H .$$

That is why we get $(\sigma_m)_{\max} = \sigma_k^{(m-1)} \sigma_{II}$.

Consequently, optimal shock waves system calculation for given M_H consists of determination of the deceleration surface angle value determination ω_i and angle shock wave front angle α_i. After that, σ of the every shock wave of the system and, finally, amounts of $(\sigma_m)_{\max}$ are determined. Remained geometric dimensions of the optimal system are determined by the given air flow rate, shock waves placement on the shell and continuity equation.

Diffuser profile is calculated by the values $\omega_1, \sigma_{k2}, M_1$ of the first angle shock wave for different α_H and given M_H. The curve is plotted by the results of the calculation and later used for optimal arrangement parameters determination. On the i-S diagram shock wave air compression on the direct shock wave and three-step system are compared with the same initial conditions. Compression in every weak shock waves is followed by the slight entropy increasing and total pressure decreasing. That's why total losses are less than for direct shock wave $\sigma_{2k+II} > \sigma_{II}$. Correspondingly, air static pressure, density and kinetic energy after compression in the shock wave system are higher and temperature is lower than after compression in the direct shock wave.

If the M_H is between 1,8 and 2,0, the system with two shock waves is used. If M_H is between 2,0 and 2,5, the system with three shock waves is used and etc.

Optimal arrangement of the diffuser correspond to only calculated M_{Hp} number and design engine regime. Arrangement lose its optimum due to the unavoidable deviations of the M_H from the M_{Hp} and engine regimes changing. For example, if $M_H < M_{Hp}$ angle shock waves angles increase and these shock waves are separated from the shell edge and transform to the detached shock wave. It leads to losses increasing, i.e. to decreasing of the air feed $S_H < S_1, \psi < 1$. Besides, interaction of the shock wave with boundary layer causes its separation and unstable operation of the inlet device stall. System optimum suffer also when $M_H > M_{Hp}$.

To provide optimal operation of the inlet device during the different M_H and engines regimes, these device are constructed with regulated elements: changing of the deceleration surfaces angles ω, relative axial displacement of the shell, regulation of the air flow rate by bypassing and boundary layer control.

During supersonic flight subsonic flow in diffuser after the direct shock wave accelerates again in the narrowing channel to $\lambda \simeq 1$ in the inlet device throat and to $\lambda > 1$ in the expansion channel to transform to a subsonic flow $\lambda < 1$ in the direct shock wave. After that subsonic flow decelerate in the expansion subsonic diffuser to a given value $\lambda_\beta \simeq 0,5$ before the compressor. With such organization of the flow slight changing of the engine operation regime and, consequently, volumetric flow rates, influence only on the place of the direct shock wave and does not disturb calculated shock wave system. Closing shock wave acts a positive part of the gas-dynamic regulator for air mass flow rate continuity with changing volumetric flow rate by means of losses changing.

To decrease a harmful effect of the boundary layer to shock waves (separation and distortion) different ways of boundary layer control are applied. The list of them include: draining, suction and refrigeration of the deceleration surfaces.

Chapter 10. MAGNET GAS DYNAMIC THEORY

10.1 Application area

During electrically conducting fluid flowing in the electric and magnetic fields electromagnetic body force appears ,which is sometimes called the ponderomotive force which acts on all the fluid particles. Furthermore, during the passage of electric current through the liquid, Joule heat is generated.

In the study of electrically conducting fluid motion in electric and magnetic fields these two new effects must be taken into account, adding to the equations of motion and energy corresponding two additional terms. This leads to an increase in

the number of variables and the need for a corresponding increase in the number of equations; such additional equations are the equations of Maxwell's electrodynamics. Set of Maxwell's equations, Navier – Stokes equations, which include the electromagnetic body forces, the energy equation including the Joule heat, and the equation of state, is a system of differential equations of magnetic fluid dynamics.

At high temperatures of the order of several thousand degrees and at very low pressures the gases are ionized and therefore electrically conductive, like metals liquid droplets and some other liquid electrolytes. The effects of electric and magnetic fields on an electrically conductive fluid, and the mainstreaming of this influence mentioned above are also applied to ionized gas.

Astrophysics, aircraft and rocket technique and energetic need development of the magnet gas dynamics.

Astrophysicists study the structure of the Sun and other stars, in which the gas is in a highly ionized state under the influence of very high temperatures, as well as "cold" interstellar gas, ionized at very low density.

Modern aircraft and rocket industry manufacture vessels which are fly in the atmosphere with a speed near several kilometers per second. Air temperature near body surface at that speed approaches to electric arc temperature. It phenomenon causes pronounced ionizing of the air. If electric and magnet fields are added to such flow, electromagnet volumetric force appears which with a certain conditions can gain a value comparative to aerodynamic forces.

The feature of the electromagnet volumetric force is, that in contrast with other volumetric forces (gravity, inertial forces), it can be controlled by exposure on the causing electric and magnet fields. Intensity and shape if the shock wave can be influenced by changing of the electromagnet force value. It also allows to increase Reynolds number during the flow transfer from the laminar flow to turbulent one, to decelerate or accelerate electric conductive fluid (or gas) flow, to cause velocity profile deformation and boundary layer separation.

Electric current generator, in which direct transfer from the heat energy to electric one is accomplished, can be created by using electric conductive fluid or gas. Magnetic dispensers, flowmeters and pumps for liquid metals and mercury also find its application.

Nowadays, two areas of magnet gas dynamic are showed up: the first one, which consider infinite electric conductivity of the media (astrophysics) and the second one, which consider finite electric conductivity of the media (technical magnet gas dynamics).

10.2. Electromagnetic fields

Electromagnetic fields in common case are described by the next system of integral Maxweel relations:

1. Relation, which connects magnet field stress vector circulation integral H by the closed circuit l with total force of the direct current, which flow through this circuit area:

$$\oint Hidl = -\int_s j_n dS \qquad (1)$$

2. Relation, which connects total electrostatic induction through the closed surface with area S with total free charge in the *v* volume, which is seized by this surface:

$$\int_s D_n ds = \int_v \rho_{v0} dv \qquad (2)$$

3. Relation, which seized electric field stress vector circulation integral E by the closed circuit l with a time of the magnetic induction flow changing through the area seized by this circuit:

$$\oint Eidl = -\int_s \frac{\partial Bn}{\partial t} dS \qquad (3)$$

4. Magnet induction flow B through the closed surface continuity expression:

$$\int_s B_n ds = 0 \tag{4}$$

This integral relations should be added by expression of the electromagnet fields stress vectors to induction vectors transition:

$$D = \varepsilon_a E,\ B = \mu_B H \tag{5}$$

and consolidated Ohm's law:

$$\text{j} = \sigma_R\{\text{E} + [\text{W X B}]\} \tag{6}$$

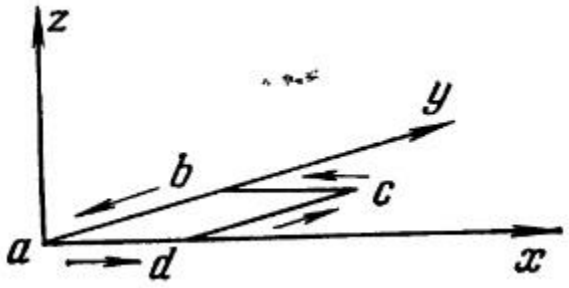

Fig. 10.1 – Coordinate system for Maxwell equations

Not let's express Maxwell equations in the differential form. To do so we need to split them into two systems.

The first system is for direct current magnet field.

Current density projection u is connected only with H_x and H_y projections of the magnet field in the same point of space, because stress lines of magnet fields lie in the plane which is perpendicular to current direction. Stress vector circulation integral by the infinitively small circuit abcd consists of next terms (counterclockwise orientation):

$$\Gamma_{abcd} = -H_y dy + H_x dx + \left(H_y + \frac{\partial H_y}{\partial x} dx\right) dy - \left(H_x + \frac{\partial H_x}{\partial y} dy\right) dx =$$

$$= \left(\frac{\partial H_y}{\partial x} - \frac{\partial H_x}{\partial y}\right) dx dy \tag{7}$$

On the other hand, circulation integral of the H vector should be equal to force of the current, which is flow through this area:

$$\Gamma_{abcd} = I_z = j_z dxdy \tag{8}$$

So, we have:

$$\frac{\partial H_y}{\partial x} - \frac{\partial H_x}{\partial y} = j_z \tag{9}$$

Similarly, for current density projections on the other axis we find:

$$\frac{\partial H_z}{\partial y} - \frac{\partial H_y}{\partial z} = j_x \quad \frac{\partial H_x}{\partial z} - \frac{\partial H_z}{\partial x} = j_y \tag{10}$$

Equations (10) connect conductivity current density j with space derivates of magnet field stress H. If the equation, which connects electrostatic induction vector D c free charge distribution density in the volume p_vo

$$\frac{\partial D_x}{\partial x} + \frac{\partial D_y}{\partial y} + \frac{\partial D_z}{\partial z} = \rho_{v0} \tag{11}$$

to equations (10) we'll get the first Maxwell equations system, which can be presented in vector form as:

$$\text{rotH=j} \quad \text{divD=}\rho_{v0} \tag{12}$$

This system is fair for uniform magnetic materials, which fill entire field, because in this case magnet current field stress does not depend on media magnet penetration.

The second Maxwell equation system is received by using consolidation of the Faraday induction law.

Let's compose an expression for electric field stress circulation integral E by the infinitively small circuit abcd, which is caused by changing of the magnet induction vector *∂B /∂t* , which is perpendicular to E vector, in time:

$$\Gamma_{abcd} = -E_y dy + E_x dx + \left(E_y + \frac{\partial E_y}{\partial x} dx\right) dy - \left(E_x + \frac{\partial E_x}{\partial y} dy\right) dx =$$

$$= (\frac{\partial E_y}{\partial x} - \frac{\partial E_x}{\partial y}) dxdy \qquad (13)$$

Vector E circulation integral by the closed circuit is equal to derivate of the magnet induction through the area, seized by this circuit and taken with negative sign:

$$\Gamma = -\frac{\partial \Phi}{\partial t} = -\frac{\partial B_z}{\partial t} dxdy \qquad (14)$$

Here we have:

$$\frac{\partial E_y}{\partial x} - \frac{\partial E_x}{\partial y} = -\frac{\partial B_z}{\partial t} \qquad (15)$$

Similarly:

$$\frac{\partial E_z}{\partial y} - \frac{\partial E_y}{\partial z} = -\frac{\partial B_x}{\partial t}, \quad \frac{\partial E_x}{\partial z} - \frac{\partial E_z}{\partial x} = -\frac{\partial B_y}{\partial t} \qquad (16)$$

Adding to the equations (15) magnet induction lines continuity equation:

$$\frac{\partial B_x}{\partial x} + \frac{\partial B_y}{\partial y} + \frac{\partial B_z}{\partial z} = 0 \qquad (17)$$

we gain the second Maxwell equation system, which has a next vector form:

$$\text{rote} = -\frac{\partial B}{\partial t}, \quad divB = 0 \qquad (18)$$

In case of non-uniform media on its separate areas boundaries without surface charges and currents the next conditions must be satisfied:

$$\frac{D_{1t}}{\varepsilon_{a1}} = \frac{D_{2t}}{\varepsilon_{a2}} \quad D_{1n} = D_{2n} \qquad (19)$$

$$\frac{B_{1t}}{\mu_{a1}} = \frac{B_{2t}}{\mu_{a2}} \quad B_{1n} = B_{2n} \qquad (20)$$

Let's except vectors of current density j and electric current stress E from the differential equations of Maxwell. Ohm's law transformed into current density field vorticity equation is used for this purpose:

$$\text{rotj} = \sigma_R\{rot\text{E} + \text{rot}\,[\text{W X B}]\}. \quad (21)$$

Equation for magnetic field stress vector vorticity is substituted by equation of the magnetic induction vector vorticity

$$\text{rotB}=\mu_B j \quad (22)$$

As it is known from the field theory:

$$\text{rot rotB}=-\Delta B = -\left(\frac{\partial^2 B_x}{\partial x^2}+\frac{\partial^2 B_y}{\partial y^2}+\frac{\partial^2 B_z}{\partial z}=\right) \quad (23)$$

If σ_R = const, we find that

$$-\Delta B = \mu_B rot\, j = \mu_B \sigma_R \{rotE + rot[W\ x\ B]\} \quad (24)$$

From the equation (18) we have

$$rotE=-\frac{\partial B}{\partial t} \quad (25)$$

Substituting this expression to (24) we get

$$\frac{\partial B}{\partial t} = rot[W\ x\ B] + \frac{1}{\mu_B \sigma_R}\Delta B \quad (26)$$

This equation, which connects magnetic field with velocity field in electric conductive fluid, is called magnetic induction equation. In case of very high media electric conductivity ($\sigma_R \to \infty$) the second term of the right part of the equation (26) can be neglected. After that it gains the next form:

$$\frac{\partial B}{\partial t} = rot[W\ x\ B] \quad (27)$$

This equation is equal to velocity vortex equation in hydrodynamic of the ideal fluid which means that vortex lines are moving together with fluid. Similarly, magnetic fields lines are connected with media and they move together.

The “freezing-in” of the magnetic lines is connected with the fact that during magnetic induction vector flow through the circuit changing, electric currents appear in it and resist to this flow changing. The resistance is stronger, if σ_R is higher. If $\sigma_R \to \infty$ induction flow changing became impossible. Moving along vector line doesn’t affect the field. Vector lines move edgeways together with media.

In case of fixed media (W=0) induction equation has a form of diffusion equation or transient heat conductivity (Fourier equation)

$$\frac{\partial B}{\partial t} = \frac{1}{\mu_B \sigma_R} \Delta B \tag{28}$$

It shows that in the body placed in the magnetic field from outer sources, magnetic field disappear not immediately after turning this sources off. Magnetic stream lines gradually “infiltrate” into the body and weakens.

For example, in a copper sphere of radius 1 m magnetic field decreases as within about 10 seconds: The higher order magnetic conductivity of the field, the weaker field damping.

The value

$$\frac{1}{\mu_B \sigma_R} = \nu_R \tag{29}$$

is similar to transition coefficient in the diffusion and heat conductivity equation and it has dimension similar to kinematic viscosity. That’s why it is called magnetic viscosity. Numerical values of the magnetic viscosity are usually much larger than values of the kinematic viscosity. In common case, when no one term in the right side of the equation cannot be neglected, stream lines aim to move together with media and simultaneously infiltrate the media.

10.3. Magnetic gas dynamic equations

Hydrodynamics (and gas dynamics) equations for electric conductive fluid with presence of electric and magnetic fields unlike hydrodynamic equations of

non-conductive fluid must contain additional term which take electromagnet volumetric force into account. From the magnetic field to the conductor (or conductive fluid) volumetric element dv Ampere force acts in the case when current with density j flow:

$$df_H = [\text{jX B}]\, dv, \tag{30}$$

From the electric field Coulomb force acts on such elements:

$$df_c = E\rho_{c0}dv \tag{31}$$

where ρ_{c0} — charge density in the volume of $dv(\rho_{c0}dv = dq)$.

Thus, total electromagnetic force applied to the volume:

$$df = df_c + df_H = \{\rho_{c0}E + [j\ X\ B]\}\text{dv} \tag{32};$$

Force, applied to the elementary volume:

$$F = \frac{df}{dv} = F_e + F_H = \rho_{r0}E + [j\ X\ B] \tag{33}$$

The estimation of the term order in the equation (32) shows that Coulomb force can be neglected. Thus, with taking (22) into account we get the expression for electromagnetic force, applied to elementary volume:

$$\text{F=[j X B]=}\frac{1}{\mu_B}\text{[rotB X B]} \tag{34}$$

Projections of the electromagnetic force vector to the axes of rectangular coordinate system are:

$$F_x = \left(j_y B_z - j_z B_y\right)\ \ F_y = (j_z B_x - j_x B_z) F_z = (j_x B_y - j_y B_x) \tag{35}$$

or in the other form (with substitution current density vector by magnetic induction vector according to (22))

$$\mu_B F_x = a_y B_z - a_z B_y = B_x \frac{\partial B_x}{\partial x} + B_y \frac{\partial B_x}{\partial y} + B_z \frac{\partial B_x}{\partial z} - 1\backslash 2 \frac{\partial B^2}{\partial x}$$

$$\mu_B F_y = a_z B_x - a_x B_z = B_x \frac{\partial B_y}{\partial x} + B_y \frac{\partial B_y}{\partial y} + B_z \frac{\partial B_y}{\partial z} - 1\backslash 2 \frac{\partial B^2}{\partial y} \qquad (36)$$

$$\mu_B F_z = a_x B_y - a_y B_x = B_x \frac{\partial B_z}{\partial x} + B_y \frac{\partial B_z}{\partial y} + B_z \frac{\partial B_z}{\partial z} - 1\backslash 2 \frac{\partial B^2}{\partial z}$$

Here, $B^2 = Bx^{2+}\ By^{2+}\ Bz^2$ is a value of the magnetic induction vector, a = rotB.

During the (36) expression the condition of the magnetic stream line continuity was used.

Taking force F (34) into account we get an equation of the electric conductive fluid moving in the electric and magnetic fields in vector form (with $\mu = const$)

$$\rho \frac{dW}{dt} = R - gradp + \mu \Delta W + 1\backslash 3 \mu grad(divW) + [j\ X\ B] \qquad (37)$$

or

$$\rho \frac{dW}{dt} = R - gradp + \mu \Delta W + 1\backslash 3 \mu grad(divW) + \frac{1}{\mu_B}[rotB\ X\ B] \qquad (38)$$

For gas the system of differential equation show include energy equation. In case of electric conductive gas placed in the electric and magnetic fields it will take the form of (with $\lambda = const, \mu = const$):

$$\rho \frac{di}{dt} = \frac{dp}{dt} + \lambda \Delta T + \mu \Phi + \frac{j^2}{\sigma_R} \qquad (38)$$

or with taking (22) into account

$$\rho' \frac{di}{dt} = \frac{dp}{dt} + \lambda \Delta T + \mu \Phi + \frac{1}{\mu_B^2 \sigma_R}' [rotB] \quad ^2 \qquad (39)$$

Magnetic induction equation (26)

$$\frac{\partial B}{\partial t} = rot[W\ x\ B] + \frac{1}{\mu_B \sigma_R} \Delta B \qquad (40)$$

hydrodynamic continuity equation

$$\frac{\partial \rho}{\partial t} + div\, \rho W = 0 \qquad (41)$$

and condition equation, which in case of perfect gas is a Clapeyron equation

$$p = f(P, T), \qquad (42)$$

should be added to equations (37) and (38).

System of equation (38) – (42) is a full system of differential equations of the magnetic gas dynamics.

If motion energy is used in the form (37), equation system should include Ohm's law, Maxwell equations (12), (18) and equations (22) and (26).

In these equations Coulomb force is neglected. If we take Coulomb into account we get full system of electromagnetic gas dynamic equations.

For incompressible fluid equations system (37) – (42) is simplified because fluid equations are solved independently from energy equation. The necessity to solve condition equation (42) is no longer exist and continuity equations (41) and motion equations (37) are simplified.

Thus, full system of the incompressible fluid magnetic hydrodynamic equation system in vector form consist of motion equation

$$\rho \frac{dW}{dt} = R - grad\, p + \mu \Delta W + [j\ X\ B] \qquad (43)$$

or

$$\rho \frac{dW}{dt} = R - grad\, p + \mu \Delta W + \frac{1}{\mu_B}[rotB\ X\ B], \qquad (44)$$

energy equation, which is solved independently from the other equations:

$$\rho \frac{dT}{dt} = \lambda \Delta T + \mu \Phi + \frac{j^2}{\sigma_R}, \qquad (45)$$

magnetic induction equation

$$\frac{\partial B}{\partial t} = rot[W\ x\ B] + \frac{1}{\mu_B\, \sigma_R} \Delta B \qquad (46)$$

continuity equation

$$divW=0 \tag{47}$$

If motion and energy equations are used in the form of (44) and (45), to gaining of closed system it is necessary to add Ohm's law equation, Maxwell equations (12) and (18) and equation (22).

Switching to projections to the rectangle coordinates xyz system axes vector motion equation (44) divide to the three motion equation:

$$\rho\left(\frac{\partial u}{\partial t}+u\frac{\partial u}{\partial x}+v\frac{\partial u}{\partial y}+w\frac{\partial u}{\partial z}\right)=-\frac{\partial p}{\partial x}+\mu\left(\frac{\partial^2 u}{\partial x^2}+\frac{\partial^2 u}{\partial y^2}+\frac{\partial^2 u}{\partial z^2}\right)+$$

$$+\left(j_y B_z-j_z B_y\right),$$

$$\rho\left(\frac{\partial w}{\partial t}+u\frac{\partial w}{\partial x}+v\frac{\partial w}{\partial y}+w\frac{\partial w}{\partial z}\right)=-\frac{\partial p}{\partial z}+\mu\left(\frac{\partial^2 w}{\partial x^2}+\frac{\partial^2 w}{\partial y^2}+\frac{\partial^2 w}{\partial z^2}\right)+$$

$$+\left(j_x B_y-j_y B_x\right) \tag{48}$$

$$\rho\left(\frac{\partial v}{\partial t}+u\frac{\partial v}{\partial x}+v\frac{\partial v}{\partial y}+w\frac{\partial v}{\partial z}\right)=-\frac{\partial p}{\partial y}+\mu\left(\frac{\partial^2 v}{\partial x^2}+\frac{\partial^2 v}{\partial y^2}+\frac{\partial^2 v}{\partial z^2}\right)+$$

$$+\left(j_z B_x-j_x B_z\right)$$

Motion equation system by using dependencies (35) and (36) to next form:

$$\rho\left(\frac{\partial u}{\partial t}+u\frac{\partial u}{\partial x}+v\frac{\partial u}{\partial y}+w\frac{\partial u}{\partial z}\right)=-\frac{\partial p_c}{\partial x}+\mu\left(\frac{\partial^2 u}{\partial x^2}+\frac{\partial^2 u}{\partial y^2}+\frac{\partial^2 u}{\partial z^2}\right)+$$

$$+\frac{1}{\mu_B}\left(B_x\frac{\partial B_x}{\partial x}+B_y\frac{\partial B_x}{\partial y}+B_z\frac{\partial B_x}{\partial z}\right),$$

$$\rho\left(\frac{\partial w}{\partial t}+u\frac{\partial w}{\partial x}+v\frac{\partial w}{\partial y}+w\frac{\partial w}{\partial z}\right)=-\frac{\partial p_c}{\partial z}+\mu\left(\frac{\partial^2 w}{\partial x^2}+\frac{\partial^2 w}{\partial y^2}+\frac{\partial^2 w}{\partial z^2}\right)+$$

$$+\frac{1}{\mu_B}\left(B_x\frac{\partial B_z}{\partial x}+B_y\frac{\partial B_z}{\partial y}+B_z\frac{\partial B_z}{\partial z}\right) \tag{49}$$

$$\rho\left(\frac{\partial v}{\partial t}+u\frac{\partial v}{\partial x}+v\frac{\partial v}{\partial y}+w\frac{\partial v}{\partial z}\right)=-\frac{\partial p_c}{\partial y}+\mu\left(\frac{\partial^2 v}{\partial x^2}+\frac{\partial^2 v}{\partial y^2}+\frac{\partial^2 v}{\partial z^2}\right)+$$

$\frac{1}{\mu_B}(B_x\frac{\partial B_y}{\partial x}+B_y\frac{\partial B_y}{\partial y}+B_z\frac{\partial B_y}{\partial z})$

In these equations there is a value of

$$\backslash p_c = p + \frac{B^2}{2\mu_B} \tag{50}$$

which is called effective pressure and it is a sum of hydrodynamic (p) and magnetic ($p_m = \frac{B^2}{2\mu_B}$) pressure.

Note, that in the equations (48) non-electromagnetic forces (gravity etc.) are omitted for sake of brevity.

Vector induction equation (46) in rectangle coordinates system is also divided in three equations:

$$\frac{\partial B_x}{\partial t} = \frac{1}{\mu_B\sigma_R}\left[\frac{\partial^2 B_x}{\partial x^2}+\frac{\partial^2 B_x}{\partial y^2}+\frac{\partial^2 B_x}{\partial z^2}\right]+\frac{\partial uB_x}{\partial x}+\frac{\partial uB_x}{\partial y}+\frac{\partial uB_x}{\partial z}-B_x(\frac{\partial u}{\partial x}+\frac{\partial v}{\partial y}+\frac{\partial w}{\partial z})$$

$$\frac{\partial B_y}{\partial t} = \frac{1}{\mu_B\sigma_R}\left[\frac{\partial^2 B_y}{\partial x^2}+\frac{\partial^2 B_y}{\partial y^2}+\frac{\partial^2 B_y}{\partial z^2}\right]+\frac{\partial vB_y}{\partial x}+\frac{\partial vB_y}{\partial y}+\frac{\partial vB_y}{\partial z}-B_y(\frac{\partial u}{\partial x}+\frac{\partial v}{\partial y}+\frac{\partial w}{\partial z}) \tag{51}$$

$$\frac{\partial B_z}{\partial t} = \frac{1}{\mu_B\sigma_R}\left[\frac{\partial^2 B_z}{\partial x^2}+\frac{\partial^2 B_z}{\partial y^2}+\frac{\partial^2 B_z}{\partial z^2}\right]+\frac{\partial wB_z}{\partial x}+\frac{\partial wB_z}{\partial y}+\frac{\partial wB_z}{\partial z}-B_z(\frac{\partial u}{\partial x}+\frac{\partial v}{\partial y}+\frac{\partial w}{\partial z})$$

In energy equation (38) a term, which take Joule heat into account, can be expressed through the magnetic induction, Maxwell equation (22) should be used for this purpose. As result we get:

$$\rho\frac{dT}{dt} = \frac{dp}{dt}+\lambda\Delta T+\mu\Phi+\frac{1}{\sigma_R\mu_B^2}\,(rotB)^2 \tag{52}$$

where correspondingly with field theory

$$(rotB)^2 = (\frac{\partial B}{\partial x})^2+(\frac{\partial B}{\partial y})^2+(\frac{\partial B}{\partial z})^2 \tag{53}$$

Ohm's law in projection on the coordinate axes has a form of:

$$j_x = \sigma_R[E_x+(vB_z-\omega B_y)]$$

$$j_y = \sigma_R[E_y + (vB_x - \omega B_z)] \quad (54)$$

$$j_z = \sigma_R[E_z + (vB_y - \omega B_x)]$$

If $\rho = const$ hydromagnetic continuity equation has a form of:

$$\frac{\partial u}{\partial x} + \frac{\partial v}{\partial y} + \frac{\partial w}{\partial z} = 0. \quad (55)$$

That's why magnetic induction equations are simplified because the last terms in the right side of these equations are equal to 0.

In many cases motion and induction equations can be significantly simplified, by neglecting one or another small terms.

Often, energy equation is used in the form where enthalpy and kinetic energy are united in total enthalpy. To transform to corresponding magnetic hydrodynamic energy equation form additional motion energy term – electromagnetic force

$$F=[j \text{ X } B] \quad (56)$$

should be used by projection to the axes of the rectangular coordinate system. Later, projection of this vector should be multiplied on corresponding velocity projection. Then gaining products are summarized and we get additional electromagnetic term.

$$f_x u + f_y v + f_z w = [u(j_y B_z - j_z B_y) + v(j_z B_x - j_x B_z) + w(j_x B_y - j_y B_x) =$$
$$= [j_x(wB_y - vB_z) + j_y(uB_z - wB_x) + j_z(vB_x - uB_y)] \quad (57)$$

During this expression composition expressions (35) were used for electromagnetic force terms. In other words, scalar product of the velocity vector ad electromagnetic force vector was presented in the form of:

$$Wf = -j [W \text{ X } B] \quad (58)$$

From the Ohm's law:

$$\frac{j}{\sigma_R} - E = [W\ X\ B] \tag{59}$$

Substituting this expression into the previous equation, we get:

$$\text{W}\cdot\text{f}=-\frac{j^2}{\sigma_R} + jE \tag{60}$$

If this additional term. which represent electromagnetic force work, is summarized with Joule heat

$$Q_e = \frac{j^2}{\sigma_R} \tag{61}$$

we get final expression for additional “electromagnetic” term of energy equation

$$Q_H = \text{j} \cdot \text{E}. \tag{62}$$

Then, gas energy equation with presence of electromagnetic field is written in the form of:

$$\rho \frac{di^*}{dt} = \frac{\partial p}{\partial t} + \lambda \Delta T + \mu \Delta \left(\frac{W^2}{2}\right) + \frac{1}{3}\mu (W\nabla) divW + \frac{1}{3}\mu (divW)^2 + 2\mu\Omega + jE \tag{63}$$

In many cases, work of the electromagnetic forces is represented in other form, which can be gained by substitution (22) of current density in scalar product (62) by magnetic induction

$$Q_H = \frac{E}{\mu_B} rotB \tag{64}$$

and by using known expression from the field theory

$$\text{div[E X B]=B rote-ErotB}. \tag{65}$$

In case of steady magnetic field ($\frac{\partial \text{B}}{\partial \text{t}} = 0$) from (18) we know that rot E = O, and correspondingly

$$\text{ErotB= – div [E X B]}. \tag{66}$$

Sunstituting this result to (64) we go on next expression for additional electromagnetic term in the energy equation:

$$Q_H = -\frac{1}{\mu_B} div \text{ [E x B]}. \quad (67)$$

After the substitution in the (63) of the last term by expression (67) we get another energy equation form for magnetic gas dynamics:

$$\rho \frac{di^*}{dt} = \frac{\partial p}{\partial t} + \lambda \Delta T + \mu \Delta \left(\frac{W^2}{2}\right) + \frac{1}{3}\mu (W\nabla) divW + \frac{1}{3}\mu (divW)^2 + 2\mu\Omega -$$

$$-\frac{1}{\mu_B} div \text{ [E x B]}. \quad (68)$$

In steady state and without viscosity and heat conductivity, energy equation (68) has a form of:

$$\rho \frac{di^*}{dt} = -\frac{1}{\mu_B} div \text{ [E x B]}. \quad (69)$$

After appearance of the additional term in the electric conductive fluid motion in the magnetic field equation (48) the necessity to add new similarity criteria, which takes relation of magnetic field to inertial field into account, appears. Lets transform the last term of equation (82) right side to a non-dimensional form by dividing it to the value of $\rho_0 U_0^2 \backslash l$. As result we get

$$\frac{j_0 B_0 l}{\rho_0 U_0^2} \left(\frac{j_y B_z}{j_0 B_0} - \frac{j_z B_y}{j_0 B_0}\right) \quad (70)$$

here l is characteristic dimension; ρ_0, U_0, j_0, B_6 – are fluid density, velocity, current density and magnetic induction j values in same characteristic flow point. If electromagnetic force is written as in motion equation (49), corresponding term of this equation can be presented in non-dimension form as:

$$\frac{B_0^2}{\mu_B \rho_0 U_0^2} \left[\frac{B_x}{B_0}\frac{\partial \frac{B_x}{B_0}}{\partial \frac{x}{i}} + \frac{B_y}{B_0}\frac{\partial \frac{B_x}{B_0}}{\partial \frac{y}{i}} + \frac{B_z}{B_0}\frac{\partial \frac{B_x}{B_0}}{\partial \frac{z}{i}} - \frac{1}{2}\frac{\partial (\frac{B}{B_0})^2}{\partial \frac{x}{i}}\right] \quad (71)$$

It is obvious, that dynamic similarity of the model bypassing and full-scale object in electric conductive fluid with presence of the external magnetic field require for model and object similar values of:

$$\frac{j_0 B_0 l}{\rho_0 U_0^2} = S_j = idem \tag{72}$$

or with taking $j_0 \approx \frac{1}{\mu_B}\frac{B_0}{i}$ into account according to (65) we have

$$\frac{B_0^2}{\mu_B \rho_0 U_0^2} = S_B = const \tag{73}$$

This multiplier characterize relation of the magnetic and kinetic energy of the elementary volume. Value A = $\sqrt{S_B}$ is called Alfven number. Of course it is necessary to other hydrodynamic similarity criteria (numbers of Strouhal, Froude, Mach and Reynolds) to be the same.

Considering that with finite conductivity according to the Ohm's law current density which is inducted by magnetic field is proportional to the relation

$$\sigma_{R0} U_0 \; B_0 \sim j_0 \tag{74}$$

we can gain from the (72) the magnet-hydrodynamic interaction criterion, whch express the relation of magnetic force from the inducted currents to inertial force

$$S_0 = \frac{\sigma_{R0} B_0^2 l}{\rho_0 U_0} = idem \tag{75}$$

S_o value is called magnetic-hydrodynamic interaction criterion.

By non-dimensionalizing of the Ohm's law terms:

$$\frac{j_x}{j_0} = \frac{\sigma_{R0} E_0}{j_0}\frac{\sigma_R}{\sigma_{R0}}\left[\frac{E_x}{E_0} + \frac{U_0 B_0}{E_0}\left(\frac{v B_z}{U_0 B_0} - \frac{w B_y}{U_0 B_0}\right)\right] \tag{76}$$

If j0 is conductivity current in characteristic point; $j_0 = \sigma_{R0} E_0$. Then we have:

$$\frac{j_x}{j_0} = \frac{\sigma_R}{\sigma_{R0}}\left[\frac{E_x}{E_0} + \frac{U_0 B_0}{E_0}\left(\frac{v B_z}{U_0 B_0} - \frac{w B_y}{U_0 B_0}\right)\right] \tag{77}$$

Here the relation of the current inducted by magnetic field to current of external electric field is determined with $\sigma_R = \sigma_{R0}$ by non-dimensional criterion:

$$\Pi = \frac{U_0 B_0}{E_0} = \frac{U_0}{E_0 \backslash B_0} = \frac{U_0}{W_д} \tag{78}$$

Here $W_д$ is a drift velocity. The value

$$Э = \frac{S_0}{\Pi}, \tag{79}$$

which characterizes the relation of the electromagnetic force from the current applied from the external to inertial forces, is called electric-hydrodynamic interaction criterion.

By non-dimenionalizing of the magnetic induction equation (51) we have:

$$\frac{l}{i_0 U_0}\frac{\partial \frac{B_x}{B_0}}{\partial \frac{i}{i_0}} = \frac{1}{\mu_B \sigma_R l U_0}\left[\frac{\partial^2 \frac{B_x}{B_0}}{\partial\left(\frac{x}{l}\right)^2} + \frac{\partial^2 \frac{B_x}{B_0}}{\partial\left(\frac{y}{l}\right)^2} + \frac{\partial^2 \frac{B_x}{B_0}}{\partial\left(\frac{z}{l}\right)^2}\right] + \frac{\partial^2 \frac{uB_x}{U_0 B_0}}{\partial\left(\frac{x}{l}\right)^2} + \frac{\partial^2 \frac{uB_x}{U_0 B_0}}{\partial\left(\frac{y}{l}\right)^2} + \frac{\partial^2 \frac{uB_x}{U_0 B_0}}{\partial\left(\frac{z}{l}\right)^2} -$$

$$- \frac{B_x}{B_0}\left[\frac{\partial^2 \frac{u}{U_0}}{\partial\left(\frac{x}{l}\right)^2} + \frac{\partial^2 \frac{v}{U_0}}{\partial\left(\frac{y}{l}\right)^2} + \frac{\partial^2 \frac{w}{U_0}}{\partial\left(\frac{z}{l}\right)^2}\right] \tag{80}$$

In the left side of (80) known non-dimensional criterion (Strouhal number) is placed. In the right side new non-dimensional multiplier appear. The inverse value of the multiplier is called magnetic Reynolds number:

$$R_H = \mu_B \sigma_R l U_0 \ = \frac{l U_0}{v_H} \tag{81}$$

This criterion characterizes relation of the magnetic field from the inducted currents to applied external magnetic field. Sometimes, relation of the magnetic Reynolds number to usual Reynolds number, i.e. magnetic Prandtl number, is used

$$Pr_m = \frac{R_H}{R} = \mu_B \sigma_R v = \frac{v}{v_H} \tag{82}$$

which represents the relation of the common viscosity to magnetic viscosity. If the magnetic-hydrodynamic interaction criterion is multiplied on the Reynolds number

we get the relation of the magnetic force from the field inducted by magnetic current to the viscosity force:

$$S_0 R = \frac{\sigma_R l B_0^2}{\rho_0 U_0} \frac{l U_0}{v} = \frac{\sigma_R l B_0^2}{\rho_0 v} \quad (83)$$

Square root from this value is called Hartmann number

$$\text{Ha} = l B_0 \sqrt{\frac{\sigma_R}{\mu}} \quad 84)$$

Here $\mu = \rho_0 v$ is dynamic viscosity coefficient. during Hartmann number determination opposite channel dimension is used as characteristic dimension. Hartmann number is a main similarity criterion in such magnetic-hydrodynamic tasks where viscous forces acts prime role.

Only three of listed additional criteria of magnetic hydrodynamics are mutually independent (for example, numbers П, Ha and Rн). The rest parameters (S, Э, Pr_m) can be gained from the expressions mentioned above.

At some values of the certain criteria system of the magnet hydrodynamics equations assume simplification. If Rн<1, magnetic fields from the inducted currents can be neglected and we can assume that current occurs only due to external magnet field action. Such flows take place in magnet hydro- and gas dynamics of channels (moving with presence of the electromagnetic fields of technical plasma or liquid metals in tubes, channels of magnetic pumps and magnetic gas dynamics generators of electric current) and in case of body bypassing when electric conductivity of the media is not large.

If $R_н > 1$ magnetic field became frozen in media and move with it. This area of magnet gas dynamics finds its application in astrophysics which deals with very extensive spaces of very rarefied interstellar gases or with very heated conductive stellar material, which is heated to several millions degrees (for example, solar prominence).

During the laboratory experiments with liquid metals Rн is usually equal to 0,01—0,1, and Hartmann number can reach several hundreds. In experiments with

technical plasma (temperatures near 10^4 K) it is possible to reach Rн value equal to 1, because Π number can be more or less, than 1.

10.4. Magnet gas dynamics equations for elementary jet.

The conception of the elementary jet in magnet gas dynamics doesn't find such universal application as in usual gas dynamics because only in several cases the values and directions of electric field intensity and magnetic induction vectors as well as vector of current density and electromagnetic force.

There are two examples of magnet gas dynamics flow where elementary jet conception is strictly fair.

1. Channel with a constant section area $\boldsymbol{z}$ = ±a, which is generated by two parallel walls where in the x direction electric conductive gas flow. The walls of the channel are opposite electrodes with infinite conductivity. Viscosity and heat conductivity are not taken into account.

If difference of potentials are kept on the walls electric current j_z,which induces its own magnetic field, appears. Stream lines of such field are directed perpendicularly to the flow plane (to y axis) accordingly to Ampere rule.

Flow in such channel is equivalent to flow of the elementary jet, which is placed in constant crossed electromagnetic fields W(u,0,0), E(0,0,Ez), B(0,B_y, 0), f(f_x, 0,0).

2. Uniform gas flow before and after magnet gas dynamics wave (with lines of magnetic induction, which are perpendicular to the flow direction). Let's write the magnetic gas dynamics equations for elementary jet neglecting viscosity and heat conduction. Let's consider fluid moving and magnetic field steady and vector [E X B], which determines electromagnetic force work, is directed in parallel in velocity vector W. In this case vector flow [E X B] is directed normally to opposite jet flow.

As it is known from the field theory

$$div[E\ x\ B] = \lim_{\Delta v \to 0} \frac{1}{\Delta v} \int_S [E\ x\ B] n dS \qquad (85)$$

where Δv is volume, which is seized by the closed surface S. Vector [E X B] $_{\text{п}}$ flow is directed through this surface and n is external surface normal to a surface S. In our case, with infinity small volume Δv we have

$$\int_S [ExB]dS = \Delta([ExB]_l F) . \quad (86)$$

Here F is a flow section area, l index points to vector [E X B] projection to stream line. Volume of the jet with dl length is equal to *dv=Fdl,* so

$$div[E\ x\ B] = \frac{1}{F}\frac{d}{dl}[(E\ x\ B)_l F] \quad (87)$$

Substituting this expression to the energy equation (94) b considering that *W=dl\dt* we have:

$$\rho WF\frac{di^*}{dl} = -\frac{1}{\mu_B}\frac{d}{dl}([E\ x\ B]_l F) \quad (88)$$

Because fluid mass flow rate

$$\rho WF = G_{cek} = const \quad (89)$$

along the stream line doesn't change, after integration we have:

$$\rho WFi^* + \frac{1}{\mu_B}[E\ x\ B]_l F = const . \quad (90)$$

From this expression we get effective value of total heat content

$$i_c^* = i^* + \frac{[E\ x\ B]_l}{\mu_B \rho W} = const \quad \text{or} \quad i_c^* = i \quad + \frac{[E\ x\ B]_l}{\mu_B \rho W} + \frac{W^2}{2} = const \quad (91)$$

So, effective value of the total heat content i_B^*, which include electromagnet energy, remains constant along the stream line, if electromagnetic energy flow is directed along velocity vector.

In case of E=0 or if vectors of electric magnetic fields intensity are parallel, equation (91) represents total heat content continuity condition for energetically isolated jet. Vector E can be excluded from the energy equation.

$$\text{E=(v}_{\text{H}}\text{rotB-[W x B])} \quad (92)$$

which leads to

$$[E \times B] = (V_H [\text{rot}B \times B] - \{[W \times B] \times B\}). \quad (93)$$

In projection to stream line direction we get:

$$[E \times B]_x = \{V_H [\text{rot}B \times B]_x + u(B_y^2 + B_z^2)\} \quad (94)$$

Here assumed that x axis is directed along the jet *(v= w=*0). Substituting last expression in (91) we get energy equation for jet if E_|_W and B_|_W:

$$i_c^* = i^* + \frac{v_H}{\mu_B \rho W} [rotB \; x \; B]_x + \frac{B^2}{\mu_B \rho} = const \quad (95)$$

Expression (95) can be simplified because all parameters in the opposite section of the elementary jet are considered constant. Indeed in this case ***(V = w = B_x = B_z = E_x = E_y = 0,*** т. е. W= ***u, B = B_y, E = E_z)*** terms of the magnetic induction rotor:

$$rot_x B = \frac{\partial B_z}{\partial y} - \frac{\partial B_y}{\partial z} = 0,$$

$$rot_y B = \frac{\partial B_x}{\partial z} - \frac{\partial B_z}{\partial x} = 0, \quad (96)$$

$$rot_z B = \frac{\partial B_y}{\partial x} - \frac{\partial B_x}{\partial y} = \frac{\partial B}{\partial x}$$

and term of the vector product

$$[\text{rot B} \times B]_x = (\text{rot}_y B) B_z - (\text{rot}_z B) B_y = -B\frac{\partial B}{\partial x} = -\frac{1}{2}\frac{dB^2}{dx} \quad (97)$$

Substituting this expression to (95) we can get the next form of the energy equation for the jet placed in the crossed electromagnetic fields:

$$i_c^* = i^* + \frac{v_H}{\mu_B \rho W}\frac{dB}{dx} + \frac{B^2}{\mu_B \rho} = const \quad (98)$$

If gas has a very high conductivity ($\sigma_R \to \infty, v_H \to 0$**),** last term in the (98) equation can be neglected. After that condition of effective total heat content continuity for jet in crossed fields is written as

$$i_c^* = i^* + \frac{B^2}{\mu_B \rho} = const \tag{99}$$

Magnetic induction equation (51) applied to elementary jet is significantly simplified.

Only one term of the current density in energy equation in crossed electromagnetic field ($B_x = B_z = E_x = = E_y = v = w =$ д/ду = д/дz = 0, W = и, B =B_y, E = $E_г$, j =j_z) is saved

$$j_z = \sigma_R(E_z + uB_y) . \tag{100}$$

From the Maxwell equation (27) for stationary field $(\partial B/\partial t = 0)$ we have

$$E = E_z = \text{const} \tag{101}$$

and from the Maxwell equation (22) we have

$$j_z = \frac{1}{\mu_B} rot_z B = \frac{1}{\mu_B}\frac{dB_y}{dx} \tag{102}$$

Here we have induction equation for jet in opposite crossed field

$$uB_y = \frac{1}{\mu_B \sigma_R}\frac{dB_y}{dx} + const \tag{103}$$

where

$$\text{const} = —E_z \tag{104}$$

If the gas conductivity is very high (($\sigma_R \to \infty$), magnetic induction for elementary jet placed in the opposite magnetic field equation transform to very simple form:

$$uBy = \text{const} \tag{105}$$

In case of non-viscous fluid (μ = 0, p = const) it is possible to gain another energy equation form for elementary jet. Motion equation (49) is used for this purpose which in projection to jet direction *(W=u, v = w =* 0) with opposite magnetic field *(B =* B_y, $B_x = B_z = 0$) has a next form:

$$\rho u \frac{\partial u}{\partial x} = -\frac{\partial}{\partial x}\left(p + \frac{B^2}{2\mu_B}\right) \tag{106}$$

After integration of (106) we have

$$p_c^* = p + \rho \frac{u^2}{2} + \frac{B^2}{2\mu_B} = const \tag{107}$$

or

$$p_c^* = p^* + \frac{B^2}{2\mu_B} = const. \tag{108}$$

Equation (108) is Bernoulli equation for the jet of incompressible electric conductivity fluid which is placed in opposite magnetic field. The third term of this equation is called magnetic pressure $p_m = \frac{B^2}{2\mu_B}$. After summarizing of the p_m with total pressure p^* we get effective total pressure p_c^* which is constant along the jet length.

If jet is affected by the direct-axis magnetic field *(B =* B_X, *By =* B_z *= 0)*, integration of the (49) equation lead to usual (hydraulic) form of the Bernoulli equation:

$$p + \rho \frac{u^2}{2} = p^* = const \tag{109}$$

because during this:

$$-\frac{\partial}{\partial x}\left(\frac{B^2}{2\mu_B}\right) + \frac{1}{\mu_B} B_x \frac{\partial B_x}{\partial x} = 0 \tag{110}$$

Let's compose momentum equation for jet placed in the electromagnetic fields. Common form of the momentum equations for elementary jet is fair for all cases of motion:

$$P_x = G(u_2 - u_1) \quad (111)$$

Taking magnetic field action into account is that projection of the total force is divided into two parts:

$$Px = Pxp + Pxm, \quad (112)$$

where P_{xp} is a projection of the all hydrodynamic forces, P_{xm} is a projection of electromagnetic volumetric forces, applied on the jet 1-2 area.

Projection of the electromagnetic force, applied to the elementary volume, according to (34) is equal to

$$f_x = [j\ x\ B]_x = \frac{1}{\mu_B}[rot\ B\ x\ B]_x \quad (113)$$

Projection of the force, acting on the elementary volume, on the x axis is equal to

$$dP_{xm} = f_x F dx \quad (113)$$

here F is an area of the jet opposite section, dx is a length of its elementary area (in the direction of velocity vector u),

Elementary force, acting on the jet 1-2 area, projection is

$$P_{xm} = \int_1^2 \frac{F}{\mu_B}[rot\ B\ x\ B]_x dx \quad (114)$$

Electromagnet force, applied to the finite area of elementary jet of constant section with opposite magnetic field, is equal to

$$P_{xm} = \frac{F}{2\mu_B}(B_1^2 - B_1^2) \quad (116)$$

The force of the hydrodynamic pressure in this case is equal to:

$$P_{xm} = F(p_1 - p_2) \quad (117)$$

Because of that momentum equation for elementary jet of constant section with opposite magnetic field has a next form:

$$Pxp + Pxm = G(u_2 - u_1) \quad (118)$$

Here, according to continuity equation ($G = \rho u F = const$) we have:

$$p_1 - p_2 + \frac{(B_1^2 - B_1^2)}{2\mu_B} = \rho_1 u_1 (u2 - u1) = \rho_2 u_2^2 - \rho_1 u_1^2 \quad (119)$$

Introducing effective pressure, which is equal to hydrodynamic and magnetic pressure sum, to (119) equation

$$p_c = p + p_m = p + \frac{B^2}{2\mu_B} \quad (120)$$

we transform momentum equation for the elementary jet of constant section with opposite magnetic field to next simplest form:

$$p_{c1} + \rho_1 u_1^2 = p_{c2} + \rho_2 u_2^2 \quad (121)$$

Sometimes, it is comfortable to present momentum equation in the next form:

$$p + \frac{B^2}{2\mu_B} + \rho \ u^2 = const \quad (122)$$

Momentum equation (122) on the contrary from the Bernoulli equation (108) is suitable not only for incompressible fluids but also for gases, i.e. media with changing density.

10.5. Action inversion condition for gas flowing in the electromagnetic field

Let's consider steady 1-d flow ($W(x) = (u, 0, 0)$) of non-viscous and non-heat-conductive gas with finite conductivity in opposite crossed magnet and electric fields.

Assuming, that inducted magnetic field can be neglected, let's specify distribution of the section-mean values of the electric field intensity and magnetic induction along the channel with changing section length $E(x) = (0, E_y, 0)$, $B(x) = (0, 0, B_z)$. It allows solving the task without introducing Maxwell's equations.

Derivating continuity equation

$$\rho u F = const = G \tag{123}$$

by the direction of motion we get

$$\frac{1}{\rho}\frac{d\rho}{dx} + \frac{1}{u}\frac{du}{dx} + \frac{1}{F}\frac{dF}{dx} = 0 \tag{124}$$

Similarly from the condition equation for ideal gas we have

$$\frac{d\rho}{dx} = R\rho\frac{dT}{dx} + \frac{a^2}{k}\frac{d\rho}{dx} \tag{125}$$

Motion equation (49) for 1-d flow of non-viscous and non-heat-conductive gas with opposite electromagnetic fields can be transformed to form of:

$$\rho u\frac{du}{dx} + \frac{dp}{dx} = \sigma_R[E - uB]B \tag{126}$$

Energy equation of such 1-d flow we get from (63) and (54)

$$\rho u\frac{di^*}{dx} = \sigma_R[E - uB]E \tag{127}$$

Considering that $i^*=i+u^2\backslash 2$, $R=c_p-c_v$ and $c_p = \kappa c_v$ energy equation (127) with при c_p = const has a next form:

$$\frac{k}{k-1}R\rho u\frac{dT}{dx} + \rho u^2\frac{du}{dx} = \sigma_R E[E - uB] \tag{128}$$

In these equations all parameters depend only on velocities of the magnetic and electric fields with $u(x)$ velocity directed to x axis and intensities of the magnetic and electric fields are directed perpendicularly to each other and to motion direction. Let's consider functions B_z and E_y and also F(x) as describing channel section area are set.

System of equations (124)-(127) in common case cannot be solved in explicit form but it helps to determine how velocity and Mach number derivatives depend on main task parameters.

Excluding from (125) and (129) temperature gradient we gain:

$$\frac{k}{k-1}\left(\frac{dp}{dx}-\frac{a^2}{k}\frac{d\rho}{dx}\right)+\rho u\frac{du}{dx}=\frac{\sigma_R E}{u}[E-uB] \qquad (129)$$

Substituting density gradient in this expression by (124) we get an expression:

$$(M^2-1)\frac{1}{u}\frac{du}{dx}=\frac{1}{F}\frac{dF}{dx}-\frac{k}{\rho a^2}\frac{\sigma_R E}{u}\left(\frac{E}{B}-u\right)\left(\frac{E}{B}\frac{k-1}{k}-u\right) \qquad (131)$$

which shows how changing of the section area and factor that reflect electromagnetic field behavior (second term in the right side) influence on changing of the velocity along the channel length.

If electromagnetic field is absent, equation (131) is transformed into the known relation for the Laval nozzle. If terms which characterize changing of the mass flow rate, friction work, addition of heat and mechanical work are added equation (131) by some elementary transformations can be transformed to inverse condition.

$$(M^2-1)\frac{1}{u}\frac{du}{dx}=\frac{1}{F}\frac{dF}{dx}-\frac{1}{G}\frac{dG}{dx}-\frac{1}{a^2}\frac{dL}{dx}-\frac{k-1}{a^2}\frac{dQ_{\text{нар}}}{dx}-\frac{k}{a^2}\frac{dL_{\text{тр}}}{dx}-$$

$$\frac{k}{\rho a^2}\frac{\sigma_R E}{u}\left(\frac{E}{B}-u\right)\left(\frac{E}{B}\frac{k-1}{k}-u\right) \qquad (132)$$

The term, which takes electromagnetic action into account, in equation (132) is differ from the rest terms of this expression because it includes the values of real parameters rather than their derivates and, besides, his value depends on absolute gas velocity and pressure values and its sign is determined by product of two differences: the first is difference between gas velocity *u* and drift velocity $W_Д=E/B$, and the second one is difference between gas velocity and next velocity

$$U_1=\frac{E}{B}\frac{k-1}{k}=W_Д\frac{k-1}{k} \qquad (133)$$

Thereby, if all actions except for the electromagnetic are neglected, i.e. considering ideal 1-d flow in the heat isolated channel of constant section with

presence of crossed electromagnetic fields, inverse condition for velocity derivate can be written as:

$$(M^2-1)\frac{du}{dx} = -\sigma_R E \frac{k}{\rho a^2}(u-U1)(u-W_Д) = \frac{\sigma_R B^2}{p}(u-U1)(u-W_Д) \quad (134)$$

During the gas flow with drift velocity inducted electric field is equal and opposite to applied that results in absence of the current through the gas and magnetic hydrodynamic interaction. As it can be seen, with constant value of the electromagnetic action the sign of velocity derivate is changed during the transfer from the subsonic flow (M<1) to supersonic (M>1) and vice versa.

Inverse condition for Mach number derivate along the channel length can be expressed the same way. In case of dF\dx≠ 0 we have similar to (131) expression:

$$(M^2-1)\frac{1}{M\left(1+\frac{k-1}{2}M^2\right)}\frac{dM}{dx} = \frac{1}{F}\frac{dF}{dx} - \frac{k}{\rho a^2}\frac{\sigma_R B^2}{u}\left(\frac{E}{B}-u\right)\left(\frac{E}{B}\frac{1+kM^2}{\frac{2k}{k-1}+kM^2}-u\right) \quad (135)$$

For channel with constant section *(dF\dx=0*) we have:

$$(M^2-1)\frac{1}{\left(1+\frac{k-1}{2}M^2\right)}\frac{dM}{dx} = -\frac{k}{\rho a^3}\sigma_R B^2(u-W_Д)(u-U_2) =$$

$$-\frac{\sigma_R B^2}{ap}(u-U2)(u-W_Д) \quad (136)$$

where

$$U_2 = U_1\frac{1+kM^2}{2+(k-1)M^2} = W_Д\frac{1+kM^2}{kM^2+\frac{2k}{k-1}} \quad (137)$$

Thereby. in expression for dM/dx new characteristic velocity U2 which value depends on Mach number appear.

With the help of (135) and (136) diagram of possible 1-d gas flow regimes in crossed electric and magnetic fields. Velocity values are on the horizontal axis and Mach number values are on the vertical axis. Direct lines *u=U1*,u=Wд, M=1 and curve U2(M) divide plane on the next areas:

I. $M > 1$	II. $M < 1$
$A_1 \cdot W_д < u$	$A_2 \cdot W_д < u$
$B_1 \cdot U_2 < u < W_д$	$B_2 \cdot U_1 < u < W_д$
$C_1 \cdot U_1 < u < U_2$	$C_2 \cdot U_2 < u < U_1$
$D_1 \cdot u < U_1$	$D_2 \cdot u < U_2$

Consider u and M known in some section x. During displacement along x axis this parameters are changing in such way that in the areas A_1, B_2 and D_1 displacement takes place to the left and down, in the areas *A2, B1, B2* — displacement takes place to the up and in the areas *C1* и *C2* – to the left and up.

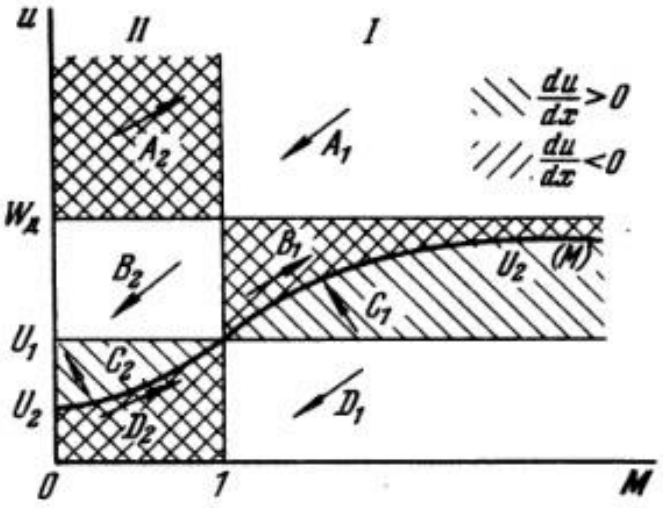

Fig. 10.1. Possible regime of the 1-d flow in crossed electromagnetic fields

From the equation (194) it is known, that on the lines $u = W_Д$ and $u = U1$ smooth transfer across the value of M =1 in the first point in the M increasing direction and in the second similar transfer in the M decreasing direction is possible.

In the C_1 and C_2 areas flow acceleration with decreasing of the M number takes place. Here speed of sound increases faster than flow velocity.

The received results are easily explained if we note that electromagnetic field influence to the gas flow results in mechanical work of electromagnetic force, applied to an elementary volume

$$—F \cdot W = —W \cdot [j \times B] \quad (138)$$

and in addition of the Joule heat. The total energy with taking this heat into account in elementary volume will be equal to

$$Q_H = Ej \quad (139)$$

In considered 1-d case the relation of mechanical work to total energy is equal to

$$\Pi = \frac{\sigma_{R[E-uB]uB}}{\sigma_{R[E-uB]E}} = \frac{u}{W_Д} \quad (140)$$

If $u > W_д$ mechanical work of the electromagnetic force exceed changing of the gas total energy, i.e. mechanical work is partially transfer to electromagnetic field energy in the form of current, which can work in the outer circuit of the generator. If $u<W_д$, energy of the electromagnetic field is transferred to a gas as mechanical work or heat (pump or accelerator).

In first case electromagnetic force is directed against gas motion, in the second –case it is directed along the gas motion. In the second case, if Π close to 1, field action is represented by electromagnetic forces work, and if if Π close to 0, they are represented by heat adding.

If $u=U_1$, i.e. $\Pi = U_1/W_Д$, heat and mechanical actions of the electromagnetic fields are compensated. That's why gas velocity doesn't change $(du/dx =0)$. If $u = W_Д$ both actions are equal to 0 so dи/dx = 0 again. Line $u = U_2$ feature is that in the point of its intersections with u(M) curves changing of the speed of sound values are proportional to gas velocity values changing, so Mach number derivate by channel length is always equal to 0 if $u = U_2$. Transfer across the $u = U_2$ on the fig. 13.20 line is possible only in vertical direction (if M=const).

Chapter 11. NUMERICAL METHODS IN GAS DYNAMICS

11.1 Analysis of the fluid motion equation and methods of its solving

Fluid mechanics is based on the assertions of classical Newtonian mechanics, thermodynamics, and the hypothesis of continuity.

The first assertion implies that the study of motion with velocities small compared to the speed of light, and macroscopic objects are considered whose dimensions are much greater than the size of the microcosm.

The second assertion suggests that in a neighborhood of each point the liquid is in a state of thermodynamic equilibrium or close to it, so you can use the thermodynamic laws.

Finally, the third statement involves replacing the real fluid (gas) with its discrete molecular structure model of continuous distribution of matter on the considered volume. According to the hypothesis of the continuity the fluid is modeled by a continuous solid medium. From a mathematical point of view this means that the functions characterizing the state of the environment should be sufficiently smooth, ie, continuous and differentiable in space and time. Discontinuity is allowed only on separate lines or surfaces. Continuity hypothesis combines liquids and gases in a single category of fluid easily deformable media.

In solid mechanics either concentrated or distributed forces are considered. In fluid mechanics only distributed forces are applied because concentrated force application leads to fluid discontinuity.

To characterize the mass forces entered the stress vector of mass forces J, having the dimension of acceleration. Expanding the vector J along the coordinate axes (unit vectors), we obtain:

$$J = iX + jY + \kappa Z,$$

where X, Y, Z – the projection of the mass forces on the coordinate axes (single mass forces), and i, j, k – unit vectors.

During mass forces considering stress vector of the surface force in the fluid point p_n, numerically equal to pressure, is introduced.

In general, the p_n depends not only on the position of the point on the surface (the coordinate x, y, z) and time t, but also on the orientation in space area ΔS, i.e. $\vec{p}_n = (x, y, z, t, \vec{n})$.

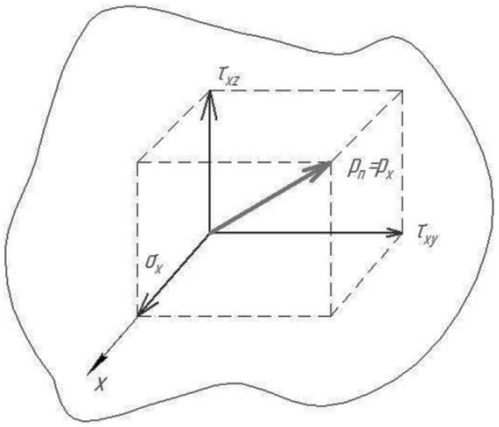

Fig. 11.1 – Elementary volume

Consequently, p_n stress is not usual vector because it can reach different values depending on area placement. If its position is fixed, p_n will be usual vector wich can be expanded along coordinate axes. For example, area perpendicular to *Ox* axis is chosen. Stress vector $p_n = p_x$ in common case doesn't coincide with surface normal n direction (in this case with *Ox* axis direction) and can be expanded on normal τ_{xy} and tangent τ_{xz} terms $p_x = i\sigma_x + j\tau_{xy} + \kappa\tau_{xz}$. The second index of tangent stresses point to axis in which direction stress τ is projected.

With area perpendicular to the axes y and x, we get two more expansions stress:

$$p_y = i\tau_{yx} + j\sigma_y + \tau_{yz},$$

$$p_z = i\tau_{zx} + j\tau_{zy} + \kappa\sigma_z.$$

At an arbitrary location of the site with the outward normal n vector p_n can be expressed in terms of vectors p_x, p_y, p_z by the following relation:

$$p_n = np_{nn} = p_x\cos(nx) + p_y\cos(ny) + p_z\cos(nz)$$

Projecting p_n on coordinate axes, we get

$$p_{nx} = \sigma_x\cos(nx) + \tau_{yx}\cos(ny) + \tau_{zx}\cos(nz),$$

$$p_{ny} = \tau_{xy}\cos(nx) + \sigma_y\cos(ny) + \tau_{zy}\cos(nz),$$

$$p_{nz} = \tau_{zx}\cos(nx) + \tau_{yz}\cos(ny) + \sigma_z\cos(nz).$$

Physical value which is characterize in that point by p_n vector, which takes on different values depending on the orientation of the area, is called the tensor. Thus, the surface tension is determined by nine scalar quantities σ_x, σ_y, σ_z, τ_{xy}, τ_{xz}, τ_{yx}, τ_{yz}, τ_{zx}, τ_{zy}. Stress tensor at an arbitrary point in space has the symmetry property (Cauchy's theorem of reciprocity of shear stresses), that is, $\tau_{xy} = \tau_{yz}$, $\tau_{zx} = \tau_{zx}$, $\tau_{zy} = \tau_{yz}$.

Consequently, the surface tension is determined by not nine but six scalar values.

Occurrence of shear stresses in a fluid is caused by its toughness and movement (relative displacement).

In motionless liquid, as well as in a moving fluid devoid of viscosity (perfect fluid), the shear stresses are zero ($\tau_{xy} = \tau_{yz} = \tau_{zx} = 0$) and surface forces are determined only by the normal stresses σ_x, σ_y, σ_z, independent of the orientation of area, i.e. $\sigma_x, \sigma_y, \sigma_z = -p_{nn}$.

Euler equations of motion for an ideal fluid in a Cartesian coordinate system have the form:

$$\left.\begin{aligned} \frac{dc_x}{dt} &= -\frac{1}{\rho}\frac{\partial p}{\partial x} + X \\ \frac{dc_y}{dt} &= -\frac{1}{\rho}\frac{\partial p}{\partial y} + Y \\ \frac{dc_z}{dt} &= -\frac{1}{\rho}\frac{\partial p}{\partial z} + Z \end{aligned}\right\} \qquad (11.1)$$

$$\left.\begin{aligned} \frac{\partial c_x}{\partial t} + c_x\frac{\partial c_x}{\partial x} + c_y\frac{\partial c_x}{\partial y} + c_z\frac{\partial c_x}{\partial z} &= -\frac{1}{\rho}\frac{\partial p}{\partial x} + X \\ \frac{\partial c_y}{\partial t} + c_x\frac{\partial c_y}{\partial x} + c_y\frac{\partial c_y}{\partial y} + c_z\frac{\partial c_y}{\partial z} &= -\frac{1}{\rho}\frac{\partial p}{\partial y} + Y \\ \frac{\partial c_z}{\partial t} + c_x\frac{\partial c_z}{\partial x} + c_y\frac{\partial c_z}{\partial y} + c_z\frac{\partial c_z}{\partial z} &= -\frac{1}{\rho}\frac{\partial p}{\partial z} + Z \end{aligned}\right\} \qquad (11.2)$$

Considered equations (11.1), (11.2) are the mathematical expression of the conservation of momentum law at each point of the liquid element: the rate of change of momentum vector is the sum of all the mass and surface forces acting on the fluid element.

The system of differential equations of motion of the Euler (11.2) with partial derivatives of the unknown functions (the projection of the velocity vector c_x, c_y, c_z, density ρ and the pressure p) is not closed in the sense that the number of unknown functions exceeds the number of equations. In addition, the system of equations is nonlinear: unknown functions and their partial derivatives are included in the form of products.

To close the system we use differential equation of continuity

$$\frac{\partial \rho}{\partial t} + \frac{\partial(\rho c_x)}{\partial x} + \frac{\partial(\rho c_y)}{\partial y} + \frac{\partial(\rho c_z)}{\partial z} = 0. \qquad (11.3)$$

This equation reflects the law of conservation of fluid mass and the condition of continuity, so takes place not only for perfect, but for a viscous fluid.

For an incompressible fluid (p = const) from (11.3) we have:

$$\frac{\partial c_x}{\partial x} + \frac{\partial c_y}{\partial y} + \frac{\partial c_z}{\partial z} = 0. \qquad (11.4)$$

Incompressible fluid motion equations, written with taking viscosity into account, are significantly complicated in comparison with (11.2) system of equations:

$$\rho\left(\frac{\partial c_x}{\partial t}+c_x\frac{\partial c_x}{\partial x}+c_y\frac{\partial c_x}{\partial y}+c_z\frac{\partial c_x}{\partial z}\right)=X-\frac{\partial p}{\partial x}+\mu\left(\frac{\partial^2 c_x}{\partial x^2}+\frac{\partial^2 c_x}{\partial y^2}+\frac{\partial^2 c_x}{\partial z^2}\right);$$

$$\rho\left(\frac{\partial c_y}{\partial t}+c_x\frac{\partial c_y}{\partial x}+c_y\frac{c_y}{\partial z}+c_z\frac{\partial c_y}{\partial y}\right)=Y-\frac{\partial p}{\partial y}+\mu\left(\frac{\partial^2 c_y}{\partial x^2}+\frac{\partial^2 c_y}{\partial y^2}+\frac{\partial^2 c_y}{\partial z^2}\right); \qquad (11.5)$$

$$\rho\left(\frac{\partial c_z}{\partial t}+c_x\frac{\partial c_z}{\partial x}+c_y\frac{\partial c_z}{\partial y}+c_z\frac{\partial c_z}{\partial z}\right)=Z--\frac{\partial p}{\partial y}+\mu\left(\frac{\partial^2 c_z}{\partial x^2}+\frac{\partial^2 c_z}{\partial y^2}+\frac{\partial^2 c_z}{\partial z^2}\right).$$

Written motion equations, which are called Navier Stokes equations, are united to one vector equation if Laplace operator is used:

$$\rho\frac{d\vec{c}}{dt}=\vec{J}-gradp+\mu\Delta\vec{c}\ .$$

For the mathematical formulation of the problem Euler and Navier Stokes equations must be supplemented by the continuity equation and other dependencies. For specific tasks it is necessary to determine the initial and boundary conditions. For an incompressible viscous fluid boundary conditions result from the hypothesis of liquid adhesion to the streamlined surface, according to which both the normal and tangential components of the velocity on the surface of the body vanish. Experiments show that this hypothesis is correspond to reality and is broken only at a strongly rarefied gases flow of solid surfaces.

For homogenous liquid with the absence of the free surface, mass forces are balanced by hydrostatic lifting force and, if pressure is difference between real pressure and stand-by pressure, these forces are excluded from the motion equation. So we have:

$$\rho\frac{d\vec{c}}{dt}=-gradp+\mu\Delta\vec{c}.$$

Differential equations of motion of the Navier-Stokes equations for a viscous incompressible fluid with constant viscosity contain the same dependent variables of Euler: c_x, c_y, c_z, p, which are included in differential equations for an ideal incompressible fluid. The difference between these equations is only in the fact that in the right sides equations systems, an additional term equal to the product of the dynamic viscosity coefficient μ on Laplace operator from the respective projections of the velocity vector appears.

Thus the introduction of viscosity resulted in an increase in of the order of partial derivatives of the velocity vector projection, and changing in the boundary conditions. If for ideal fluid it was enough to streamline the solid surface to introduce the conditions of impermeability and unseparated liquid particles, then for a viscous incompressible fluid it is necessary to introduce the condition for the fluid particles sticking to the impenetrable solid surface, i.e., vanishing full speed.

Based on the above it follows that the equations of motion of Euler and Navier Stokes equations in general, cannot be integrated.

However, with some additional conditions, such integration is possible. Thus, the simplest problem of the flow of an ideal fluid efficiently solved using the methods of the theory of functions of a complex variable. Exact solutions of the Navier-Stokes equations for some particular cases also available. These decisions relate to problems in which all the inertial terms on the left side of equations disappear. In particular, this property have so-called layered flow, which is a sign of the presence of only one component of the velocity. If this component is the velocity c_x and components c_y and c_z are zero, then the continuity equation implies that $\frac{\partial c_x}{\partial_x} = 0$ and, consequently, c_x is independent from the x coordinate. Thus, for layered flows have

$$c_x = c_x(_{y,z}),\ c_y = 0,\ c_z = 0,\ \frac{dp}{\partial y} = 0,\ \frac{\partial p}{\partial z} = 0$$

and instead of the full non-linear system of equations (11.2) we obtain for the steady (stationary) flow linear differential equation for the velocity $c_x(_{y,z})$

$$\frac{dp}{dy} = \mu\left(\frac{\partial^2 c_{\tilde{o}}}{\partial y^2} + \frac{\partial^2 c_y}{\partial z^2}\right)$$

Note that since a ratio on the left is a function of the x coordinates, and the right – the function of the coordinates y and z, then the equality of these functions is only possible at a constant pressure gradient, i.e., $\frac{dp}{dz} = \text{const}$.

Using equation we obtain exact solutions of the equations of motion for the Navier-Stokes cases: a plane-parallel flow in a channel bounded by two parallel flat walls; Couette flow and layered motion of an incompressible fluid in the pipes. In the first case, the flow rate of c_x does not depend on the coordinate z. Couette flow takes place between two parallel plates, one of which moves with constant velocity c_{xo}. This case differs from the previous one only by the boundary conditions. Layered motion of an incompressible fluid in pipes has axial symmetry. The solution of the problem is simplified by using the equations of motion of the Navier-Stokes equations written in cylindrical coordinates.

Application of the equations of motion of the Navier-Stokes equations to a variety of other cases of viscous incompressible fluid flows created great difficulties because of their non-linearity. This forced many researchers to explore the possibility of using not complete exact equations of motion, but simplified approximate differential equations.

For example, for some tasks inertial forces can be very small compared to the viscous forces. Discarding all terms in the equations on the left side we came instead of the nonlinear system to an inhomogeneous Poisson linear equations whose solutions are known. This way of linearization is most simple, but it is applicable to a very slow creeping flow.

Another example relates to simplification of equations of flow at high Reynolds numbers. In this case, you can use the method of comparative assessments of the terms in the Navier-Stokes equations, and on that basis try to simplify the original system, omit the terms that have a relatively small order. Such simplification was proposed by Prandtl in 1904 for the flow region, located

directly near the surface. This was the basis for the establishment and further development of the theory of the boundary layer. Differential equations follow from the boundary layer of the Navier-Stokes equations.

Turbulent motion is the most common form of the motion of liquids and gases in nature and technical devices. However, quite universal and valid methods for calculating turbulent flows do not exist, despite the fact that it was researched for nearly one hundred years.

Semi-empirical theory of turbulence are used mainly for flows of boundary layer (wall surface and jet). Problems with complex internal structure (spatial flows, separated flows and others.) by using semi-empirical theories are hardly calculated. This is due to the following reasons: the complexity of the mathematical description of the mechanism of the phenomenon, limited possibilities of the traditional trends in the theory of turbulence, as well as the lack of necessary detailed experimental data. Obviously, the new approaches in the theory of turbulence are necessary.

Currently, there are two points of view of the mathematical description of the developed turbulent flow. According to the first of them, based on the fundamental ideas of O. Reynolds, equations of Navier-Stokes are taken as basis and they are added by lacked relations of turbulent flow. The second view is that the turbulent motion is the random process, and hence the equations describing it must be prepared on a statistical basis.

Brief analysis on the example of the equations of fluid motion allows noting that, in dealing with complex nonlinear problems of deformable continuum, classical methods of mathematical analysis of continuous functions for obtaining quantitative information are mostly unusable.

11.1. Summary of numerical methods

As we know fluid flows can be described by the system of partial differential (or integral-differential) equations, which cannot be solved analytically, except in a few special cases. Its approximate solution in digital form can be obtained by

sampling, which approximates the differential equation system of algebraic equations. They then can be solved by a computer. An approximation is applied to small areas in space and / or time. Thus, the results of the numerical solution are provided at discrete points in space and time. The accuracy of the numerical solutions depends on the degree of perfection of the used sampling methods.

11.1.1 Possibilities and limitations of numerical methods

When using numerical methods of mathematical physics it is always necessary to remember the fact that the results are always approximate numerical solutions. There are several reasons for the discrepancies between the results of calculations and the actual physical process. Errors accumulate in each part of the process used to obtain numerical results:

- the original differential equations involve assumptions, due to an idealization of real physical processes;
- algebraic equations involve approximation error obtained during the sampling of differential equations;
- in the solution of algebraic equations iterative methods are used.

When the calculation equations are exact analytical solutions (e.g., the Navier-Stokes equations for incompressible Newtonian fluids), the calculation results can be obtained with any desired degree of accuracy. However, for many physical phenomena, such as turbulence, combustion, multiphase flow, the exact equation or impossible to formulate or impossible to get the exact numerical solution. Even if the numerical solution of the equation was accurate from a computational point of view, it would not be a good representation of reality. To test the adequacy of the models, it is necessary to attract the experimental data.

Sampling error can be reduced by using a more accurate interpolation or approximation by averaging flow parameters within the smaller areas, but this increases the time and cost of obtaining solutions. Therefore, for the application of numerical methods in engineering problems it is necessary to find a compromise.

Compromises also necessary for solving discretized equations. Direct modeling, through which you can get the exact solution in practice is rarely used because it is too expensive computationally. Iterative methods for solving more common, but during their use it is necessary to take into account the errors due to incomplete convergence of the iterative process.

11.2 The components of the numerical method

11.2.1 Mathematical model

The starting point of any numerical method – a mathematical model. It is a system of differential or integral-differential equations and boundary conditions. Everyone chooses the appropriate model for the target application (incompressible, non-viscous, turbulent, two – or three-dimensional flow, etc.). This model may include simplification of exact conservation laws. Method of solution is usually created taking into account the specifics of the system of equations.

11.2.2 Method of sampling

After mathematical model selecting it is necessary to choose appropriate sampling method, i.e. approximation method of the differential equations by system of algebraic equations for variables in some variety of discrete positions (points) in space and time. There are many of methods, most notable of which are:

- finite difference method (CDM (FD)). The advantage of this method is its simplicity. The finite difference method is used by programs FlowEr, CIAM, TsAGI et al.
- The Finite Element Method (FEM). The finite element method is used by programs Flotran, Flow Plus, Cosmos Flow et al.
- finite volume method (FVM (FV)). The classical description of this method is given in. This method is used by programs CFX, Fluent, StarCD et al.

Each method leads to the same solution if you are using a relatively dense mesh. However, some methods are more appropriate for specific classes of problems than others.

11.2.3 Coordinate system

The conservation equations can be written in different forms, depending on the coordinate system used, and basis vectors. For example, you can choose coordinate system: Cartesian, cylindrical, spherical, curved, rectangular or non-rectangular, which may be stationary or moving. Selection of the coordinate system depends on the nature of particular solved problem. The choice of coordinate system can also affect the sampling method and the type of finite element mesh.

In addition, you need to select the starting point (the beginning of the flow), which will determine the vector and tensor (fixed or variable, covariant or contravariant, etc.).

11.2.4 Estimated finite element mesh

The positions of the discrete points, where variables are calculated, are determined by calculated finite-element mesh which is discrete visualization of the flow geometric area. It split calculated area into finite number of subsectors (elements, control volumes etc.). Calculated mesh can be structured or non-structured.

Classification of unstructured grid generation is shown in Fig 11.2.

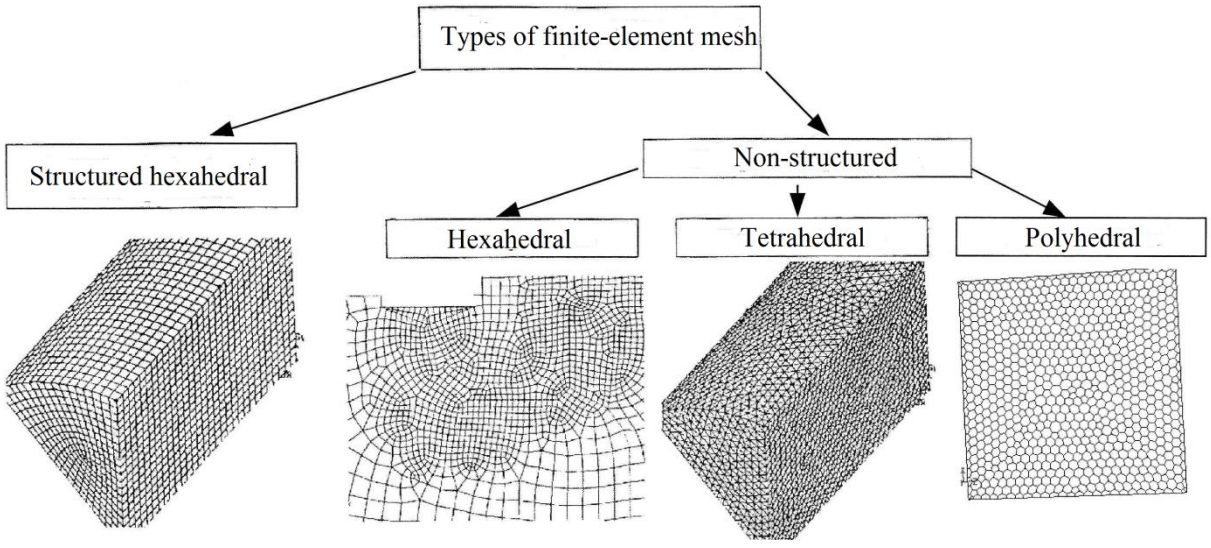

Fig. 11.2 – Classification of the finite-element meshes

Structural (regular) grids consists of rows of the grid, the elements of one kind do not cross each other and intersect each other branches of element only once. This allows numbering the line of the set sequentially. The position of any point of the mesh (or control volume) is uniquely defined within the area index in the two (in the two-dimensional field) or three numbers (three-dimensional field), for example (i, j, k). This is the most simple grid structure, as it is logically equivalent to the Cartesian coordinate system. Each point has four nearest neighbors in two dimensions and six in three-dimensional; one of the indices for each neighbor of the point P (the indices i, j, k) differs by ± 1 from the respective index P. This task of neighboring relations simplifies programming and the matrix system of algebraic equations is a regular structure that can be used in the creation of the method of solving. The disadvantage of structured grids is that they can be built only for simple geometric areas of solutions. Another disadvantage is the difficulty of controlling the distribution of grid points: a large concentration of points in a single area to ensure the accuracy of calculation results creates too small interval in other parts of the area of solutions and causes unnecessary Resource Costs. This problem is compounded in three-dimensional problems. Long, thin cells can also impede the convergence of the solution.

11.2.5 Finite approximation

After selecting of the grid type it is necessary to choose approximation algorithm which will be used in sampling process. In finite difference method approximations for derivates in the grid points must be selected. In finite element method shape forms (elements) and weight functions must be selected.

Their selection will affect the accuracy of the approximation. This also applies to the difficulty of developing a method of solutions. More accurate approximations include more nodes and provide a more complete matrix.

11.2.6 Solution method

The result of a sampling is a system with a large number of non-linear algebraic equations.

For unsteady flows methods, which are based on using time-step differential equation solution with starting conditions, are applied.

In each case in solution of elliptic task time step must be given.

Steady tasks usually use quasi time step or equivalent iteration scheme.

Since the equations are nonlinear, for their solution iterative scheme is used. These methods use a consistent linearization of the equations, and the resulting linear systems are almost always solved by iterative methods.

The choice of method depends on the type of solutions and the number of grid nodes selected to approximate the derivatives in each of algebraic equations.

11.2.7. Convergence criteria

For iteration method it is necessary to establish convergence criteria. There are usually two levels of iteration: inner iteration within which linear equation is solved and outer iteration where solving is connected with non-linearity and equation mutual effect. It is important to decide when it is necessary to stop the iterative process in terms of accuracy and efficiency.

11.3 Properties of numerical methods for solving

11.3.1 Reliability

Discretization is carried out the more accurate the closer the grid spacing tends to zero. The difference between the discretized equations and the exact solution is called the error of the method. It is usually estimated by replacing all values of a discrete approximation of the nodes in the Taylor series expansion at each point. As a result, the original differential equation is restored plus the remainder, which is the error of the method. To ensure the reliability of the method, method error tends to zero when the grid spacing $\Delta t \to \to 0$ and / or

$\Delta x_i \rightarrow \rightarrow 0$. Error of the method is usually proportional to the grid interval Δx_i and / or time step Δt. If the most important member is proportional to $(\Delta x)^n$, or $(\Delta t)^n$ method is called the nth-order approximation. For consistency n> 0 is required. Ideally, all members must be discretized with the approximation of the same order of accuracy; However, some members (such as convective members of the flow with high Reynolds number of diffusion members in the flow with low Reynolds number) may be dominant in the stream, and this calculation may require a higher accuracy than others.

Some methods of sampling lead to errors in method, which is a function of Δx_i to Δt or vice versa. In this case, the requirement of reliability is performed only if and when Δx_i and Δt must be reduced in such way that the corresponding ratio tends to zero.

Even if approximation is consistent, it does not necessarily mean that the solution of the discretized system equations will be the exact solution of the differential equation with unbounded size step reduction. In order to this to happen, the method of solution must be stable.

11.3.2 Stability

The decision of the numerical method is stable if it does not increase (not accumulate) errors that appear in the solution process. For non-stationary problems (problems with time dependence) stability ensures that the method gives the final decision whenever solution of the exact equation is limited in time. For iterative methods stable method is those which is not diverged. Stability can be difficult to diagnose, especially when the boundary conditions non-linearity are present. Therefore, the research of method stability for linear tasks is carried out with constant coefficient without boundary conditions. Experience shows that results obtained in this way can often be applied to more complex tasks, but there are exceptions.

The most widely used method for the study of stability of numerical schemes is Neumann method.

11.3.3 Convergence

A numerical method has convergence, if the solution of discretized equations tends to the exact solution of differential equations, when the grid spacing tends to zero. For linear problems with initial conditions a simple equivalence theorem (Richtmyer and Morton, 1967) states that "properly formulated linear problem with the initial conditions and approximations by finite differences, which satisfies the conditions of reliability and stability is a necessary and sufficient condition for convergence." Obviously, reliable scheme is useless if a method does not converge.

For nonlinear problems, which are influenced by the boundary conditions, stability and convergence of the method are difficult to identify. Therefore, the convergence is usually tested using numerical experiments, ie repetition of computing grids upgraded consistently. If the method is stable and all approximation that used in discretization process are compatible, the solution converges to grid independent solution. For sufficiently small mesh sizes convergence value is controlled in accordance with the error of the main component.

11.3.4 The conservation laws

Since the equations of the Navier – Stokes equations are the conservation laws, the numerical scheme must comply with these laws, both the local and global level. This means that in the steady task an amount of matter which enters the volume is equal to amount of matter that leaves the volume. If rigid form of the conservation laws and finite volume method are used it guarantees conservation law accomplishment for any individual control volume and whole calculated area. Other methods of sampling may be less accurate in the implementation of conservation laws.

It is an important property of the solution method because it determine the solution error. If mass, momentum and energy conservation laws are provided,

calculation error can be only in their inappropriate distribution in the calculated area.

11.3.5 Limitations in the calculation

Numerical solutions should be within the proper boundaries. Physically non-negative parameters such as density, turbulent kinetic energy, must always be positive. Other parameters, such as concentration, should be in the range between 0% and 100%. In the absence of sources, some of equations (for example, the heat equation for the temperature when heat sources are not available) require that the minimum and maximum values of the variables are in the range of values given on the borders of the region. These conditions must be taken into account by numerical approximation.

Observance of these limits is difficult to guarantee. Below it will be shown that only some of the first order schemes ensure compliance with this condition. Schemes of higher order can lead to a change in the results of unlimited solution. It is usually occurs only in too large grids. Therefore, the solution results, which are placed outside pointed limitations, are indicators of the fact that solution errors are large and grid require modification (at least, locally).

11.3.6. Adequacy

Models of complex phenomena, which description includes turbulence, combustion or multiphase flow, must guarantee gaining of physically realistic solution. This is not a numerical problem per se, but the wrong model can lead to unphysical solutions or divergent iterative process.

11.3.7 Accuracy

Numerical methods of the fluid flow and heat exchange calculation give only approximate solutions. In additions for errors which can be admitted during solution algorithm development or boundary condition setting, the results of the numerical solutions always include three types of systematic errors:

- modeling error, defined as the difference between the experimental results and the results of mathematical model solution;
- sampling error, defined as the difference between the exact solution of differential equations of conservation and the exact solution of the algebraic system of equations obtained by discretization of differential equations.
- iterative error, defined as the difference between iterative and exact solution of the system of algebraic equations.

Iterative errors are often called convergence errors. However, the term convergence is used not only in relation to the imperfections of the iterative procedure, but is also determined by the convergence of numerical solutions regardless of the grid and is connected to a sampling error.

It is important to know about the existence of these errors, and, what's more, to distinguish one from the other. Various errors may cancel each other so the solution obtained on the coarse grid can be coordinated better with experiment than the solution obtained on the finer grid, which, by definition, must be more precise.

Modeling errors depend on the assumptions made in the preparation of physical equations for the variables. They can be neglected in the study of laminar flow, as the Navier-Stokes equations represent sufficiently precise flow model. However, in turbulent flows, two-phase flow, combustion, etc., modeling error can be very significant. That is, even the exact solution of the equations can be qualitatively incorrect. Modeling errors are possible due to the simplification of geometry – area of solution, as well as due to the simplification of boundary conditions, etc. These errors are not known at once; their assessment can only be made by comparing the solution in which sampling and errors of convergence are insignificant with accurate experimental data or with the data obtained from more accurate models (for example, data obtained as a result of direct numerical simulation of turbulence, etc.). This comparison is very important to control the process of convergence and error estimates sampling to create models of physical phenomena.

11.4. Finite volume method

11.4.1 Introduction

When using the finite volume method, the solution space is divided into a grid on a finite number of small control volumes, which, in contrast to the finite difference method, defines the boundaries of the control volume, rather than compute nodes.

Finite volume method uses as a starting point the integral form of the conservation equations:

$$\int_s \rho\varphi\upsilon \cdot ndS = \int_s \Gamma grad\varphi \cdot ndS + \int_\Omega q_\phi d\Omega \qquad (11.1)$$

The classic method is to determine the volume of the control grid and assign a compute node in the center of the control volume. However, the structured grids may also determine the location of first node, and then create control volumes around them, so that the control volume faces lie halfway between the nodes (see. Fig. 11.3). Nodes for which the boundary conditions imposed are shown as black dots.

The advantage of the first method is that the value represents the average node value over the entire volume of volume control with higher precision (second order) than in the second method, because the node is located at the midpoint of the control volume. The second method is that the approximation of the derivatives on the faces of the control volume are more accurate in the middle of the edge between two nodes. In practice, the first option is often used.

The principles of sampling are the same for all variants. The only thing that you need to take into account is the ratio between the different locations (points) within the scope of integration.

Integral conservation equation (11.1) refers to every control volume as well as to whole solution area. If equations for every control volume are summarized we get global conservation equation because integrals by surfaces and inner faces

are balanced. Thus, global conservation is incorporated in method which provides to him one of the most important advantages.

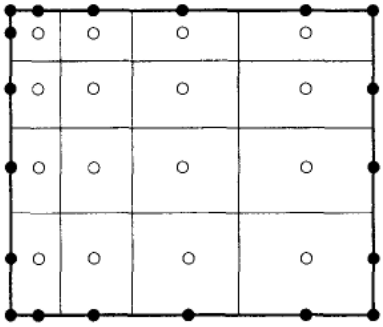

Fig. 11.3 Nodes centered in control volume

To get algebraic equations for specific control volume, surface and volume integrals must be approximated by least square method.

The typical 2-d and 3-d control volumes in Cartesian coordinates are presented on fig. 11.4 and 11.5. The surface of the control volume consists of four (in two-dimensions) or six (in three-dimensional) plane faces denoted in lower case letters corresponding to the their direction (e, w, n, s, t, and b) relatively to the central node (P). Dimensional version can be taken as a special case of three-dimensional, in which the dependent variables are independent of z.

Flow across the boundary control volume is the sum of the integrals over the four (in two-dimensional case) or six (in three- dimensional case) control volume faces:

$$\int_S f\,dS = \sum_k \int_{S_e} f dS\,, \qquad (11.2)$$

where *f* is a component of convective $\rho\phi\upsilon\cdot n$ or diffusive ($\tilde{A}grad\phi\cdot n$) flow vector in the direction normal to control volume face.

Since velocity field and fluid properties are known, the only unknown variable is $\varphi\varphi$. If velocity field is unknown, the task became more complicated and includes double non-linear equations.

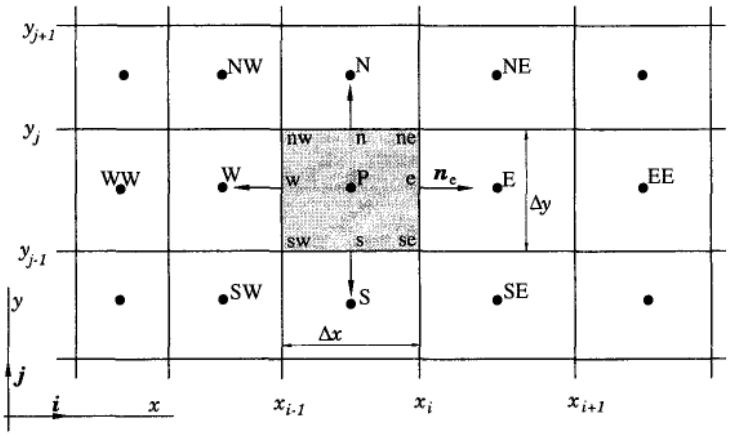

Fig. 11.4. Typical 2-d control volume in Cartesian coordinate system

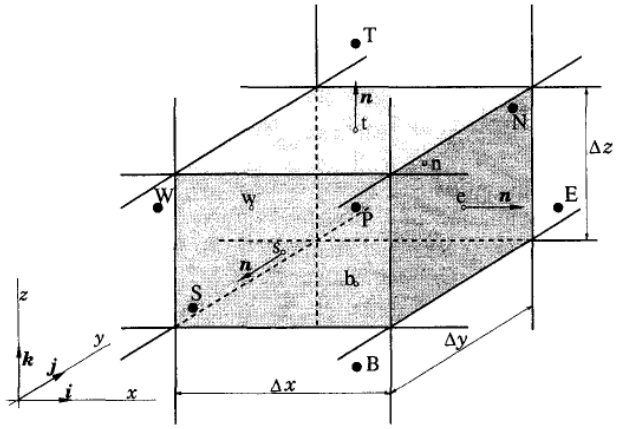

Fig. 11.5. Typical 3-d control volume in Cartesian coordinate system

To maintain the conservation equations, it is important to control volumes not to be overlapped; each face of the control volume is the only for the two control volumes, which lie on both sides.

Further, only ‘e’ face, which is typical for 2-d control volume shown on the fig. 1.3, will be considered. Similar expressions can be obtained for all facesby making the appropriate substitution of index.

To accurately calculate the surface integral in equation (11.2), the only thing you need to know – is the integrand f across the surface S_e, which is not known. Once the values of the nodes φ (center of control volume) will be calculated, the approximation may be possible. This is best done by using two-level approximation:

- integral is approximated in terms of the variable values in one or more locations on the edge of the cell;
- the nominal cell values are approximated in terms of the node (center of control volume) values.

The simplest approximation for the integral is a midpoint rule: integral is approximated as the product of the integrand in the center of the face of the cell (which is itself an approximation to the average over the surface) and cell surface area:

$$F_e = \int_{S_e} f dS = \overline{f}_{eS_e} \approx f_{eS_e}. \qquad (11.3)$$

This approximation provides the integral value of f at the location of ' e ' and has a second-order accuracy.

Since the value of f is not available in the center of the face *'e'*, it must be obtained by interpolation. To maintain the accuracy of the second order approximation of the midpoint rule surface integral value f_e must be calculated with an accuracy of at least second order.

Other second-order approximation of the surface integral for two-dimensional case is a trapezoid rule:

$$F_e = \int_{S_e} f dS \approx \frac{S_e}{2}(f_{ne} + f_{se}). \qquad (11.4)$$

In this case it is necessary to estimate the flow in the corners of the control volume.

To approximate the higher order surface integrals flow should be evaluated in more than two points. Fourth-order approximation is a Simpson rule that evaluates the integral over S_e as:

$$F_e = \int_{S_e} f dS \approx \frac{S_e}{6}(f_{ne} + 4 f_e + f_{se}). \qquad (11.5)$$

Here you need to know the values of f at the three points in the center of the face *'e'* and the two corners of the *'ne'* and *'se'*. To maintain the accuracy of the

fourth order, these values should be obtained by interpolation of nodal values at least as accurate as a rule of Simpson.

In 3-d case, midpoint rule is a simplest second-order approximation. In three dimensions, usually middle – the simplest approximation of the second order. Approximation of higher order, which require the integrand in locations other than center of the cell faces (e.g., corners and centers of the edges) are possible, but they are more difficult to implement.

If f variation, as supposed, has some specific simple form (e.g., polynomial interpolation), integration is easy to do. Then, approximation accuracy depends on order of the shape function.

11.4.3 Approximation of integrals over volume

Some variables in the initial differential equations require integration over the control volume. The simplest approximation of the second order of accuracy is to replace the volume integral by the product of the average value of the integrand and volume control volume and to approximate the form as a value in the centre of the control volume:

$$Q_p = \int_{\Omega} q d\Omega = \bar{q}\Delta\Omega \approx q_p \Delta\Omega, \qquad (11.6)$$

where q_P replaces the value of q in the center of the control volume. This amount is easily calculated; since all the variables are available at the node P, and there is no need for interpolation. The above approximation becomes exact if q – constant or varies linearly within the control volume; otherwise, it contains the second-order error.

Approximation of higher order requires values of q in more points than only in the center. These values must be obtained by interpolating the values in the nodes or equivalently, by using shape functions.

In the two-dimensional formulation volume integral becomes the integral of surface. Fourth-order approximation can be obtained by using biquadratic shape function:

$$q(x,y) = a_0 + a_1 x + a_2 y + a_3 x^2 + a_4 y^2 + a_5 xy + a_6 x^2 y + a_7 xy^2 + a_8 x^2 y^2. \quad (11.7)$$

The nine coefficients obtained by adapting the function to the values of q at nine points (*'nw', 'w', 'sw', 'n', P, V, 'ne', 'e' u 'se'*, look at fig. 1.3). The integral can then be calculated. In two dimensions, the integration gives (for grids in the Cartesian coordinate system):

$$Q_p = \int_\Omega q d\Omega = \bar{q}\Delta\Omega \approx \Delta x \Delta y \cdot \left[a_0 + \frac{a_3}{12}(\Delta x)^2 + \frac{a_4}{12}(\Delta y)^2 + \frac{a_8}{144}(\Delta x)^2 (\Delta y)^2 \right]. \quad (11.8)$$

In this case only four coefficients must be determined, but they depend on the values of q in all nine of the above points. On a uniform grid in Cartesian coordinates, we obtain:

$$Q_p = \frac{\Delta x \Delta y}{36}\left[16q_p + 4q_s + 4q_n + 4q_w + 4q_e + 4q_{se} + 4q_{sw} + 4q_{ne} + 4q_{nw}\right]. \quad (11.9)$$

Since, the value exist only in *P* node, interpolation must be used to obtain *q* values in other points. It should be at least the fourth order of accuracy, holding precision of integral approximation.

Aforementioned fourth order approximation of the volume integral in the two-dimensional case can be used to approximate the surface integrals in the three-dimensional formulation. Approximation of higher order volume integrals in the three-dimensional case are more complex, but can be found by using the same methods.

11.4.4 Interpolation and methods of differentiation

Approximation to the integrals require variable values at points other than the compute nodes (control volume centers). Integrand, mentioned in previous sections as *f*, includes product of several variables and/or variable gradients in next points: $\Delta f = \rho\phi\upsilon \cdot n$ for convective flow and $\Delta f = \Gamma grad\phi \cdot n$ for diffusive flow. Assuming that the velocity field Γ and the properties of the fluid ρ are known in all points, to calculate the convective and diffusive flow, it is necessary to know the value $\varphi\phi$ and its gradient normal to a face of the cell in one or more

points on the surface of the control volume. Integrals by source terms volume can also require these values. The must be expressed by interpolation as values terms in nodes.

11.4.4.1 Interpolation upstream

Approximation of $\phi_e\varphi_\beta$ by its value in the node, placed upstream than '*e*', is equivalent to using the reverse or direct difference approximation for the first derivate. Consequently, this approximation can be called scheme of the upstream differences calculation (UD). In UD $\phi_e\varphi_\beta$ is approximated as:

$$\phi_e = \begin{cases} \phi_p if\,(v\cdot n)_e > 0 \\ \phi_E if\,(v\cdot n)_e < 0\cdot \end{cases} \qquad (11.10)$$

This is only approximation, which unequivocally meets the criterion of restrictions, i.e., the use of this interpolation will never lead to oscillatory solutions. However, this is achieved by the numerical diffusion.

Taylor series expansion for *P P* gives (for the grid in Cartesian coordinates $(v\cdot n)_e > 0$):

$$\phi_e = \phi_Ð + (x_e - x_P)\left(\frac{\partial\phi}{\partial x}\right)_P + \frac{(x_e - x_P)^2}{2}\left(\frac{\partial^2\phi}{\partial x^2}\right)_P + H, \qquad (11.11)$$

where *HH* are variables of a higher order. Approximation UD saves only the first variable on the right side, so it is a scheme of the first level. The main error of the method is diffusion, i.e. it resembles the diffusion flux:

$$f_e^d = \tilde{A}_e\left(\frac{\partial\phi}{\partial x}\right)_e \qquad (11.12)$$

Coefficient of the numerical, artificial or false diffusion is equal to $\Gamma_e^{num} = (pu)_e\Delta x/2$. Then, the method error generates diffusion in the direction, normal to flow, as in the direction of flow, which causes serious error. Peaks or rapid variations of the variables will be removed.

11.4.4.2. Linear interpolation (CD)

Other direct approximation for the value in the center of the control volume faces is a linear interpolation between the two closest nodes. At the point *'e'* of the grid in the Cartesian coordinate system we have (see. Fig. 11.4 and 11.5):

$$\varphi_e = \varphi_E \lambda_e + \varphi_P (1 - \lambda_e), \tag{11.13}$$

where the linear interpolation factor $\lambda_{\hat{a}}$ is defined as:

$$\lambda_e = \frac{x_e - x_p}{x_E - x_p}. \tag{11.14}$$

Equation (11.11) is the equation of the second order of accuracy that can be shown by using a Taylor series expansion $\varphi\beta$ at X_P to remove the first derivative in equation (11.11):

$$\varphi_e = \varphi_E \lambda_e + \varphi_P (1 - \lambda_e) - \frac{(x_e - x_P)(x_e - x_P)}{2} \left(\frac{\partial^2 \varphi}{\partial x^2} \right)_P + H .$$

The main error of the method is proportional to the square of the grid spacing on uniform or non-uniform grids.

As with all approximations of order higher than the first order, this scheme can lead to oscillatory solutions. This is the simplest scheme of the second order. It is the most widely used. This scheme corresponds to central-difference approximation of the first derivate in finite differences method and is called CD. The assumption of a linear relationship between the nodes P and E also offers a very simple approximation of the gradient, which is necessary to evaluate the diffusion fluxes:

$$\left(\frac{\partial \varphi}{\partial x} \right)_e \approx \frac{\varphi_E - \varphi_p}{x_E - x_p}.$$

When using a Taylor expansion around ϕ_e it can be shown that the error of the method of aforementioned approximation:

$$e_\tau = \frac{\left(x_e - x_P\right)^2 - \left(x_E - x_e\right)^2}{2\left(x_E - x_P\right)}\left(\frac{\partial^2\varphi}{\partial x^2}\right)_e - \frac{\left(x_e - x_P\right)^3 + \left(x_E - x_e\right)^3}{6\left(x_E - x_P\right)}\left(\frac{\partial^3\varphi}{\partial x^3}\right)_e + H.$$

When the point 'e' is in the middle between the nodes E (for example, in a regular grid) and the approximation has an accuracy of second order, since the first term on the right-hand side vanishes, then a leading member of the residual time is proportional to $(\Delta x)^2$. When the grid is not uniform, the leading error term is proportional to the product of Δx and grid expansion coefficient. Despite the formal accuracy of first level in this circuit there is a decrease to improved grid errors, like a second-order approximation even on irregular meshes.

11.4.4.3. Quadratic interpolation against the flow (QUICK)

The next logical refinement in the direction of improving the approximation was the description of the change in the variable between the point by the parabola, and not straight. To create a parabola, it is necessary to use the data in another point. Correspondingly with convection nature, the third point is taken in the location upstream, i.e. W if the flow from *PP* to *EE* (i.e. $u_x > 0$) or *EE*, if $u_x < 0$ (fig. 11.5). So we have:

$$\phi_e = \phi_u + g_1\left(\phi_D - \phi_U\right) + g_2\left(\phi_U - \phi_{UU}\right), \qquad (11.15)$$

where D, U and UU are designations for main direction, first and second upstream node correspondingly (*E, P*, and *W* or *EP*, *PE,* and *EE* dependently on flow direction). Coefficients g_2 and g_1 can be expressed trough the node coordinates:

$$g_1 = \frac{\left(x_e - x_U\right)}{\left(x_D - x_U\right)}\frac{\left(x_e - x_{UU}\right)}{\left(x_D - x_{UU}\right)};$$

$$g_2 = \frac{\left(x_e - x_U\right)}{\left(x_U - x_{UU}\right)}\frac{\left(x_D - x_e\right)}{\left(x_D - x_{UU}\right)}.$$

For regular grids coefficients of three node values which are include in interpolation are taken: 3/8 for main direction point, 6/8 for the first upstream node and 1/8 for the second upstream node.

This scheme is somewhat more complex than the CD scheme, because the computational region is extended to one node in each direction (for two-dimensional case, the nodes included *EE, WW, NN* and *SS*). At the same time on non-orthogonal and / or non-uniform grids, the expressions for the coefficients g_i are not simple. Leonard (1979) made this scheme popular and gives it a name *QUICK* (Quadratic Upstream Interpolation with Convective Kinetics).

In this quadratic interpolation scheme error of the method corresponds to the third order accuracy either on uniform or non-uniform grids. This can be demonstrated by eliminating the second derivative of the equation (11.15), the use of ϕ_w, which, on a uniform grid in Cartesian Coordinate system with $u_x > 0$results in:

$$\varphi_e = \frac{6}{8}\varphi_P + \frac{3}{8}\varphi_E - \frac{1}{8}\varphi_W - \frac{3(\Delta x)^2}{48}\left(\frac{\partial^2 \varphi}{\partial x^3}\right)_P + H\,.$$

The first three terms on the right side represent an approximation *QUICK*, while the last term – the basic error of the method. When this interpolation scheme is used together with midpoint rule approximation of the surface integral, full approximation of second order of accuracy (Quadratic approximation accuracy). Approximation *QUICK* is little more accurate than a *CD*.

11.4.5. The implementation of the boundary conditions

Each control volume provides one algebraic equation. Integrals by volume are calculated in the same manner as for each control volume, but flows through the faces of the control volume, coinciding with the area, require special handling. These flows must be known, or expressed as a combination of values of internal and boundary conditions. Since they do not provide additional equations, they

should not give additional unknowns. There are no nodes outside the boundary, so these approximations should be based on one-sided differences or extrapolations.

Usually, convective flows are attributed to the front border. Convective flows are zero in impermeable walls and planes of symmetry, and are commonly used independent of the coordinate normal to the outflow; In this case, the upstream approximation can be used. Diffusion fluxes are sometimes defined in the wall, for example, a specific heat flow (including the special case of adiabatic surfaces with zero heat flow) or when the boundary values of variables are prescribed. In this case, the diffusion fluxes evaluated using normal approximation for unilateral gradients. If gradient itself is determined, it is used to calculate the flow, and approximation for flow can be used in terms of node values to calculate bpundary value of the variable.

11.4.6. Algebraic system of equations

Summarizing the approximations of flow and the source of variables, we create an algebraic equation that relates the variable value in the center of the control volume to values in points of several neighboring control volumes. Numbers of equations and variables are equal to number of control volumes, so the system is well laid out. There is a form [17] of algebraic equation for specific control volume and system of equations for entire solution area gives matrix form of equation.

11.5. Solution of the Navier – Stokes equations

As a result of the sampling every equation is presented as system of linear equations which have unknown values of flow parameters which are determinate from this equation solution. To solve the system of algebraic equation two groups of methods are currently used. Conjugate gradient methods are based on finding a multidimensional vector function to minimize the residuals obtained by substitution of the approximate solution to the system of linear equations. The most promising method of finding a solution to a system of linear equations is the

multigrid method. Some programs use some simplified algorithms: tridiagonal Thomas algorithm (TDMA) and Gauss-Seidel method.

To increase stability and convergence relaxation is most commonly used. Relaxation is a limit on the change of the variable during the iteration:

$$\varphi^i = \varphi^{i-1} + \alpha\Delta\varphi ,$$

where

α – relaxation coefficient;

i – iteration number.

Solution of the Navier – Stokes equations numerically itself is not difficult. The real difficulty is related to the definition of the velocity field with an unknown pressure field. The pressure gradient is part of the source term of the Navier – Stokes equations. The equations for pressure determination, however, are not introduced into the system. Therefore, the pressure field is determined by the continuity equation. If the "correct" pressure field is substituted into the Navier – Stokes equations, the velocities, obtained as result of its solution, will satisfy to the continuity equation.

One of the possible solutions of the system of equations is as follows:

- approximate pressure field is given;
- Navier-Stokes equation is solved and u^*,v^*,$w^*$are determined;
- pressure correction $p' = p - p^*$ is determined, where p – the pressure field, which satisfies the continuity equation;
- $p = p' + p^*$ is determined;
- specified values of the velocities u,v,w are determined;
- temperature distribution T is determined;
- temperature dependant media properties (λ, μ, c_p, R) are renewed;
- turbulence parameters distribution is determined;
- turbulence dependant media properties (μ_T) are determined.

This algorithm is called a semi-implicit method for connecting the pressure equations and is better known under the name SIMPLE.

The discrepancy concept is often used as a solution convergence criterion. Let for the differential equation $L(\hat{O}) = 0$ approximate solution $\bar{o}$ was found. The value $R = L(\bar{O})$ is called discrepancy. Obviously, the closer to zero the discrepancy, the closer the resulting numerical solution to a real solution of the system of equations. Convergence condition is the condition that the maximum value $|R|$ should not exceed a certain small number. Maximum discrepancy is usually appointed within $1 \cdot 10^{-2} \ldots\ldots 1 \cdot 10^{-4}$.

Учебное издание

Бирюк Владимир Васильевич,
Благин Евгений Валерьевич,
Угланов Дмитрий Александрович,
Цыбизов Юрий Ильич

MECHANICS OF COMPRESSIBLE FLUID

Учебное пособие

Редактор Н.С. Куприянова
Компьютерная верстка Л.Р. Дмитриенко

Подписано в печать 12.12.2018. Формат 60x84 1/16.
Бумага офсетная. Печ. л. 9,75.
Тираж 25 экз. Заказ . Арт. – 4(Р5У)/2018.

ФЕДЕРАЛЬНОЕ ГОСУДАРСТВЕННОЕ АВТОНОМНОЕ
ОБРАЗОВАТЕЛЬНОЕ УЧРЕЖДЕНИЕ ВЫСШЕГО ОБРАЗОВАНИЯ
«САМАРСКИЙ НАЦИОНАЛЬНЫЙ ИССЛЕДОВАТЕЛЬСКИЙ
УНИВЕРСИТЕТ ИМЕНИ АКАДЕМИКА С.П. КОРОЛЕВА»
(САМАРСКИЙ УНИВЕРСИТЕТ)
443086 Самара, Московское шоссе, 34.

Изд-во Самарского университета.
443086 Самара, Московское шоссе, 34.